Escola de Camins
Escola Tècnica Superior d'Enginyeria de Camins, Canals i Ports
UPC BARCELONATECH

TREBALL FINAL DE MÀSTER

# On the use of trapezoidal synthetic storm for breakwater stability design


Treball realitzat per:
**Eduard Cano Garcia**

Dirigit per:
**Xavier Gironella Cobos & Andrea Marzeddu**


Màster en:
**Enginyeria de Camins, Canals i Ports**

Barcelona, 16-06-2017


Departament d'Enginyeria Civil i Ambiental

# ABSTRACT

The design of a breakwater armour layer relies mostly on empirical formulations. However, is commonly accepted that a series of physical tests are necessary to verify this design. This is due to the limited number of cases studied in order to drive these expressions.

The aim of this work is to perform a comprehensive study on the methodologies for the testing of this type of structure. Stability tests on a breakwater with an armour layer composed by two layers of cubic clocks have been performed in the CIEMito, a small-scale flume at UPC. This stability has been assessed in terms of the relative damage ($N_{od}$).

A real storm, registered by a buoy in the Catalan coast, is downscaled and simulated in the flume serving as a benchmark for the assessment of other testing methodologies. From these, a synthetic storm based on the Equivalent Magnitude Storm model with a trapezium shape is compared with the real storm in terms of damage. Results from previous experiments of other synthetic models as the 'classical methodology' and the triangular synthetic storm are also exposed in the work.

The parameters used to define these synthetic storms are derived from the real storm. Concretely, $H_s$ and $T_p$ associated to the peak of the storm, and the Magnitude, which is identified as the energy associated to the storm.

The damage assessment is done with $N_{od}$ values obtained at the end of the storm (same energy delivered), but also relative damage is obtained in intermediate steps (peaks) to control the progression. For both the real and trapezoidal storm, it is observed that the most contribution to the final damage occurs during the increasing branch and between peaks, while it does not practically increase during the storm tail.

The results of the comparison between the real and trapezoidal storm put in evidence that the trapezoidal storm causes a higher damage when the dataset of both storms englobes only the author tests. Nevertheless, situation is reversed when this dataset is extended to results of other operators in charge of the breakwater construction. The research has verified that, although being fixed for all the tests the construction methodology, the placement of each single block acquires notable relevance in the structure global damage.

# TABLE OF CONTENTS

# LIST OF FIGURES

# LIST OF TABLES

# LIST OF SYMBOLS

| | |
|---|---|
| $A$ | Surface area [m$^2$] |
| $A_e$ | Eroded area [m$^2$] |
| $b$ | Section width [m] |
| $b_S$ | Small base of the trapezoidal synthetic storm [h] |
| $b_L$ | Long base of the trapezoidal synthetic storm [h] |
| $d$ | Water depth [m] |
| $D_{50}$ | Grading of stones [m] |
| $D_{equiv.}$ | Synthetic storm duration [h] |
| $D_n$ | Nominal stone diameter [m] |
| $D_{real}$ | Real storm duration [h] |
| $f$ | Frequency [Hz] |
| $f_{peak}$ | Peak frequency of the spectrum [Hz] |
| $g$ | Gravity [m/s$^2$] |
| $H_{equiv.}$ | Height of the peak storm above a fixed threshold [m] |
| $H_{max}$ | Maximum wave height [m] |
| $H_s$ | Significant wave height [m] |
| $H_{s,measured}$ | Significant wave height measured by a wave gauge in the flume [m] |
| $H_{s,peak}$ | Significant wave height of the peak storm [m] |
| $H_{s,target}$ | Significant wave height introduced in the flume program [m] |
| $H_T$ | Fixed threshold wave height [m] |
| $K_D$ | Dimensionless stability coefficient [-] |
| $L$ | Wave length [m] |
| $M_{equiv.}$ | Magnitude of the synthetic storm [h x m] |
| $M_{real}$ | Magnitude of the real storm [h x m] |
| $n$ | Number of breakwater layers [-] |
| $N_L$ | Prototype to model scale ratio of length [-] |
| $N_{\rho,stone}$ | Prototype to model scale ratio of stone density [-] |
| $N_{\rho,water}$ | Prototype to model scale ratio of water density [-] |
| $N_o$ | Number of blocks displaced more than one nominal diameter [-] |
| $N_{od}$ | Dimensionless damage parameter [-] |
| $N_s$ | Stability number [-] |
| $N_z$ | Number of waves [-] |
| $P$ | Layer porosity [%] |
| $R_c$ | Breakwater coronation [m] |
| $s_{om}$ | Wave steepness found with the mean wave period [-] |
| $s_p$ | Wave steepness found with the peak wave period [-] |
| $S$ | Damage level [-] |
| $T_m$ | Mean wave period [s] |
| $T_p$ | Peak wave period [s] |
| $T_{p,input}$ | Peak wave period introduced in the flume program [s] |

| | |
|---|---|
| $T_R$ | Return period [year] |
| $w_r$ | Unite weight for the armour unit [kg/m$^3$] |
| $W$ | Single stone weight [kg] |
| $W_{50}$ | Median of the mass distribution curve [kg] |
| $\alpha$ | Energy scale parameter in JONSWAP spectrum [-] |
| $\gamma$ | Peak enhancement factor in JONSWAP spectrum [-] |
| $\gamma_s$ | Specific weight of the stone [N/m$^3$] |
| $\gamma_w$ | Specific weight of the water [N/m$^3$] |
| $\Delta$ | Relative density of the stone. $\Delta = \frac{\rho_{stone} - \rho_{water}}{\rho_{water}}$ [-] |
| $\eta$ | Free surface elevation [m] |
| $\theta$ | Structure slope [º] |
| $\mu_N$ | Mean of a sample [-] |
| $\xi_z$ | Surf similarity parameter [-] |
| $\rho_s$ | Density of the stone [kg/m$^3$] |
| $\rho_w$ | Density of the water [kg/ m$^3$] |
| $\sigma$ | Peak width parameter in JONSWAP spectrum [-] |
| $\sigma_N$ | Standard deviation of a sample [-] |
| $\phi$ | Packing density [-] |
| $\phi_{spm}$ | Packing density as defined in the Shore Protection Manual [-] |
| $\psi^*$ | Narrow bandedness parameter of Bocotti's storm model [-] |

# 1. INTRODUCTION

A rubble mound breakwater is a maritime structure designed to protect a valuable part of the coast. In general, it works by reducing (eliminating) the transmission of the energy of waves in inshore waters providing safe harbourage or reducing coastal erosion. For that purpose, and in order to ensure the breakwater integrity and the infrastructure serviceability by limiting the time of unserviceability, a comprehensive structural design of this structure is required. Attaining to this, the stability of the armour layer plays a crucial role.

Historically, maritime infrastructures as rubble mound breakwaters have been designed using analytical expressions to calculate the stability. These formulations are obtained from test results and are used for a great variability of situations, but not take into consideration all the variables that can affect the stability of the breakwater. These analytical expressions are normally fitted only with few results coming from experiments where the main parameters to be defined (slope of the breakwater, porosity, cross section…) are maintained constant between tests. Then, these formulations are not flexible enough to adapt to geometrical or conceptual differences (addition of a berm, structure toe…) that could report important difference in the results obtained. Therefore, this situation can lead to a design, which in terms of safety and economics is not optimized at all.

The design variables for maritime infrastructures are the significant wave height, the wave period, storm direction and water level. Basing on a treatment of this data, physical model tests either in 2D or in 3D should be carried out in order to verify before the construction the results obtained with the analytical formulations. The experiments aim to solve the shortcomings of the analytical expressions and see if the infrastructure to be constructed must be redesigned or optimized. They can lead to have a global overview of the problem and not only focus on the stability, but also in the risk associated to the possibility to have economical loses. A more reliable and fitted design comprises minor expenses in construction materials, which is an essential factor for the companies englobed in the construction process.

The methodology for the design of a breakwater is a standardized process and starts by knowing the zone where the breakwater is going to be constructed. Depending on the structural characteristics (both physical and economical), the economic impact in case of failure (partial or total) and the possibility of human losses, a return period (associated to the lifetime) will be selected (ROM 02-90). Once it has been selected, the significant wave height associated to this return period ($H_s$=$H_s(T_R)$) can be obtained. In general, the selected return period is larger (or comparable) than the available sea state time series (preferably from a wave buoy) and data extrapolation should be performed. The time series is divided into independent storms ($H_s$>threshold) and the value of $H_s$ associated to the peak of each individual storm is then selected. These values are supposed to follow a probability density function (normally a tri-parametric Weibull). Once the probably density function is fitted with the selected data, and the parameters of the latter are obtained, the $H_s$ associated to the design return period is calculated.

The next step is to correlate the significant wave height with the peak wave period ($T_p$), but the adjustment normally shows a scattered diagram. Empirical formulations exist, as the one proposed in Del Estado, P. (2015), $E(T_p)$=$aH_s{}^c$, that create a relationship between both variables by adjusting them with the least squares method. However, $E(T_p)$ is only an expected or probable value of the peak wave period for a storm characterized with that $H_s$. A constant

wave steepness ($H/L$) can be chosen, considering typical values associated to storm conditions (ranged normally between 0.02 and 0.06). Once a steepness value is selected, the wave conditions composed by the paired data ($H_{s,}T_p$) can be find out.

With this characterization of the wave conditions and knowing the geometry of the structure breakwater, stability can be assessed for the main parts of it (toe, filter, armour layer). Among them, the armour layer is the one having more repercussion when evaluating the damage.

When calculating the armour layer stability of a breakwater with the analytical formulation, essential parameters as $D_{n50}$ and $W_{n50}$ can be obtained for the design (Hudson, 1974 and Van der Meer, 1988b). Depending on the $W_{n50}$, and attaining at the material disposition, it must be decided whether the breakwater is rubble mound or made out with artificial blocks.

Regarding the construction process, the packing density was analysed in many works (Medina *et al.,* 2014*)* and was found to be very important for the stability of a cubic armour breakwater, because a significant increase of porosity (increase of packing density) can lead to a decrease of stability. However, popular equations on breakwater stability (Van der Meer, 1987) only take into consideration a specific value for the porosity (generally 0.4 or 0.6), directly related with this packing density. It was not until later works (Van der Meer, 1999) when he considered the effect of the packing density in a redefined formula.

Frens (2007) also discussed the importance of the placement method in the packing density, which will be a crucial aspect in the damage assessment depending on the operator who constructs the breakwater and carries out the experiment.

Coming back to the necessity to carry out physical models to verify the design of a new or remodelled breakwater, some of them are defined and characterized straight away.

The classical experimental stability test of a breakwater armour layer is the proposed by Owen and Allsop (1984) and is composed of a series of tests with the 60, 80, 100 and 120% (safety factor) of the significant wave height ($H_s$) selected for the design with the associated peak wave period. The suggested number of waves are 3000-5000, a number typically associated with the duration of a storm.

In these recent years, the works of Martín-Hidalgo *et al.* (2014) and Martín Soldevilla *et al.* (2015) have focus on the analytical study of the damage evolution of a cubic armour layer with real and synthetic storms, which are schematic representations of a real storm. These authors have shown that the damage evolution is affected by the storm sequencing in terms of maximum energy flux model (Melby and Kobayashi, 2011). Martín Soldevilla *et al.* (2015) made an exhaustive analysis between all these possible synthetic models in the research. From this comparison, it is suggested that the Equivalent Magnitude Storm model (EMS) is the one that gives the best results regardless of the type of storm. The most appropriate shape to use depends of the storm conditions (sea, swell or a combination of both).

In order to better understand the phenomena and to try to solve shortcomings encountered during the literature review, a series of small-scale experiments have been carried out in the CIEMito flume, which is located in the Maritime Engineering Laboratory (LIM) at the UPC. These experiments performed for this research are conducted in the frame of an European project H2020 (Hydralab+). This Thesis represents a part of all the research that is intended to be done. In fact, this work is a continuation of previous researches done in the CIEMito facility in the last year.

The target of this study is to understand the effects of the storm sequencing on the stability of a two layers cubic block breakwater under the application of a real storm and a trapezoidal storm. By comparing the effects of both storms, it will be seen if this real storm can be synthetized with such synthetic model. With these tests done in laboratory, it is always intended to try to give more reliable results in comparison with the ones obtained with the analytical expressions. Depending on the test results, a redesign or optimization of the breakwater could be considered.

For the assessment of the damage in the armour layer of the breakwater, the damage parameter $N_{od}$ (relative damage) proposed by Van der Meer (1999) has been used. The aim of this research is to compare different physical model test methodologies for the design process of a breakwater armour layer by means of comparing the level of damage caused by the synthetic storm model and the scaled real storm (unsteady phenomena).

In addition, the influence in the final damage of variables as the operator in charge of the breakwater construction and the wave generation seeding will be deeply assessed.

## 1.1. Objectives

The main objectives of this work are:

- Assess the influence of the different tested storm sequences on the stability of a two layers cubic block breakwater by means of damage caused. Have a global overview of the damage caused by the different test methodologies with the parameter $N_{od}$, but focusing on the real and trapezoidal storm.

- Compare damage caused by the real storm and synthetic trapezoidal storm in order to see possible similarities to see if the real storm can be synthetized in the flume with such this trapezoidal model.

- Evaluate how the damage progresses during a sequence of events to know the contribution of each stretch to the final damage.

- Assess the influence of variables as the operator in charge of the breakwater construction and the wave generation seeding in the damage results.

## 1.2. Outline

The Thesis is divided in 6 chapters. In Chapter 2 “Literature review”, is showed a background synthetic storm models, wave spectra and the classical testing method is given. In addition, it is included general information of the analytical expressions that define the breakwater stability and the damage assessment.

The explanation of the methodology is done in the Chapter 3 “Experiments methodology”. This section aims to describe the physical 2D model, including the definition of the breakwater structure and the construction procedure and main properties of the armour layer cubes, the storm data used, the test programs of the different test methodologies studied for this work and the analysis of the data.

The damage results for all the kind of storms are given and analysed in the Chapter 4 “Results”. The results of the real and trapezoidal storm are compared and an assessment of the variables that influence the damage is done.

With the analysis of the results, some conclusions are drawn and different approaches for further investigation are stated in the Chapter 5 “Conclusions and recommendations”.

Finally, the references used for this work and the Annex are exposed.

# 2. LITERATURE REVIEW

## 2.1. Breakwater stability

Breakwater is an important infrastructure in the development and planning of a port, which function is to protect a valuable area, preventing it from wave attack. The relevance of this infrastructure is even better when dealing with large ports, because if vessels or infrastructures located behind the coast are affected during heavy water storms, the economic and environmental consequences are higher. These large ports accommodate tankers, containerships and chemical vessels that have to be always in extreme safety conditions.

The water force produced on the breakwaters is due to wave breaking, reflection, refraction and resulting rip currents. Usually, most of the conventional and low crested breakwaters are composed of armour layers of different units (concrete cubes or rubble mound), a filter layer of different smaller materials which makes the transition from the armour layer to the core, the core and toe protection.

The resulting forces on the breakwater itself affect its stability (including amour, toe and rear side of the breakwater). In order to check the stability of these infrastructures under wave attack, the designed breakwater should be tested in the laboratory before it is constructed following the results of analytical expressions.

The common used physical models, which are escalated representations of prototype elements, are very useful to improve the understanding of the physical processes that occur in the reality and that can be very complex to assess with numerical methods.

### *2.1.1. Notions of breakwater's stability*

Design of breakwaters consists of two main stages, the functional design, which determines the specifications of the breakwater, and the hydraulic or structural design, which deals with the wave attack and the stability of the breakwater when wave forces incise on it.

Structural design generally focuses on larger waves in the wave climate since these waves represent critical conditions, which can endanger the structure stability. The criteria to evaluate structural stability are normally stated in terms of extreme conditions, which are the conditions that a maritime structure must deal with without sustaining significant damage. In general, the critical design conditions are the wave height and water level combinations that result in maximum forces or minimum structural stability.

The structural stability assessment determines the required armour units that must be placed in a breakwater to resist to the selected design wave height and water level conditions. This structural stability can be divided in two types: static and dynamic. For stability tests, the breakwater must be designed to remain statically stable or allow the damage assessment.

The stability of breakwater structure can be influenced by many parameters, including the significant wave height, the armour characteristics (size, shape, method of placing…), crest elevation, slope of the structure, width and permeability. In addition, some dimensionless parameters take part in the stability obtaining, including the stability coefficient and the stability number.

### *2.1.2. Stability of rubble mound breakwaters*

These kind of breakwaters are design to do not receive any damage, or at least less than 5% of structural damage under the design conditions.

The stability formula of Hudson states the following:

$$W = \frac{w_r * H^3}{K_D * (S_r - 1)^3 * cotg\theta} \quad (1)$$

Where $W$ is the weight of the armour unit, $w_r$ is the unit weight of the armour unit, $H$ is the design wave height, $K_D$ a dimensionless stability coefficient, $S_r$ the specific gravity of the armour unit and $\theta$ the angle of the breakwater slope.

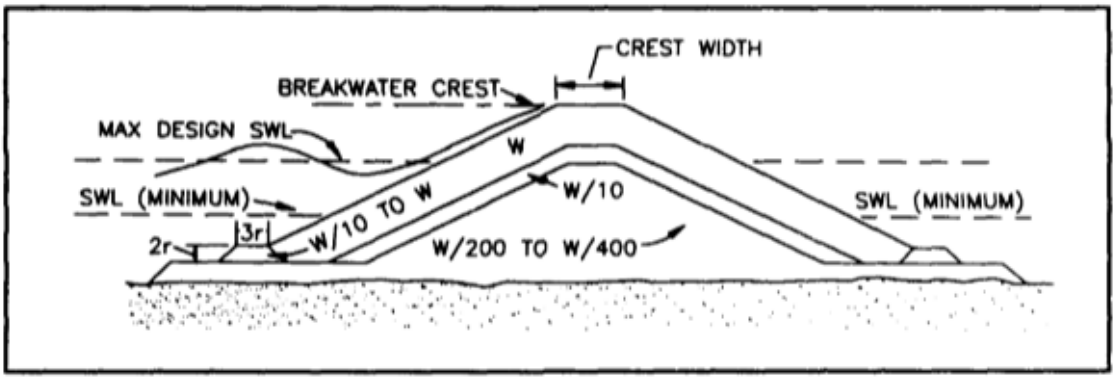


*Figure 1. Cross section for conventional rubble mound breakwater with moderate overtopping (Shore Protection Manual, 1984).*

Although the Hudson formula has been used for many years for the stability assessment, it presents shortcomings as the lack of influence of wave period that have been overcome with additional research. Among them, it can be highlighted the investigation carried out by Van der Meer (1987), who derived in two stability equations, one for breaking waves (plunging) and one for non-breaking waves (surging).

*Breaking waves (Plunging)*

$$\frac{H_s}{\Delta * D_{n50}} = 6.2 * P^{0.18} * \left(\frac{S}{\sqrt{N}}\right)^{0.2} * (\xi_z)^{-0.5} \quad (2)$$

*Non-breaking waves (Surging)*

$$\frac{H_s}{\Delta * D_{n50}} = 1.0 * P^{-0.13} * \left(\frac{S}{\sqrt{N}}\right)^{0.2} * \sqrt{cotg\ \theta} * (\xi_z)^P \quad (3)$$

Where $\xi_z$ is the surf similarity parameter, also called Irribarren number. Its expression is the following:

$$\xi_z = \frac{\tan\theta}{\sqrt{\frac{2\pi * H_s}{g * T_z^2}}} \quad (4)$$

All the variables that appear in the two stability formulas and in the Irribarren parameter expression are presented below:

$\Delta$ = relative mass density of stone ($\Delta = \frac{\rho_a}{\rho_w}$)
$\rho_a$ and $\rho_w$ = mass densities of armour and water
$D_{n50}$ = nominal diameter of stone ($D_{n50} = \left(\frac{W_{50}}{\rho_a}\right)^{\frac{1}{3}}$)
$W_{50}$ = median of the mass distribution curve
P = permeability coefficient of the structure defined by Van der Meer (Figure 2)
S = damage level ($S = \frac{A_e}{D_{n50}{}^2}$)
$A_e$= eroded cross-sectional area in profile
N = number of waves
$T_z$ = average wave period.

The term on the left side of the breaking waves and non-breaking waves stability formulas presented by Van der Meer (1987) can be named as the stability number $N_s$, whose expression is the following:

$$N_s = \frac{H_s}{\Delta * D_{n50}} \quad (5)$$

In comparison to the Hudson stability expression, the Van der Meer equations include more dependence on important parameters that govern the problem. The dependence with the wave period can be observed with the surf similarity parameter. They are also included the permeability, the storm duration and the damage level of the structure. Although this improvement, the formula is used only for specific values for this variables.

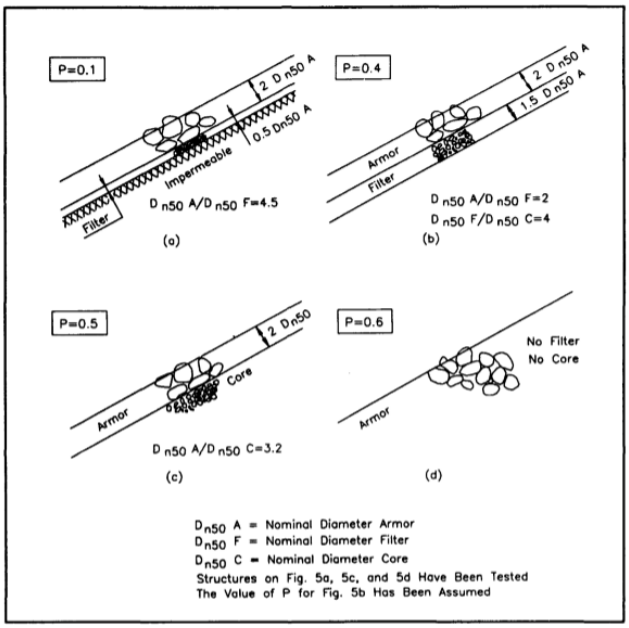


*Figure 2. Permeability coefficient P (Van der Meer, 1987).*

### *2.1.3. Stability of concrete armour layer breakwaters*

The Hudson formula for rubble mound breakwaters gives us different default $K_D$ values for rock. This range of values can be extended for a large number of concrete armour units. The most important $K_D$ values, considering that they are applicable either in breaking and non-breaking waves are the following (Shore Protection Manual, 1984):

- ***Cubes***: 6.5-7.5
- ***Tetrapods***: 7-8
- ***Dolosse***: 15.8-31.8

Extended research by Van der Meer (1988b) on breakwaters with cubic concrete units was based on the variables exposed when evaluating the stability of rubble mound conventional breakwaters. In the work carried out by him, the study was limited only to one cross-section for each armour unit, leading to have no slope angle or permeability variation. Therefore, in the stability formula deducted for breakwaters with concrete cubes in the armour layer there is no presence of these variables.

As the prototype breakwater (Van der Meer) used to construct the model in the flume facilities has a double armour layer made out of concrete cubes, the final stability formula to be used in this Thesis is the one proposed by Van der Meer (1988b) related to cubes, which is shown below:

$$\frac{H_s}{\Delta * D_{n50}} = \left(6.7 * \frac{{N_{od}}^{0.4}}{N^{0.3}} + 1.0\right) * {s_{om}}^{-0.1} \qquad (6)$$

With:
$H_s$= significant wave height
$\Delta$ = submerged density
$D_{n50}$= length of the side of the cube
$N_{od}$= relative damage
$N$ = number of waves
$s_{om}$ = wave steepness associated to the mean wave period.

If no-damage criterion was stablished ($N_{od} = 0$), the equation would be reduced until having the next expression:

$$\frac{H_s}{\Delta * D_{n50}} = 1.0 * {s_{om}}^{-0.1} \qquad (7)$$

Pretending not having damage in a maritime structure that is constantly being attacked by waves is practically impossible. No damage would be a very strict criterion and would lead to armour layers designed with very large concrete units.

The stability equation for concrete cubes decreases with an increasing in the wave steepness. This trend happens also in the plunging area for rubble mound breakwaters.

Some works continued to explore the influence of some other characteristics in the stability of the armour units, a for example the crest height and packing density (Van der Meer, 1998) Regarding the crest height he found out that the stability increases when the crest height

decreases. What respect to the packing density, and after carrying out some experiments, it was deducted that a lower packing density leaded to lower stability. Therefore, this influence could be incorporated by adding a value proportional to the packing density in the total stability equation for tetrapods (not important for the development of this Thesis).

After all this research on the influence of the packing density of tetrapods in the corresponding stability formula, Van der Meer thought that an update of the stability formula ( 6 ) for concrete cubes could also be done. Attaining that, he exposed a new revised formula (Van der Meer, 1999):

$$\frac{H_s}{\Delta * D_{n50}} = \left(6.7 * \frac{{N_{od}}^{0.4}}{N^{0.3}} + 1.0 * (0.4 + 0.61 * \frac{\phi}{\phi_{spm}})\right) * {s_{om}}^{-0.1} * \left(1 + 0.17 * \exp\left(-\frac{0.61 * R_c}{D_n}\right)\right) \quad (8)$$

Where $\phi$ represents the packing density, $\phi_{spm}$ the packing density as it is treated in the Shore Protection Manual (1984) and $R_c$ the crest height.

Although this formula has never been confirmed by investigation, the noticeable aspect is that both the packing density and the number of waves affect directly the result of the stability number. As this stability number must be assessed in the laboratory tests, both the packing density and the number of waves must be well represented in these tests.

Regarding the total number of waves, this is an assumed value when working with the classical method. On the other hand, for the synthetic storm run in the flume (Equivalent Magnitude Storm with trapezium shape in this Thesis), the total duration of it gives us directly the number of waves. This transformation will be seen in the Chapter 3.2.2.

What respects to the packing density, this is a difficult variable to control in the tests. Because of the randomly placing of the cubes in the armour layer, the construction of the breakwater will never be the same between two different tests. Although in every test is tried to have the same density distribution of cubes, the structure packing density of the two armour layers could be different.

### *2.1.4. Packing density*

The packing density is directly related to the porosity, which can be described as the percentage of voids in a granular system. Although the porosity seems to be a clear concept to work with, it must be firstly defined the armour thickness for randomly placed concrete cubes.

This thickness is normally obtained as one or two times the nominal diameter of the cubes, which can be expressed as the cubic root of the cubic amour unit volume for single-layer or double-layer armours ($D_n = (W/\gamma_r)^{1/3}$). The formula proposed by Hudson (1974) of the average thickness of an armour made out of cubes is the following:

$$t = n * k_\Delta * (\frac{\gamma_r}{W})^{\frac{1}{3}} \quad (9)$$

Where $n$ is the number of armour layers, $k_\Delta$ is a layer coefficient, $\gamma_r$ the mass density of the stone and $W$ the mass of a single armour unit.

Once the average thickness is defined, the placing density can be expressed in terms of this average thickness, but also adding the armour porosity (P %). Therefore, this placing density (φ [units/m$^2$]) will be controlled by the placement of the cubes and is directly related to the nominal armour porosity and the layer coefficient, having the next equation:

$$\phi = \frac{N_a}{A} = n * k_\Delta * (1 - P) * (\frac{\gamma_r}{W})^{\frac{2}{3}} \quad (10)$$

Where $N_a$ is the number of armour units placed on a surface $A$.

As this placing density is given in function of the porosity and layer coefficient, different combinations of both values can lead to the same placing densities. Frens (2007) analysed some misinterpretations caused by use of different criteria in some works regarding both parameters. For example, a porosity of 47% with a layer coefficient of 1.10 is equivalent to porosity of 42% with a layer coefficient of 1.00. The Coastal Engineering Manual specifies a layer thickness factor for cubes (modified) of 1.10.

| Armour Unit | n | Placement | Layer Coeff., $k_\Delta$ | Porosity (p') % |
|---|---|---|---|---|
| Quarrystone (rough) | 2 | random | 1.15 | 31 |
| Cube (modified) | 2 | | 1.10 | 47 |
| Tetrapod | 2 | | 1.04 | 50 |
| Quadripod | 2 | | 0.95 | 49 |
| Dolos | 2 | | 1.00 | 63 |
| Quarrystone | graded | random | - | 37 |

*Table 1. Layer coefficient and porosity (%) for different armour units (Coastal Engineering Manual).*

Although the description of the placing density is well known, the variable that will govern the problem and the calculations of the laboratory tests is the packing density ($\phi$). This is also associated to the armour porosity and number of layers, but is written as a dimensionless form of the placing density, using as length unit the equivalent cube size, $D_n$. The expression of this packing density is the one that appears in the Shore Protection Manual (1984).

$$\phi_{spm} = \phi(D_n)^2 = n * k_\Delta * (1 - P) \quad (11)$$

In addition to all this research, Van der Meer (1999) also proposed a very similar formula of the packing density.

$$\frac{N_a}{A} = \frac{\phi}{{D_n}^2} \quad (12)$$

In order to prevent the misunderstandings described by Frens (2007), Medina *et al.* (2011) proposed a criterion for the armour porosity, described as $p = (1 - \phi/n)$, corresponding to a layer coefficient of $k_\Delta = 1$. With this layer coefficient, the average thickness of a two-layer armour is assumed to be equal to 2*$D_n$.

The packing density value proposed by Van der Meer for cubes (1.17) and found in the literature will be the one used as a reference to find the porosity necessary in the construction of the modelled breakwater.

### *2.1.5. Placement method*

The armour layer placement and shape affect the stability of the structures. The impact of armour shape, porosity and placing methods has been examined in different studies, as the one carried out by Pardo *et al.* (2013).

The placement of the concrete cubes to construct the two-layer armour can be irregular or regular. Irregular placement can also be named as randomly placement and consists on depositing the cubes with no pattern or fixed method. An example of breakwater constructed with irregular placement was the one of the Antifer harbour.

*Figure 3. Example of irregular placement.*

In breakwaters in which the construction quality could be difficult to control, or when there is height uncertainty about the wave climate or the instability of the foundation is better to choose an irregular placement method instead of a regular one. For example, when a first layer of a breakwater constructed with a regular method is deformed due to instability, this deformation spreads and affect directly to the second layer. Another advantage of the random placing is that when damage occurs, with only adding more blocks it can be repaired.

From different works found in literature (Pardo*, et al.* 2013) about the random placing, it was generally concluded that it was difficult to obtain the desired porosity. The reason was that the first layer placing conditions the second one. Then, it was proved that it was very important to place the first layer of blocks as irregular as it was possible, avoiding the alignment of consecutive sides and trying to sustain the blocks with their sides instead of with their bottom. If all these considerations were taken into account, the generated second layer would have the searched thickness and irregular surface.

The two-layer armour of the modelled breakwater used in the laboratory tests in this Thesis is constructed with an irregular placing, trying in each construction to maintain a constant porosity with both layers.

## 2.2. Breakwater damage

The assessment of the breakwater damage is vital for the maritime engineering and for the design of the structures that protect the coast from wave storms. In fact, the damage is what defines the design of the breakwater.

Concerning the stability, many works have been developed to know further about this topic, but not too much work has been done to quantify the damage progression of a breakwater, which is crucial to determine the life cycle costs or to prioritize maintenance requirements for various projects.

Traditionally, the breakwaters and other maritime infrastructures have been inspected visually. This visual inspection is done by filling forms, which include a list of possible degradations of the structure and levels to classify its severity. Nowadays, new methodologies are growing up, trying to monitor all the damage assessment process.

### *2.2.1. Levels of damage*

For visual assessment of the damage degree for conventional breakwaters in physical modelling studies, the damage is categorized qualitatively in four armour-damage levels, according to the work of Losada*, et al.* (1986)*:*

1. ***Nd***: no damage (may be one or two loose units start rotating)
2. ***ID***: initiation of damage (a few units start to move in the upper armour layer)
3. ***IR***: Iribarren damage (big holes in the outer armour layer, but the filter layer is not visible)
4. ***D***: destruction (filter layer is exposed to direct wave attack and several units have been removed from this filter layer).

### *2.2.2. Damage assessment*

The damage of concrete blocks in an armour layer of a breakwater has been conventionally expressed by $D(\%)$, percentage of the number of damaged blocks against the total number of blocks, or preferably, to the number of units within a specific zone around still water level (SWL).

The expression of the damage, given as the relative displacement, which determines it for the whole breakwater is:

$$D = \frac{number\ of\ damaged\ blocks}{total\ number\ of\ blocks} \qquad (13)$$

However, a new equation proposed by Van der Meer proved to be easier to use. This equation permit to obtain the dimensionless damage parameter ($N_{od}$) for the concrete block armour units, which is the same that appears in the right side of the stability formula proposed by Van der Meer (1988b).

$$N_{od} = \frac{N_o * D_{n50}}{b} \qquad (14)$$

Where $N_o$ is the total number of moved units out of their place and $b$ is the width of breakwater section that is considered.

Van der Meer (Van der Meer, 1999) defines the relative damage $N_{od}$ as the actual number of units displaced a distance higher than one $D_{n50}$ ($N_o$) related to a width (along the longitudinal axis of the structure).

According to the Shore Protection Manual (1984) and Van der Meer, the start of the damage occurs for $N_{od}$ values around 0.5, while failure of the structure occurs with $N_{od}$ of more than 2 for the multi-layer elements with side slope of 1:1.5.

This damage parameter $N_{od}$ can also be referred as a percentage of the damage. If the total number of armour units that are deposited in a row with a length of one $D_{n50}$ (the width is always $b$) are known, the percentage of damage is found by making the ratio between $N_{od}$ and the number of armour units. Therefore, if the cross-sections were different, different percentages of damage will result with a similar level of damage ($N_{od}$).

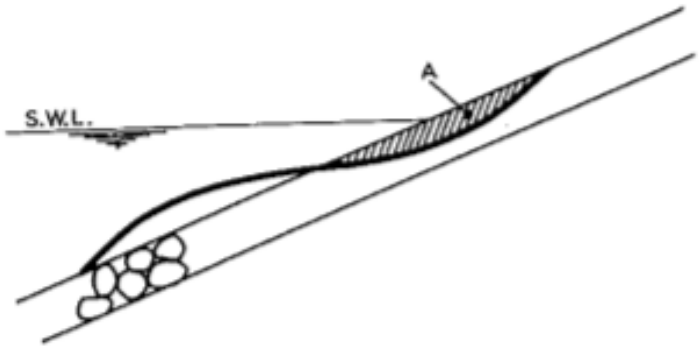


*Figure 4. Typical damage profile of a rubble mound breakwater (Van der Meer, 1987).*

Damage can also be defined according to Van der Meer (1987) with the damage parameter S as it follows:

$$S = \frac{A_e}{\left[\frac{M_{50}}{\rho_a}\right]^{\frac{2}{3}}} = \frac{A_e}{{D_{n50}}^2} \qquad (15)$$

Where $A_e$ is the cross-sectional eroded area, $D_{n50}$ is the nominal diameter of the stone, that in case of cubes is equal to the length of the side and $S$ is a dimensionless parameter, which characterises the damage in the breakwater.

Unlike the parameter $N_{od}$, this new damage parameter $S$ is normally used for rock-armoured breakwaters. This value is independent of the size (slope angle and height) of the structure, which results as an advantage to use this definition of damage, and takes only into account the vertical settlements that occur in the armour layers after receiving a wave attack.

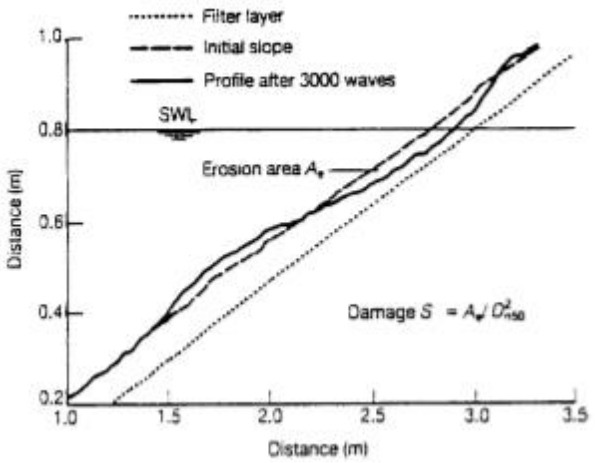


*Figure 5. Damage S based on erosion area $A_e$ (Van der Meer, 1998).*

A physical description of $S$ is the number of cubic stones with a side of $D_{n50}$, eroded within a width of one $D_{n50}$. In general terms, the "no-damage" criterion of Hudson advanced in the Chapter 2.4 is normally taken when the value of $S$ is between 1 and 3, which is related to a 0-5% of damage. Concerning the failure, this is defined as exposure of the filter layer and for $S$ values higher than 15-20, the deformation of the structure results in an S-shaped profile.

Van der Meer (1992) presented examples of damage parameter $S$ for a two-diameter thick armour layer and for different damage stages.

| slope | initial damage | intermediate damage | failure (under layer visible) |
|---|---|---|---|
| 1:1.5 | 2 | 3-5 | 8 |
| 1:2 | 2 | 4-6 | 8 |
| 1:3 | 2 | 6-9 | 12 |
| 1:4 | 3 | 8-12 | 17 |
| 1:6 | 3 | 8-12 | 17 |

*Table 2. Design values of S for a two-diameter thick armour layer (Van der Meer, 1992).*

The definition of $N_{od}$ and $S$ are comparable, although the second one includes displacement and vertical settlement, but does not consider the porosity of the armour. Generally, the value of the $S$ is twice the value of $N_{od}$ (Van der Meer, 1999).

Some investigations have focused on coupling these two parameters, highlighting the relationship established in the Coastal Engineering Manual:

$$N_{od} = G * (1 - P) * S \qquad (16)$$

Where G is a grading coefficient ($G = D_{n85}/D_{n15}$) and $P$ is the porosity of the breakwater armour layer.

The porosity is considered in arrange between 0.4 and 0.6 and the G coefficient in a concrete armour is equal to 1 (U. S. A. C. O., 2011). The Coastal Engineering Manual suggests using an approximation of $S$=1.4*$N_{od}$, although some tests have proved that this 1.4 can be higher.

## 2.3. Synthetic storm models

### *2.3.1. Storm evolution*

The evolution of a storm is essential for the assessment of the damage progression in maritime structures. These structures, as rubble mound breakwaters, can face heavy storms and the knowledge of its possible failures can lead to a better approach of its future maintenance or the redesign of the sizing dimensions if it is needed.

The lifetime of a maritime structure is established with a return period ($T_R$), which is always related with the extreme actions generated by waves during storms with a high energy associated. Due to the irregularity of the waves during a storm, it is required a statistical characterization to define the main variables taken into account to define it. Traditionally the storms are characterized mainly by the significant wave ($H_s$), the mean period ($T_m$) and the duration of it ($D$), but the dependency between these variables it is not in the most of the cases taken into account. Consequently, as a concrete relationship is not established, the risk associated to the maritime structures security remain unknown.

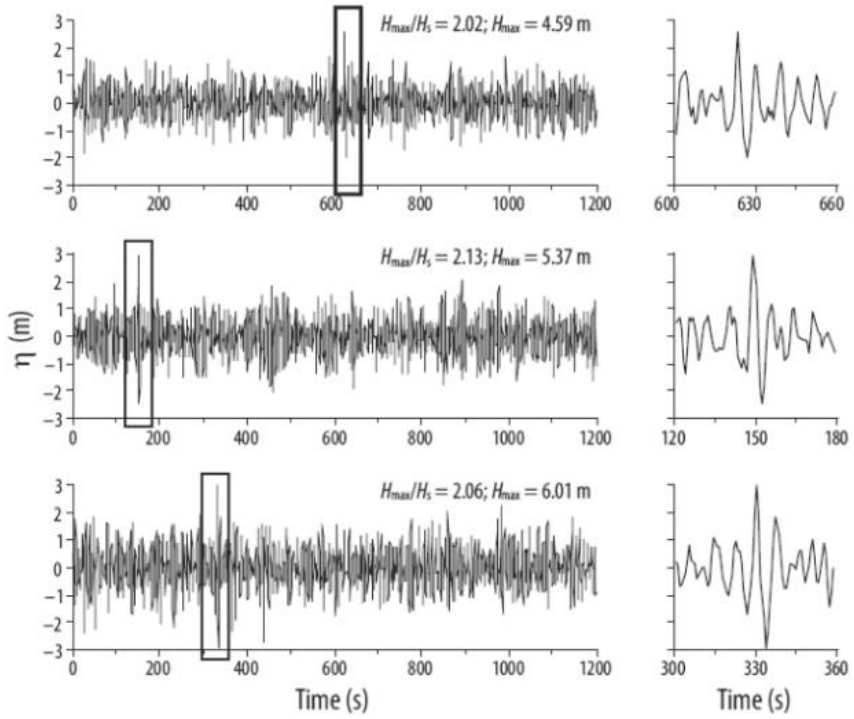


*Figure 6. Examples of wave height evolution with extreme regime. $H_{max}$, $H_s$ and η (Sulisz et al., 2016).*

In order to deal with this disconnection between the representative variables, some works in the coastal engineering ambit (Soares and Scotto, 2001), deal with this problem using the copula functions. These copula functions can be used to achieve a direct relationship between $H_s$-$T_m$ but also to reflect the dependency between the wave height and the duration or with the significant wave height ($H_s$), the duration ($D$) and the sea level.

These works mentioned have helped a lot in the development of the multivariate statistical characterisation. Although they focus on a useful approach to the variables determination, they do not try to characterize the storm history, which is fundamental, as it has been commented, to assess the damage progression in maritime structures.

To face this shortcoming, different models have been used to incorporate the storm history. The description of them, including the advantages and the drawbacks of each of them, can be seen in the works of Martín-Hidalgo *et al.* (2014) and Martín-Soldevilla *et al.* (2015).

### *2.3.2. Types of models*

In the last years, many multivariate storm models have been used to reproduce a real storm. The goodness of each method is given by the damage progression that they produce in the maritime structures. The similar the damage caused with respect the produced by the real storm, the better will behave the model.

The synthetic storm models are models that describe theoretically a storm based on the real characteristics of it. The parameters known of the real storm are:

- ***Significant wave height at the peak of the storm ($H_{s,peak}$)***
- ***Storm magnitude***, which is the surface area under the storm profile above the chosen threshold of wave height ($M_{real}$)
- ***Storm duration ($D_{real}$)***
- ***Number of waves of a storm ($N_z$)***→ normally the synthetic storm models work with the duration or with the number of waves
- ***Storm shape***

The different approaches that have taken into account the storm history characterization are developed in the next lines.

#### Equivalent triangular storm (ETS)

This model was firstly elaborated by Boccotti (2000), who adopted a triangular shape to reproduce the variation of the wave height ($H_s$) during the time and predict the return period of extreme rain events. It was the first model that tried to represent the storm evolution.

In this model, the height of the triangle, called "a", is imposed to be equal to the significant wave height registered at the peak storm ($H_{s,peak}$). The other main dimension of the created triangle, the base "b", representing the duration of the equivalent triangular storm, has a value such that the maxim expected wave height of the triangular storm is the same as the maximum expected wave height of the real storm. This maximum expected wave height can be obtained from different formulas, including the one considered in the work of Boccoti (2000), which is determined as it follows:

$$H_{max} = \int_0^{\infty} 1 - exp\left\{\int_0^{Dreal} \frac{1}{T_m|h(t)|} * ln|1 - P(H: H_s - h(t))|dt\right\} dH \qquad (17)$$

Where $Dreal$ is the real storm duration, $h(t)$ is the significant wave height evolution during the storm, $T_m$ is the mean period, and $P(H: H_s - h(t))$, the probability of the wave height calculated with the expression proposed by Bocotti (2000):

$$P(H: H_s - h) - exp\left[-\frac{4H^2}{H_s^2(1+\psi^*)}\right] \qquad (18)$$

Where $\psi^*$ is the defined narrow bandedness parameter that, for typical wind waves, normal values could be those between 0.65 and 0.75. On the other hand, and when we are dealing with swell waves, these values are normally below 0.60. Although this range of values are the

proposed in this work (Bocotti, 2000), other different values for this parameter are proposed by different works, where is stablished a more selective classification in order to differentiate $\psi^*$ values for different kind of sea states.

The narrow bandedness parameter proposed by Bocotti and the expression to calculate the mean period ($T_m$) that appears in the work of Rice in 1945 must be considered. With them, and starting from an initial base, "b1"; some iterations will must be done until the maximum expected wave height for the ETS model corresponds to the maximum wave height of the real storm.

The expressions ( 19 ) and ( 20 ) of the mean period ($T_m$) and the maximum wave height with the ETS model using the known parameters are stated below:

$$T_m = 6.6 * \pi * \sqrt{\frac{H_s}{4g}} \qquad (19)$$

$$H_{max} = \int_0^{\infty} 1 - exp\left\{\frac{b}{a}\int_0^{a} \frac{1}{T_m|h(t)|} * ln|1 - P(H{:}\, H_s - h(t))|dh\right\} dH \qquad (20)$$

Once are known the main dimensions of the triangular storm model ("a" and "b") it is important to know the part of the storm that is going to produce more damage to our structure. For this reason, a reference threshold of the wave height is fixed and the different states of $H_s$ above this limit conform the equivalent sea. Therefore, the equivalent sea is defined by the equivalent wave height ($H_{equiv.}$), which is the difference between the significant wave height at the storm peak ($H_{s,peak}$) and the storm condition ($H_T$) defined with the threshold, and the time $D_{ETS}$ during which the modelled storm with the triangular shape remains above this threshold.

All these mentioned concepts and ETS model parameters are represented in the next image:

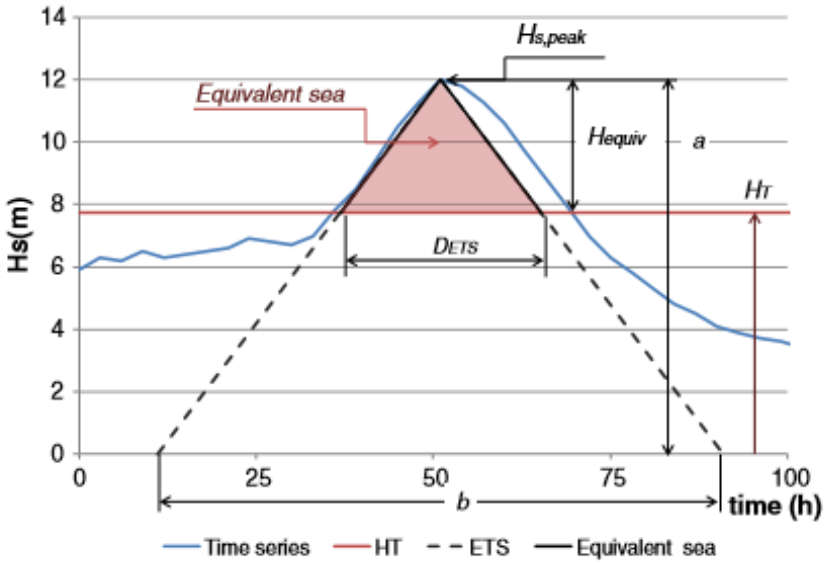


*Figure 7. ETS model parameters and example of modelling (Martín-Hidalgo et al., 2014).*

Using as a base this model, some authors have investigated other forms to represent the real storms by making use of different concepts. This triangular storm model can be extended and

generalized to include other plausible realistic descriptions of the temporal history of significant wave heights.

### Equivalent triangle duration storm (ETDS)

This model, used by Corbella and Strech (2012), considers a triangular shape of equivalent height ($H_{equiv.}$) and base $D$, which is assumed to be the duration associated to the time the real storm is above the wave height threshold limit, also known as $H_T$.

The next figure shows an overview of the model parameters.

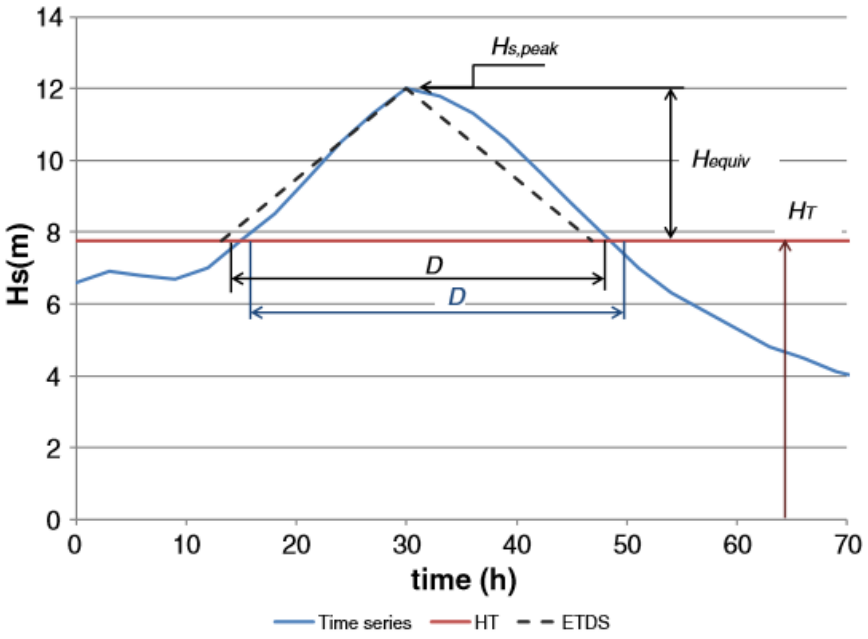


*Figure 8. ETDS model parameters and example of modelling (Martín-Hidalgo et al., 2014).*

It can be observed that the $H_{s,peak}$ of the modelled storm coincides with the one from the real storm. When considering the threshold, this wave height peak is reduced, being for the calculations $H_{equiv.}$. As the triangle shape adopted for the synthetic storm must be symmetric respect a vertical axis which includes the $H_{s,peak}$, and focusing on this specific case, the duration of this synthetic storm is a little bit displaced when comparing with the real one.

### Equivalent Triangle Magnitude Storm (ETMS)

Another model that adopts the triangular shape to represent the real storm is the proposed and firstly introduced by De Michele *et al.* (2007). The height of the triangle is considered to be equal to the equivalent height of the real storm ($H_{equiv.}$), which is the significant wave height peak considering as reference 0 the threshold. What respect to the base of the triangle, which represents the synthetic storm duration ($D_{equiv.}$), is established such that the magnitude of the synthetic storm (area below the synthetic storm history and above the wave height threshold $H_T$) is the same that the one of the real storm.

This called magnitude refers to the energy associated to the storm, when wave heights and higher than the imposed threshold. In order to find the duration of the synthetic storm, the triangle area must be equal than the one of the real storm.

The next figure shows an overview of the model parameters.

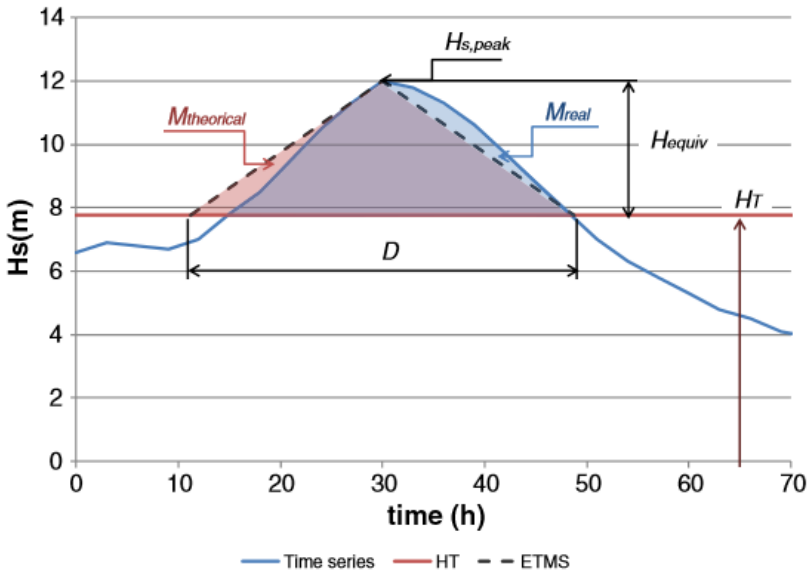


*Figure 9. ETMS model parameters and example of modelling (Martín-Hidalgo et al., 2014).*

### Equivalent Triangle Number of Waves Storm (ETNWS)

The last modelled approach to the real storm that uses as a shape the triangle, considers that the synthetic triangular storm is defined with a height equal to the equivalent wave height, $H_{equiv.}$, and with a base constructed in terms of the real storm number of waves, $N_z$.

This method it is based in the same principle as the Equivalent Triangle Duration Storm (ETDS), but with the difference that in this case, the duration of the synthetic storm is defined with the total number of waves that are above the threshold wave height ($H_T$).

The next figure shows an overview of the model parameters.

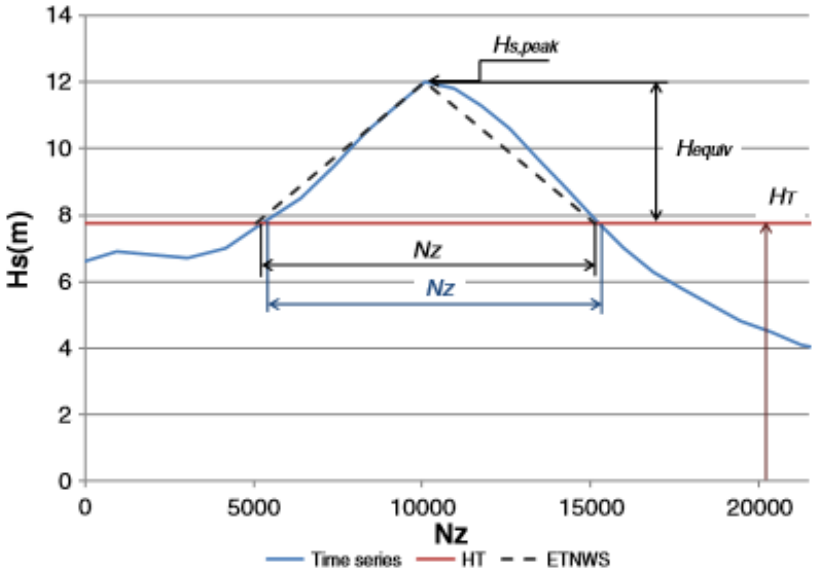


*Figure 10. ETNWS model parameters and example of modelling (Martín-Hidalgo et al., 2014).*

### *2.3.3. Model shapes*

Although the models analysed previously are all made out with a triangle shape, also another more recent shape is beginning to be used and is gaining strength, the trapezium.

#### Triangle

It is the most common shape to construct the synthetic storm. Is the shape used by the ETS, ETDS, ETMS and ETNWS models. The maximum significant wave height of the real storm is assumed to be at the midpoint of the modelled storm history. In other words, the triangle will be always symmetric with a vertical axis that cross the wave height peak of the storm.

#### Trapezium

The trapezium form is normally used to work with the Equivalent Magnitude Storm model (EMS) seen also with the triangular shape. To define the trapezium shape, the real storm (or the storms if the work englobes more than one) is transformed with an escalation, obtaining with this a pattern for the evolution of the storm.

This escalation process involves dividing all the equivalent significant wave heights available of the real storm analysed ($H_{equiv.}$) by the equivalent significant wave height of the storm peak ($H_{eq.,peak}$). Moreover, the corresponding time of the data available is divided by the total duration of the real storm. With these operations, the obtained storm is characterized by a significant wave height at the storm peak equal to 1 m and an equivalent total duration of 1h, which can be expressed in terms of number of waves, having $N_{z,St} = 10^4$. Therefore, this new escalated storm is constructed with normalized equivalent wave heights and durations going from 0 to 1.

The transformation scheme, done for 3 different storms in the work of Martín Soldevilla *et al.* (2015), is shown in the next figure:

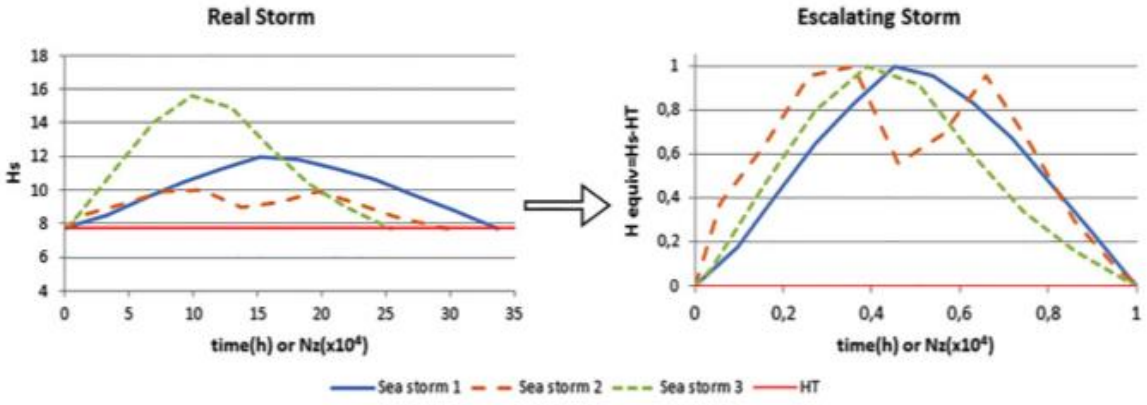


*Figure 11. Storm transformation (Martín Soldevilla et al., 2015).*

The area below the real storm, $M_{Real,St.}$, represents the energy associated to it and is considered to set the equivalent trapezium pattern (parallel bases). Once the escalated storm is obtained, the area below the storm evolution ($M_{Escalated,St.}$) can be calculated. In addition, the height and the longest base of the trapezium are known values equal to 1. Therefore, the unknown smallest base of the trapezium can be obtained by making use of the trapezium area equation:

$$M_{Escalated,St.} = (1/2) * (b_L + b_S) * h \qquad (21)$$

Finally, the duration of the EMS model will be obtained with the trapezium formula, but now from the real storm.

$$M_{Real,St.} = (1/2) * (1 + b) * H_{equiv.} * D_{trapezium} \quad (22)$$

### *2.3.4. Comparison of the models*

The conclusions on which methods fit better when dealing with specific sea states have been extracted from the analytical study done by Martín Soldevilla *et al.* (2015) and with the support of the work of Martín-Hidalgo *et al.* (2014).

In general, the Equivalent Magnitude Storm model (EMS) gives us the best results when comparing with the real storm. It behaves well regardless of the kind of storm we are dealing with (predominant sea, swell or both). On the other hand, the Equivalent Duration Storm model (EDS) and the Equivalent Number of Waves Storm model (ENWS), which are based on the same principle, also give use interesting results, but they tend to underestimate or overestimate the damage, depending on the characteristics of the storms.

The performance of every synthetic model is subject to the kind of sea typical of the zone. The influence of sea and swell wave components in the region is determinant to decide which model can approximate in a more accurate way the real conditions. After trying with all the different models and possible shapes, the results noticed that the triangle works better for preponderant wind-sea storms, while the trapezium shape is more representative of places where the storm conditions are more developed. If a triangular shape were used in such conditions, it would probably be underestimating the damage produced by the waves.

Regarding the damage, the trapezium shape will lead to an overestimation of the damage in all kind of storms, because the storm peak is maintained during few hours, while in the reality, although two similar storm peaks can exist, the storm power is not always the maximum between them.

In summary, all the results of the analysis done by Martín Soldevilla *et al.* (2015) are presented in the next table, offering a visual recognition of all the parameters to take into account when trying to decide which method and shape could work better. The study has focused on storm data of the SIMAR-1042072 and SIMAR-2083039 points, corresponding to developed sea states and preponderant wind-sea storms respectively.

| Model | Shape | SIMAR-1042072 | | | | | | SIMAR-2083039 | | | | | |
|---|---|---|---|---|---|---|---|---|---|---|---|---|---|
| | | Damage | | | Overtopping | | | Damage | | | Overtopping | | |
| | | R2 | MSE | MSE 3rd_OS | R2 | MSE | MSE 3rd_OS | R2 | MSE | MSE 3rd_OS | R2 | MSE | MSE 3rd_OS |
| EDS | Isosceles trian. | 0.941 | 0.100 | 0.510 | 0.910 | 864 | 2313 | 0.966 | 0.052 | 0.159 | 0.954 | 673 | 932 |
| | Scalene trian. | 0.941 | 0.100 | 0.512 | 0.910 | 864 | 2308 | 0.966 | 0.052 | 0.160 | 0.954 | 673 | 935 |
| | Parabola | 0.929 | 0.245 | 4.989 | 0.888 | 2637 | 46,176 | 0.888 | 0.359 | 6.275 | 0.865 | 4161 | 39,128 |
| | Trapezium | 0.925 | 0.259 | 5.821 | 0.902 | 2139 | 40,107 | 0.920 | 0.222 | 3.413 | 0.914 | 2099 | 11,557 |
| | Trapezoid | 0.977 | 0.054 | 0.296 | 0.957 | 635 | 3644 | 0.969 | 0.063 | 0.469 | 0.945 | 1111 | 3667 |
| EMS | Isosceles trian. | 0.984 | 0.029 | 0.384 | 0.990 | 118 | 1240 | 0.992 | 0.012 | 0.093 | 0.997 | 51 | 144 |
| | Scalene trian. | 0.984 | 0.029 | 0.385 | 0.990 | 118 | 1236 | 0.992 | 0.012 | 0.094 | 0.997 | 51 | 144 |
| | Parabola | 0.980 | 0.053 | 0.959 | 0.986 | 221 | 2963 | 0.962 | 0.091 | 2.054 | 0.993 | 129 | 2242 |
| | Trapezium | 0.960 | 0.120 | 2.582 | 0.968 | 561 | 9341 | 0.956 | 0.106 | 1.811 | 0.982 | 337 | 1614 |
| | Trapezoid | 0.992 | 0.017 | 0.030 | 0.993 | 101 | 89 | 0.993 | 0.013 | 0.177 | 0.996 | 64 | 557 |
| ENWS | Isosceles trian. | 0.945 | 0.102 | 0.176 | 0.926 | 789 | 410 | 0.966 | 0.061 | 0.268 | 0.953 | 800 | 1767 |
| | Scalene trian. | 0.946 | 0.101 | 0.175 | 0.926 | 789 | 410 | 0.965 | 0.061 | 0.269 | 0.953 | 800 | 1767 |
| | Parabola | 0.902 | 0.379 | 8.478 | 0.845 | 4343 | 89,908 | 0.848 | 0.577 | 11.501 | 0.806 | 7520 | 100,512 |
| | Trapezium | 0.920 | 0.288 | 6.867 | 0.892 | 2507 | 54,366 | 0.906 | 0.285 | 5.789 | 0.896 | 2846 | 33,922 |
| | Trapezoid | 0.968 | 0.082 | 0.968 | 0.949 | 836 | 11,742 | 0.955 | 0.101 | 1.405 | 0.928 | 1665 | 16,145 |

*Figure 12. Summary of parameters for the different approaches considered in the study of Martín Soldevilla et al., 2015).*

The other interest point in this study is the final damage in the maritime structures generated by the synthetic storm models in comparison with the real storms. The results of damage progression are also discretized depending on the shape used to construct the synthetic model.

In the next figures it can be seen the evolution of the significant wave height and the damage evolution caused by real and synthetic storm models.

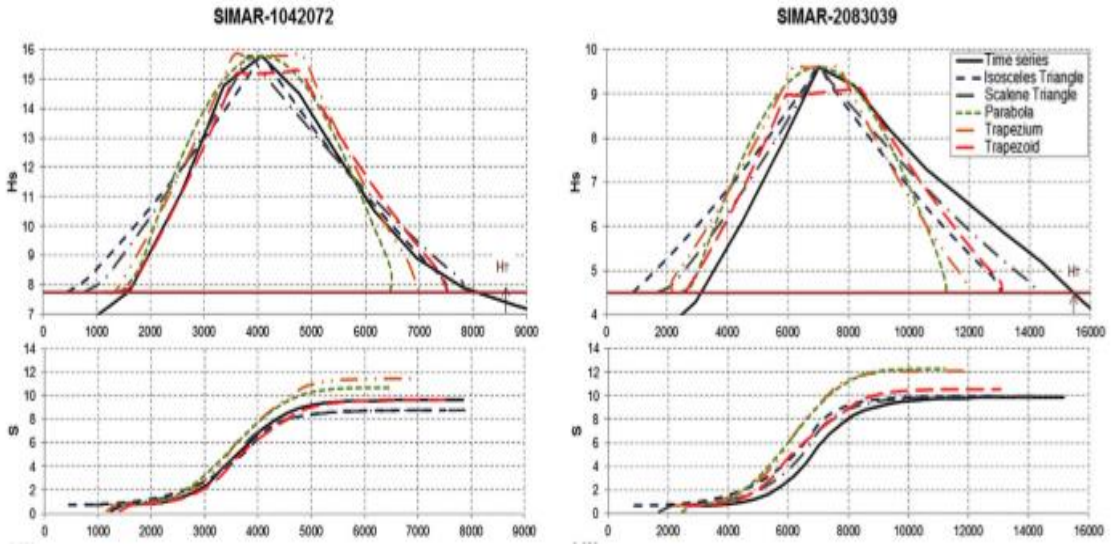


*Figure 13. Damage evolution caused by real and synthetic storm models, SIMAR-1042072 and SIMAR-2083039 (Martín Soldevilla et al., 2015).*

As it can be observed, the synthetic model using trapezium shape is the one that gives as more overestimated results, leading to a greater evolution of the damage in the structure analysed.

### *2.3.5. Proposed model*

This equivalent magnitude storm model (EMS) will be the one used in the Thesis to create a schematization of a real storm and be able to apply it in the flume facility. The shape used to define the synthetic storm will be the trapezium one.

This storm model is based on the energy generated within the storm evolution, called magnitude of the storm. Regarding the shape, it has been seen that a trapezium could fit and approximate

the storm evolution better than the triangle shape. As the storm analysed, developed in the Chapter 3.2.1, has two similar peaks in terms of wave height, the small base of the trapezium can adapt better the real changing of the storm conditions.

This model will be constructed with a trapezium shape drawn above a certain threshold, which will be the minimum wave height from which the storm is considered. The peak wave height of the storm will represent the top of the trapezium. This top is not only achieved in a singular moment, so this equivalent height will be maintained during the time of trapezium small base ($b_S$). The long base ($b_L$) of the trapezium represents the synthetic storm duration ($D_{equiv.}$). Both the $H_{equiv.}$ and the $D_{equiv.}$ are chosen in such a way that the magnitude of the synthetic storm is equal to the magnitude of the real storm.

In this synthetic model, the top small base of the trapezium is located in the middle of the total duration, which means that the figure is symmetric, so the increasing branch in terms of wave height of the trapezium will have the same slope but with opposite sign that the decreasing branch after the peak.

## 2.4. Classical testing method

A breakwater is always designed for a specific wave condition. This wave condition does not occur punctually, but it represents the peak situation in the gradual built-up and decay of the design storm.

Different methodologies are found in literature when trying to test a specific breakwater in the laboratory. The most implemented and used is the classical testing method, which tries to test a breakwater with wave conditions of increasing severity.

When it is required to know the response of a breakwater to the wave attack, the initial wave heights introduced in the test program before it is run should be about 50% of the wave height for which the breakwater has been designed. Then, this wave height tested should be increased gradually until it is achieved the designed wave height. If after arriving to this value the breakwater stills more less intact and seems stable, this wave height should be incremented until a value 20% higher than the one of the desired design. This process tries to see the response of the breakwater with more damage than the real one in order to do not construct overdesigned armour layers (Owen and Allsop, 1984).

With this premise, the classical testing methodology tests a breakwater with a range of wave heights from 50% of the designed wave condition (equal to the peak of the storm) and 120% of it. Generally, the first tested wave height is about 60% of the significant wave height of the design. After running the test with this value, this wave height is increased in steps of 20%, having tests with 80%, 100% and finally 120% of the designed wave condition.

The duration of each test, represented with the total number of waves, will depend on the information available of the storm. Typical values used for the total number of waves are ranged between 1000 and 5000, being 3000 waves the number of waves used nowadays in the main laboratories dealing with this topic.

Finally, some advantages of using this method can be highlighted. The way of testing the breakwater, with increasing wave heights rather than a start near to the design wave condition, can tell us which is the wave height at failure when having an under designed breakwater. Therefore, the breakwater can be redesigned. In addition, this way of testing represents a better

approximation to the reality, where the infrastructure always receives lower wave heights, which tend to settle down the breakwater increasing its stability, before the peak storm comes.

## 2.5. Wave spectra

The evolution of the free surface level of the water with the time is unique in each storm. The waves developed on a sea are not simple sinusoids and the water surface then, is composed of multiple random waves of different lengths and periods. Due to this phenomenon, the water surface level cannot be easily described. However, there are simplifications that try to describe this evolution with only few parameters.

These simplifications are based on the concept of the spectrum of ocean waves. The random alternation of waves during a storm can be expressed in a spectrum that gives the distribution of wave energy among different wave frequencies of wavelengths.

This concept of the spectrum was a conclusive result of the work of Fourier, who presented the Fast Fourier Transform (FFT). He showed that almost any function could be reproduced as the sum of an infinite series of sinusoidal functions with harmonic wave frequencies. Applying these ideas to the sea surface, any storm with irregular waves can be described by a linear super-position of real, regular sinusoidal waves with different wavelengths, frequencies and phases.

Once we have defined the individual sinusoidal functions, each of them can be characterized with a value of the amplitude and period (frequency). These paired values of all the functions are represented in a plane to create the spectrum of the wave-height, which gives the distribution of the variance on sea-surface height (amplitude of the waves or the height the sea surface would have with no waves) as a function of frequency or period.

The sea state of a specific place will determine the kind of spectrum that is chosen to represent it. As the work in this Thesis is done with a non-fully developed sea, the JONSWAP wave spectrum will be used. This is based on the Pierson-Moskowitz spectrum, which was proposed by Pierson and Moskowitz (1964). This assumed that the waves would become into an equilibrium with the wind if it blew steadily for a long time over a large area (fully developed sea concept).

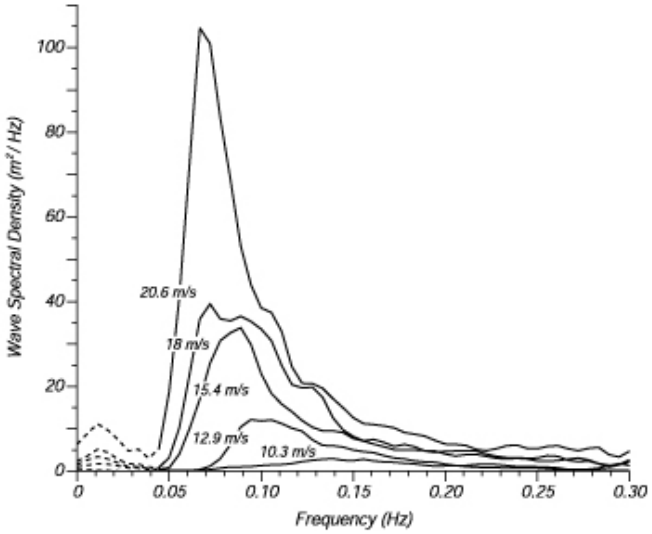


*Figure 14. Wave spectra of a fully developed sea for different wind speeds according to Pierson and Moskowitz, 1964.*

To obtain of the one observed in the Figure 14, measurements of waves made by accelerometers on British weather ships were used. The wave spectral density was calculated for various wind speeds, leading to have different wave spectres.

$$S(w) = \frac{\alpha * g^2}{w^5} \exp(-\beta * \left(\frac{w_p}{w}\right)^4) \quad (23)$$

Where $w = 2\pi f$; $f$ is the frequency; $\alpha$ and $\beta$ two dimensionless parameters equal to 0.0081 and 0.74 respectively; $w_p = \frac{g}{U_{19.5}}$ the peak wave frequency and $U_{19.5}$ the speed of the wind at 19.5 m above the sea surface.

Hasselmann (1973) created the JONSWAP spectrum taken as a base the previous wave spectrum. He found out that the wave spectrum is never fully developed, continuing to develop through non-linear wave-wave interactions even for long time and distances. To improve the results of Pierson-Moskowitz he added a factor, resulting in an extra peak factor $\gamma^r$.

$$S(w) = \frac{\alpha * g^2}{w^5} \exp\left[-\frac{5}{4} * \left(\frac{w_p}{w}\right)^4\right] * \gamma^r \quad (24)$$

Where $r = exp\left[-\frac{(w-w_p)^2}{2\sigma^2 {w_p}^2}\right]$

With the data collected during the JONSWAP experiment, the values of the parameters were calculated:

$$\alpha = 0.076 * \left(\frac{U_{10}^2}{Fg}\right)^{0.22} \quad (25)$$

$$w_p = 22 * \left(\frac{g^2}{U_{10}F}\right)^{1/3} \quad (26)$$

$$\sigma = \begin{cases} 0.07 & w \leq w_p \\ 0.09 & w > w_p \end{cases} \quad (27)$$

$$\gamma^r = 3.3$$

Where $F$ is the distance from lee shore, called fletch, or the distance over which the wind blows with constant velocity. For the values of the peak enhancement factor $\gamma^r$ there are other more complex approaches to get it, but 3.3 seems to be generalized.

In general terms, the JONSWAP spectrum is similar to the Pierson-Moskowitz one, with the exception that waves continues to grow with distance and the peak in the spectrum is more pronounced. A visual comparison between both can be observed in the Figure 15.

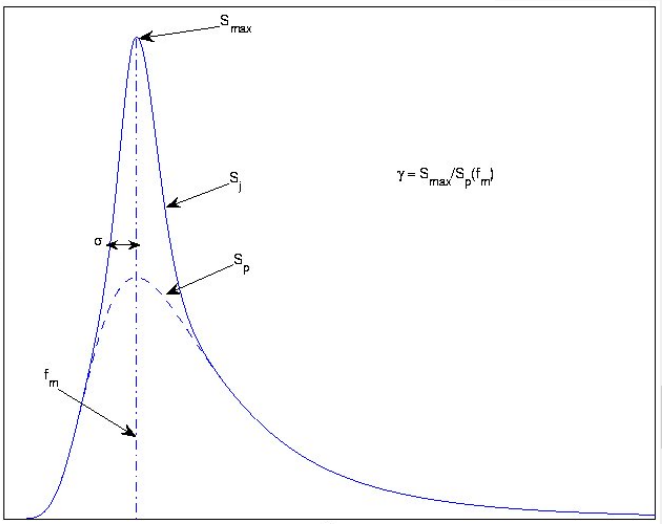


*Figure 15. JONSWAP and Pierson-Moskowitz spectra.*

The significant wave height, which is the main parameter to define the storms in this work, is calculated from the integral of $S(w)$.

## 2.6. Significant wave height and period dependency

The main parameters to define a synthetic storm are the total duration and the significant wave height. Each point of the real storm history is always represented with the significant wave height and a peak wave period related to this wave height. When constructing the synthetic storm model, the oscillating profile of the real storm must be transformed in a profile constructed with steps defined with the paired data $H_s$, $T_p$.

The problem comes when trying to know the wave period of the different steps of the synthetic model. Although the significant wave height is available from the synthetic storm profile, the wave period has to be determined. The correlation between both parameters is not direct and easy to obtain, because there only exist empirical formulation. This is an important shortcoming when trying to analyse the damage progression of a maritime structure, because both the wave height and the wave period determine the total energy flux that impact the structure during its lifetime.

In order to avoid this limitation, some studies have been carried out to try to get a general correlation between both parameters that could be used in specific cases. In the work of Martín-Hidalgo *et al.* (2014) three different approaches are presented to analyse this effect, trying to get always the mean wave period ($T_m$).

Although these approaches are useful to get the desired value, the dependency of the wave height and wave period used in this Thesis is based on the assumption that the wave steepness is constant during the real storm. Normal values of wave steepness from storm conditions range between 0.02 and 0.06.

According to the wave steepness expression, the correlation between the significant wave height and the peak wave period can be expressed by this way:

$$s_p = \frac{2\pi * H_s}{g * T_p^2} \qquad (28)$$

## 2.7. 3D modelling

The simulation of the real wave conditions and the prototype breakwater in the laboratory must be done with an undistorted physical 2D model. To evaluate the damage progression of the breakwater under these wave conditions, a 3D model has to be composed in order to have a visualization of the structure in the space.

There exist many different methods to construct this 3D model, but the most used in general is the multi-view 3D reconstruction. This Multi-view 3D reconstruction is a process, which consists on taking many overlapping pictures of the target element to obtain a final 3D model. In addition, there is available technology that allows the reconstruction of the model without a specific order of the taken pictures.

This type of 3D reconstruction can be done with freely available software in the network, which do not require advanced skills in this area. If we add that there is a large distribution of high-resolution cameras in the market, these reconstruction methods become simple and low cost (Favalli et al., 2011).

Regarding the realization of the target pictures, they must be taken from different points of view that vary significantly from one another, taking into account that pictures from the same point are useless. The element to be modelled, in this Thesis the breakwater, must be well lightened and fixed in the same position while the pictures are being taken. The higher number of pictures is used, the more accuracy of the model will be achieved.

The new emerging method that the different software are using of the 3D reconstruction is the Structure-from-Motion (SfM). On the one hand, it works as the classic photogrammetry, constructing the 3D structure with a series of overlapping pictures. On the other hand, it differs a lot from the photogrammetry in terms that the geometry, the camera positions and orientation are solved without the need to have 3D known positions of the points or a series of control points. Instead, these are solved simultaneously with an iterative adjustment procedure. Generally, high degree of overlapping is required in the pictures to use this method (Snavely, 2008).

The main problem of SfM is that there is no scale or orientation, as it was with the 3D known positions. Therefore, the 3D point clouds are generated in a coordinate system of the image, which must be transformed into a real-world coordinate system. This process can be done through a series of control points with known coordinates. In this Thesis, 2 control points will be set in the breakwater toe, and 2 more in the top of it.

An important free software without need of subscription is the one provided by AutoCAD, called Autodesk Recap 360. This will be the software used in this Thesis, which will scan all the pictures taken from the breakwater to construct the desired 3D model.

# 3. EXPERIMENTS METHODOLOGY

## 3.1. Physical model

### *3.1.1. CIEMito wave flume*

The CIEMito is the small-scale wave flume used to do the tests. It is located in the Maritime Engineering Laboratory at the Polytechnic University of Catalonia and was constructed to allow the realization of research studies in maritime and coastal engineering field.

It is made with cold rolled metal structure, while walls and bottom are made from tempered glass with 5+5 mm thick. The main dimensions are:

- ***Length***: 18 m
- ***Width***: 0.38 m
- ***Depth***: 0.56 m
- ***Maximum draft***: 0.36 m

It has two wells of 0.2 m diameter with filling and emptying equipment and a controlled water recirculation by means of stream generation system. It also includes a 3 $m^3$ tank and an own pumping-filtering system to maintain its independence from the rest of the installations.

The wave generation is performed by a reciprocating blade with 1 m linear actuator piston and with a maximum response speed of about 1.6 m/s. The maximum theoretical capacity for a maximum draft of 0.36 m corresponds to a 1.7 s period and 0.28 m high wave. The generation software allows creating regular and irregular waves and reproducing time series.

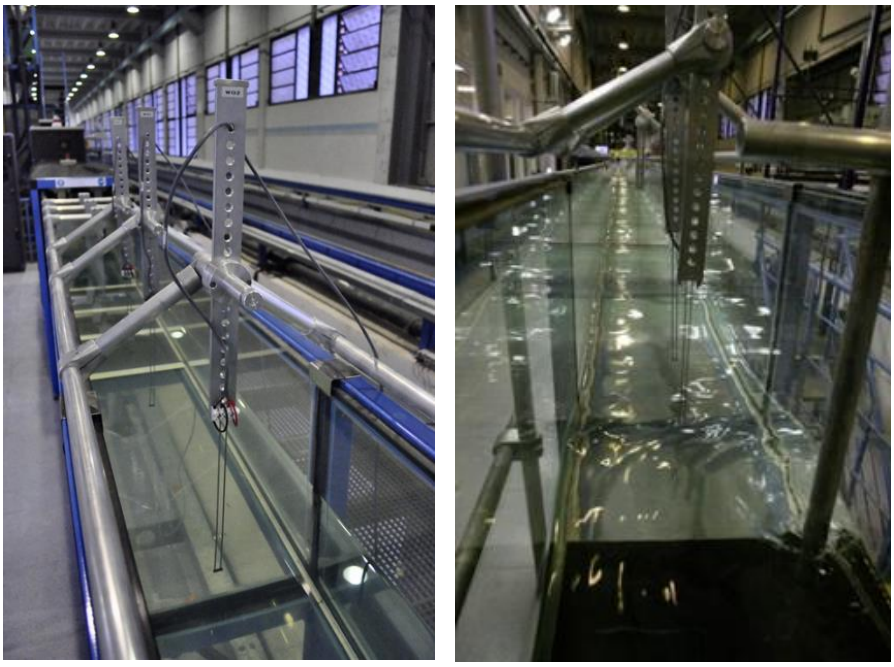

*Figure 16. Wave flume view.*

### *3.1.2. Measuring equipment*

#### CIEMito sensors

For the measurement of the produced waves, 8 resistive wave gauges are available. Between two metal electrodes circulates an electric current with a constant intensity. The water mass creates a resistance in this current when being in contact with the sensors, so the magnitude of this resistance will depend on the height of the water surface. Knowing the intensity and the resistance caused by the water, the voltage is found out applying the Ohm's law.

As the relationship between the variables that appear in the Ohm's law is linear, the software of the CIEMito wave flume can do the calibration by only knowing two voltage values. With these values a straight can be plotted and the different available sensors in the flume can be calibrated before the beginning of the test.

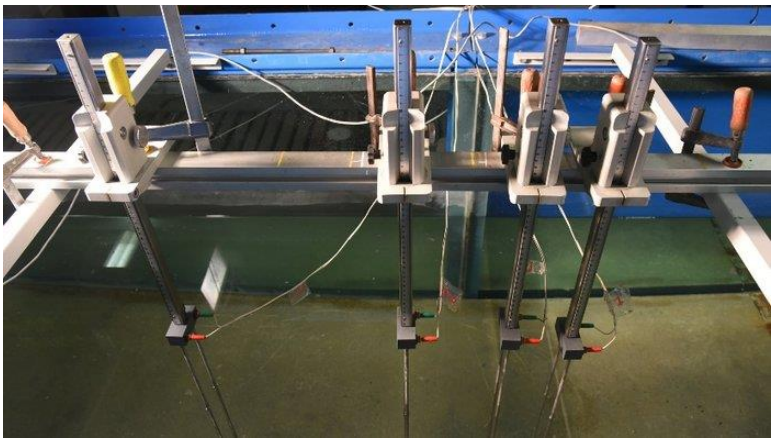

*Figure 17. Resistive wave gauges of a flume.*

#### Equipment to assess damage progression

In order to assess the damage progression of the breakwater, some photographs are going to be taken. It will be make a comparison between the photographs taken after each step in order to see the number of cubes that have been moved due to the wave attack.

For the photographs it is going to be used the following material:

- Nikon DLSR
- 2 GoPro cameras
    - GoPro Hero 4 Silver
    - GoPro Hero 3+
- 2 Full HD black and white cameras, that can be controlled directly with PC

One of the GoPro's will be mounted in a fixed position parallel to the slope of the modelled breakwater. With this position, it is ensured that the view is always perpendicular to the slope. This GoPro will take photographs before and after any test developed in the flume.

The other GoPro is used to take photographs of the breakwater from different angles. These photographs are then imported to the PC, where a program will combine them in order to create a 3D model of the breakwater. To have a reliable 3D model the approximate number of photographs that must be taken are from 80 to 100.

These GoPro's are used because the program used to create the 3D model from the pictures, Autodesk Recap 360, works good with pictures coming from those cameras. The disadvantage

is that the images created are highly distorted due to the "fish eye" model characteristic of this kind of cameras.

### *3.1.3. Scaling procedure*

The optimal laboratory tests should be the ones that behave like a version of the prototype that is modelled. Obviously, this situation never occurs due to the imperfections associated to the model construction. Although the difficulty to get a similar behavior, if all the variables are in proportion between the model and the prototype, a good representation of the reality could be achieved. It is important to notice that there will be many factors that due to their small values, the scaling would not be significant to the global process.

The scaling procedure of the prototype to obtain an experimental model can vary with the considered problem. For example, in fluid mechanics, the similarity between the model and the prototype can be divided in three main classifications: dynamic similarity, geometric similarity and kinematic similarity (Hughes, 1993).

In the case of the CIEMito wave flume, the most important properties to be scaled are the presented in the next table. Each variable will have a different scaling factor.

| Property | Unit | Scaling factor |
|---|---|---|
| **Lenght** | m | $\lambda$ |
| **Mass** | Kg | $\lambda^3$ |
| **Density** | Kg/m$^3$ | 1 |
| **Time** | s | $\sqrt{\lambda}$ |

*Table 3. Scaling factors for different properties according to Froude criterion.*

As it can be seen, the scaling factor for the density is 1. Therefore, density is a property that cannot be scaled in the laboratory tests. On the other hand, properties as the length (wave height), the mass of the breakwater stones and the time (wave period) must be scaled for this Thesis by finding out this scaling factor λ and then using the respective relationship.

The geometric scaling factor of the model is determined with the maximum significant wave height of the real storm used (storm peak). As will be seen later in the Chapter 3.2.1, the storm peak has a wave height associated of 465 cm. In order to assess the damage progression in the breakwater, this maximum wave height must deliver important damage to the breakwater, since otherwise is difficult to compare the damage caused by new test methodologies.

Knowing the dimensions of the breakwater and making use of the Van der Meer formula seen before ( 6 ) with an associated $N_{od}$ of 2 that corresponds to the breakwater's failure, the corresponding significant wave height that generates this expected $N_{od}$, is approximately 6 cm. Then, the scaling factor can be directly deduced applying this formula:

$$\lambda = \frac{H_{s,peak}}{H_{model\ failure}} = \frac{465\ cm}{6\ cm} = 77.5 \qquad (29)$$

For simplicity, the scaling factor used for this Thesis will be 80. Then, the other properties as the mass and the time can be also modelled by applying the relations seen in the previous table.

### *3.1.4. Model and scale effects*

The model and scale effects can distort modelling results. The first ones are induced while the construction of the model in the laboratory, for example by creating artificial boundaries. A clear example of it would be the glass walls of the CIEMito, which are in charge of maintain the breakwater in a fixed position. The second ones, the scale effects, occur when the scaling law used is not the correct one, leading to an incorrect reproduction of the physical conditions of the prototype at model scale.

These effects sometimes can be difficult to estimate and depend on the investigated parameters. The work of Hughes (1993*)* try to discuss about how to deal with these effects.

In a short-wave hydrodynamic model like the one used in this Thesis, often only a section of the prototype configuration is modelled. Therefore, the positioning of the model in the wave flume should be such that it minimizes the boundary effects and that reproduces the responses associated to the scale used.

The models represented in a wave flume are very susceptible to the reflection of the incident waves. Therefore, these reflections are reduced, but not eliminated, by making use of wave absorbers as it is done in the final meters of the CIEMito.

Although these possible effects when scaling, as the damage between test methodologies is compared with the same conditions, results will not have any affection.

### *3.1.5. Breakwater model*

The chosen design for the breakwater has been the same than the used by Van der Meer (1988b). The reason is to be able to obtain a damage compatible with the formulas he developed. Therefore, the stability formulas for the cubes used in this Thesis will correspond and will be based on this design.

Due to the size of the Van der Meer design of the breakwater, this structure will need to be scaled down with a factor of 3 in order to fit into the flume dimensions. The length scale ($N_L$) between the model and the prototype will be 80 as it was previously determined.

#### Van der Meer breakwater characteristics

Van der Meer used a breakwater with a uniform foreshore with a slope of 1:30 and a slope for the breakwater of 1:1.5. The characteristics of the different layers that conform the breakwater are:

- ***Core***: gravel of $D_{n50} = 11$ mm
- ***Filter layer***
  - Thickness: 6 cm
  - Gravel with a 20-25 mm grading
- ***Armour layer***
  - 2 layers of cubes
  - Thickness: 9 cm
  - Mass of the cubes: 0.204 kg
  - $D_{n50}$ of the cubes: 0.045 m

The coronation of the armour layer is +1.15 m and the coronation of the filer layer is +1.07 m.

In the Figure 18 the cross section of the Van der Meer's breakwater structure is shown:

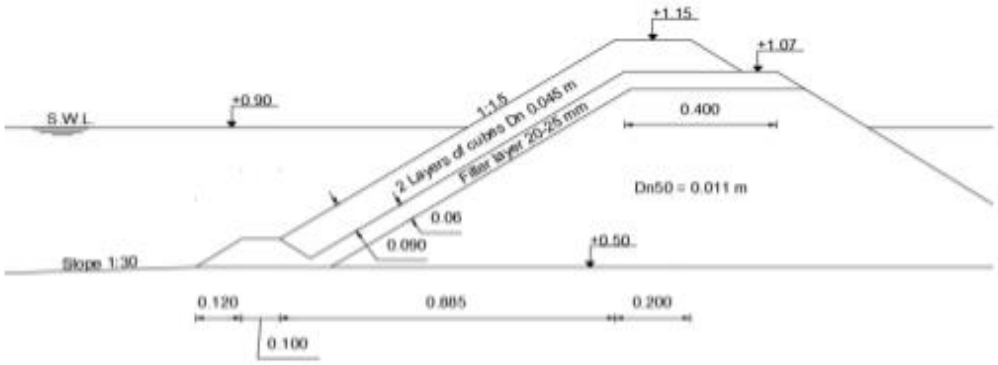


*Figure 18. Breakwater cross-section used by Van der Meer (1988b).*

## Modelled breakwater characteristics

As it has been mentioned, the wave flume facility is not suited for this sizing and the dimensions of the breakwater are downscaled by a factor of 3. This breakwater now fits in the flume dimensions and the research can be developed.

In the Figure 19 it is displayed the cross section of the breakwater that is going to be used in the laboratory tests. The damage progression caused by the different test methodologies will be assessed in further chapters.

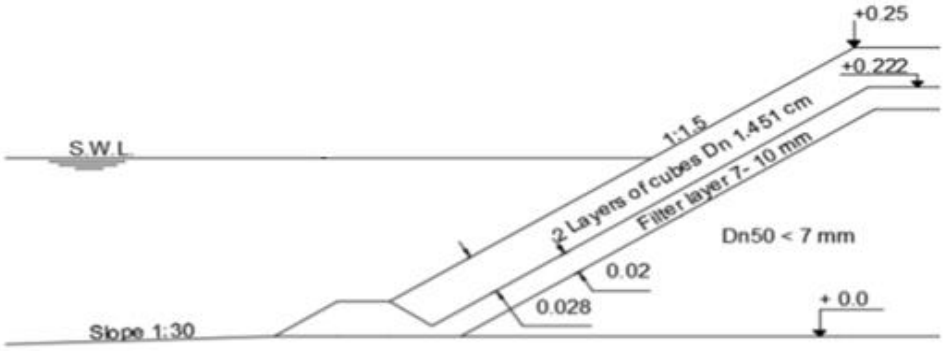


*Figure 19. Breakwater cross-section used in de flume model.*

The geometric properties of the modelled breakwater materials are the following:

- ***Core***: consists of sand available in the laboratory with a $D_{n50} < 7mm$ and more less about 3.7 mm, which is the nominal diameter of the Van der Meer core gravel divided by 3.
- ***Filter layer***: applied between the armour layer and the core, which are layers with an important difference of their grain sizes. In other words, it ensures that the change in particle size is not abrupt at all. It is basic to protect the core material against the wave attacks and to avoid excessive water pressures.
  It consists of rubble stone with the following characteristics:
  - $D_{n50} = 0.7 - 1\ cm$
  - Thickness: 2 cm
  - ρ= $2.65\ \frac{g}{cm^3}$

- ***Armour layer***: composed of two layers of cubic blocks that are made out of resin with a peace of lead in the middle that adds weight. The elaboration of these cubes was carried out by researcher Andrea Marzeddu and former master student Jordi de Leau (De Leau, 2017) from Delft University. The characteristics of these cubs are:
  - $D_{n50} = 1.45\ cm$
  - $V_{50} = 3cm^3$
  - ρ= 2.242 $\frac{g}{cm^3}$

### *3.1.6. Water depth*

The water depth in the flume is chosen to be 30 cm in front of the foreshore. This depth in the model corresponds to a depth of 24 m in the reality, because of the scaling factor applied of 80. As the real storm, and consequently the synthetic storm created, is measured with a buoy located at a depth of 65 m, waves must be propagated until a depth of 24 m, which is the one of our interest. This propagation must take into account the shoaling and refraction process that occur while the waves are moving towards the coast.

These processes will modify the wave heights, having at 24 m depth a different wave height than it was at 65 m depth. In order to see the wave height variation from 64 m to 24 m, SwanOne has been used. This mentioned coefficient will be determined by using as input a 1m wave height.

As this coefficient varies with the wave period, it is need to see the trend when giving to the wave period values from 5 to 15 s. In the Figure 20 is deployed the evolution of this wave height propagation coefficient and the equation of the tendency polynomic associated to this variation.

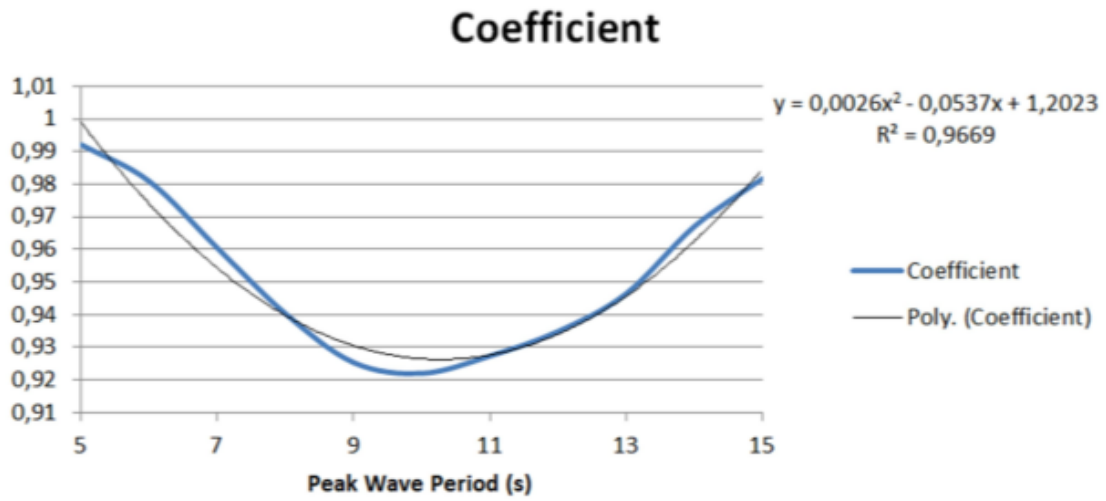


*Figure 20. Wave height propagation coefficient related to the peak period at a depth of 24m (calculated with SwanOne).*

The tendency line is determined with the Excel and gives as the possibility to find the different coefficients in terms of the wave period by using a mathematical expression easy to applicate. Once the dependency is clear, each coefficient calculated from a wave period associated to a significant wave height will be multiplied by this wave height measured at 65 m to have the wave height at 24 m depth. Consequently, the storm profile will be available at this depth.

### *3.1.7. Characterization of the cubes*

The cubes that conform both layers of the armour are an essential object to be studied in this Thesis. Their properties, the process of elaboration and colocation are transcendent to the response of the breakwater structure against wave attack.

As all the elaboration process and characterization of the cubes was done by doctor Andrea Marzeddu and former Master student Jordi de Leau, the explanation of the properties related to that is done following the structure of the Thesis of De Leau (2017).

#### Density

In order to avoid possible problems in the scaling of the cubs weight, the density of these elements should be such a value that can be comparable to the density of the real armour cubes. It has to be taken into account that the water used in the flume is fresh water but the one attacking the real breakwater is marine. To determine the density of the cubes, the formula of the relative density (Δ) has been used. This relative density, attaining at what it has been explained, should be equal for the model and the reality.

$$\Delta = \frac{\rho_{element} - \rho_{water}}{\rho_{water}} \qquad (30)$$

In the Van der Meer (1988b) breakwater, the cubes that conform the two layers of the armour had a $D_{n50}$ of 4.5 cm, while the weight was about 0.204 kg. Therefore, the density associated to these cubs is 2.24 gr/cm$^3$, which can be also expressed as 2.24 kg/m3. As the Van der Meer breakwater is the prototype from which the model has been constructed, this density is related to this prototype. This value is not as big as the expected for reinforced concrete, but as the objective is to reproduce as well as it is possible the scaled version regarding the prototype, the density used for the modelled cubes is 2.24 gr/cm$^3$ (De Leau, 2017).

#### Material

The prototype cubes are normally made out of concrete with a reinforcement of steel bars. As the size of the modelled cubs needed for the tests in this Thesis does not permit the use of any kind of reinforcement, the first try was to make them of a mixture of cement, sand and lead. This addition of lead was necessary in order to increase the density of them, knowing that with sand and cement the required density was not achieved.

The combination of these base materials did not lead to have consistent cubes, so they could not be used in such these experiments.

The second option was to make out them of resin.As the resin by itself proved to harden quickly, the strength and consistency of the cubes was achieved this time. The only problem was that the resin itself is light, with an approximate density of 1.124 g/cm$^3$. Therefore, it was introduced a piece of lead (density of 10.787 g/cm$^3$) in the middle of the cubes to ensure that the cubes had the required density. For the lead, different possibilities were contemplated such as scraped lead from a block or a lead wire. The second option was the used at the end.

The weight of lead that was needed for each cube was calculated in terms of the cube volume. As it is about 3 cm$^3$, the piece of lead inside each cube weights approximately 7.6 gr. To enable the introduction of the lead inside the resin cube the elaboration process followed three steps.

In the first one, a resin layer was poured into the mold. Then, in the second step, the lead piece was put above the resin layer. Finally, all the space left over was filled up with resin to get the entire cube.

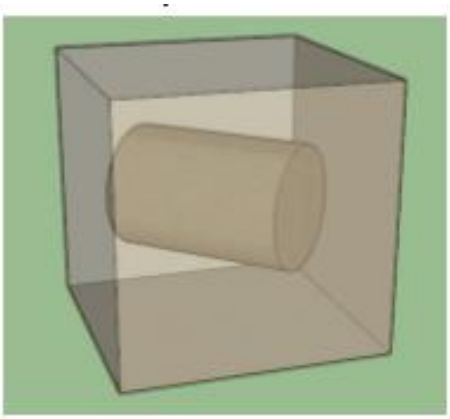

*Figure 21. Schematization of a modelled cube made out of resin (De Leau, 2017).*

This process is done manually so there are possibilities to have inaccuracies in the final element. These inaccuracies and key differences between this modelled cubes and the prototype ones, could lead to have unfair cubes. Therefore, this elaboration process does not ensure that the gravitational center of the cub has the same tridimensional position than the geometric center.

### Fairness

This concept is normally used when talking about dices. Since the fairness of the cubes must be checked, and they can be compared with dices, some testes were done in order to see the reliability of the resin cubes. These tests consisted on throwing lots of numbered cubes and see if the number of times each number appears was similar for all of them. If the gravity center were in the same position as the geometric center, the probability in one attempt to get any of the six numbers would be 1/6.

In this test, 7 randomly chosen cubs were numbered from 1 to 6 in each side in order to have the same appearance than the dices. These cubes were thrown 200 times. The results proved that although some of the cubes seemed to be fair, some of them did not give the expected results, probably due to the irregularity of the cubes during the elaboration process.

To prove the goodness of the testes and in order to see the fairness of the cubes, the parameter $\chi^2$ was measured for each of the cubes with the expression shown below.

$$\chi^2 = \sum \frac{(observed\ results - expected\ results)^2}{expected\ results} \qquad (31)$$

This unfairness of some of the 7 cubes (low fairness probability) was caused by the production process of the cubes. During this process, the cubes were dried in the mold and the surfaces (mainly the top surface) became in some cases not as flat as it would be necessary, leading to unevenness between points of the same side.

A solution to face this unfairness was to apply sand to the sides to get a flattened surface. This process was applied to the unfair dices and 150 more throws of each dice were done. After all this process, and by looking at the results obtained, it was noticed that the dices had become

fairer. Moreover, the value of the fairness probability obtained for these dices was even nearer to 50% that the dices that in the set of 200 throws were quite fair.

The fairness is very important, but it is not achievable at all. The prototype cubes are pretended to be fair, but the irregularities and the sharpness of the stones can lead to have unfairness in the reality.

### Moment of inertia

The moment of inertia when comparing the resin cubes (first try) and the ones recovered by sand (second try) were different regardless of the axis through the middle that is being evaluated. This is due to the difference in weight and the distribution of it in the cubes.

Concerning the resin cubes, the fact that the piece of lead is surrounded by resin, which is a lighter material, makes the moment of inertia smaller than for the sanded cubes. Consequently, it will be needed less force to get the same rotation velocity for resin cubes.

Although the moment of inertia is not easy to obtain with elements that have been handmade elaborated, an approximation to a sphere shape with the piece of lead in the middle can be done. Therefore, the values for both kind of cubes can be calculated, obtaining expected results. The values obtained are 1.36 $gr \cdot cm^2$ for the resin cubes and 2.28 $gr \cdot cm^2$ for the cubes with the weight evenly distributed.

As the cubes in the armour layer are generally supported in the slope, the difference between inertia moments will not affect the damage at all. The resin cubes are able to rotate easily when not being supported at all, but not when laying on the slope and being well supported (De Leau, 2017).

### Colors

To distinguish between the cubes and the two different layers that conform the armour, these have been painted with different colors:

- ***Black***
- ***Blue***
- ***Red***
- ***White***

The use of colors in the cubes enables to obtain easily the damage progression. This differentiation in 4 colors makes easier to see what is happening and in which part of the breakwater the damage is more accentuated.

These cubes are also numbered by a unique number, which is the same in all the sides. This numeration allows knowing the exact position of the cubes along the breakwater at the beginning of each test and at the end of it. Therefore, the displacement of each cub due to the wave attacks can be obtained. In total, about 800 cubes are used.

For all the testes carried out, these cubs are placed in the armour layer, so on the top of the filter layer. The positioning of the cubes in the armour layer follows the following pattern:

- ***First armour layer***: constructed with black and blue cubes, placed firstly in 5 rows alternatively and then in 2 rows until the breakwater coronation is achieved. Each row contains 17 cubes and the first rows, beginning at the toe of the breakwater. First rows are composed of black cubes.

- ***Second armour layer***: constructed with red and white cubes, with the same steps that in the first armour layer. The first rows are made with red cubes.

*Figure 22. Distribution of cubes in the first armour layer (bottom layer).*

*Figure 23. Distribution of cubes in the second armour layer (top layer).*

This cube placement is done by considering an approximate porosity of 40%. This porosity must be similar to the one used in the Van der Meer breakwater, when trying to model as well as it is possible the conditions of the prototype breakwater. Moreover, this placement is done randomly, as it occurs in the reality, by placing the cubes with no linearity and with different orientations. Consequently, the armour layer get more and more compacted and the strength achieved in all the structure is higher.

The Figure 22 shows the configuration of the first amour layer cubes (colors black and blue), and the Figure 23 the configuration of the upper armour layer (colors red and white).

### Packing density

Another influence on stability is the packing density. This influence has been investigated in many works, as De Jong (1996) did with tetrapods. In this study, it was exposed that this packing density could be involved in the equations of the breakwater stability by a factor $f(\phi)$. This contribution supposes an addition of stability.

As it has been advanced previously, the objective is to use the same package density ($\phi$) as the one used by Van der Meer for a concrete cube distribution in the armour layer, 1.17, which corresponds to a porosity of 41.5%.

The porosity equation provided in the work of Medina *et al.* (2011) is shown below:

$$p = 1 - \frac{\phi}{n} \quad (32)$$

Where $p$ is the porosity, $\phi$ the packing density and $n$ the number of layers.

By getting back to the Van der Meer expression of the packing density seen previously, an interlacement between both formulas can be done in order to get the necessary number of cubes to implement.

$$\phi = \frac{N_a * D_n^2}{A} \quad (33)$$

The porosity necessary can be obtained by substituting this last value of the packing density inside the formula of the porosity. The deducted equation is the following:

$$p = 1 - \frac{N_a * D_n^2}{n * A} \quad (34)$$

Where $N_a$ is the number of blocks necessaries to obtain the fixed porosity, $A$ is the surface area of the slope and $D_n$ is the nominal diameter of the cubes.

Being 41.5% (approximately 40%) the desired porosity in the modelled breakwater, and knowing the values of the nominal diameter of the cubes, the slope and the number of layers (2); the number of cubes necessaries ($N_a$) to place in the two layers of the armour are approximate 700.

This amount of cubes is always the same in each experiment but their placing differs from one experiment to the other, because of the randomness process of colocation. Depending on the situation, these cubes can be placed nearer to obtain denser rows or more separated to increase the porosity.

## 3.2. Storm data

### *3.2.1. Real storm*

The storm chosen for this Thesis was measured with a buoy located next to the city of Blanes in the Mediterranean Sea. This buoy is englobed in the XIOM net, a set of facilities located in different parts of the Catalan coast that measure the most important coastal variables.

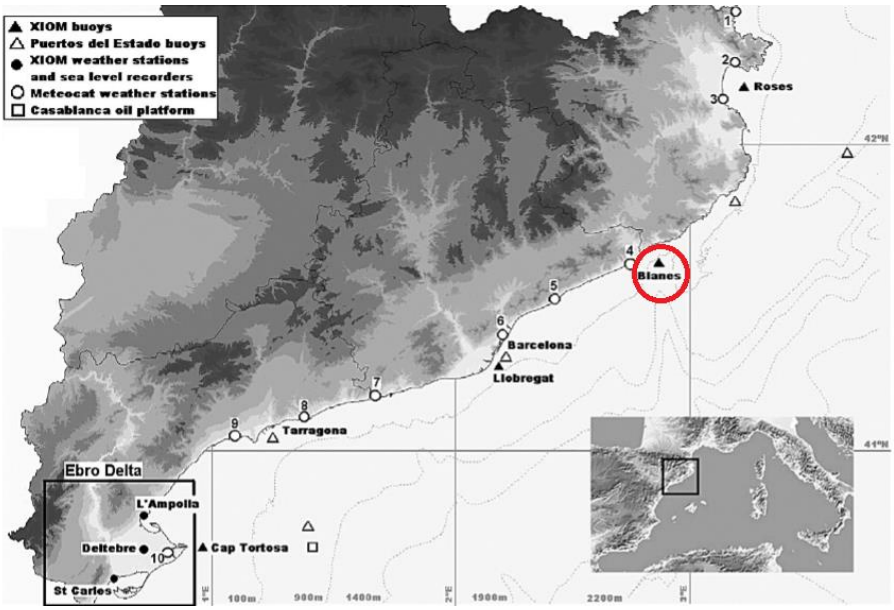


*Figure 24. Representation of the XIOM network instrumentation and location, highlighting the Blanes buoy (Bolaños et al., 2007).*

The XIOM network is constituted by 9 elements, including weather stations, tide gauges, scalar buoys and directional buoys. Regarding the directional buoys, there are a total of three and they measure the direction of the waves in real time. The buoy of Blanes is one of these ones.

The first condition was to choose a storm that would have caused damages to the protection breakwater. At first, different heavy storms were considered, but decidedly opted for the happened during the Sant Esteve's day in 2008 (26-12-2008), which was one of the 5 or 6 biggest storms with the available data.

This storm will be transformed to a synthetic storm, whose construction will be explained in the Chapter 3.2.2. This synthetic storm and the real one will be reproduced in the wave flume.

The buoy characteristics are the following:

- ***Location***: Blanes 41.64ºN 2.81ºE
- ***Depth***: 65 m
- ***Type of measurement***: Waves
- ***Sampling rate***: 20 minutes every hour
- ***Main output parameters***: Wave statistics and spectra
- ***Instrument type***: Datawell waverider
- ***Location of the coast respect to the buoy***: 326º and about 3.5 km away


*Figure 25. Example of XIOM buoy.*

The main characteristics and parameters to consider about the storm are the following:

- Threshold chosen: 3 m. It has been observed with other experiments in the wave flume that took in consideration a threshold of 1.5 m, that the wave heights above this limit and below 3 m did not cause enough representative damage to the breakwater when comparing with the wave heights above 3 m.
- At 13:00 AM on the 26th of December 2008, the significant wave heights raised above the fixed threshold of 3 m, so at this time it is considered the beginning of the real storm.
- At 10:00 A; on the 27th of December 2008, the significant wave height reached the value of 3m, due to it decreasing during the previous hours, so this time it is considered the final of the storm. *(*Note that although in the two next hours there are wave height values of 340 cm and 304 cm, this short peak has not been considered. It has been thought that it would not cause damage to the breakwater at all when it has been exposed previously to higher peak wave heights*)
- Total duration: 21 h
- $H_{s,peak}$ is 465 cm
- The period associated with the $H_{s,peak}$ ($T_{p,peak}$) is 11.8 s

If the considered threshold had been 1.5 m, the storm history (profile) would have been the one plotted below. The duration of the storm would have been greater (74 h).

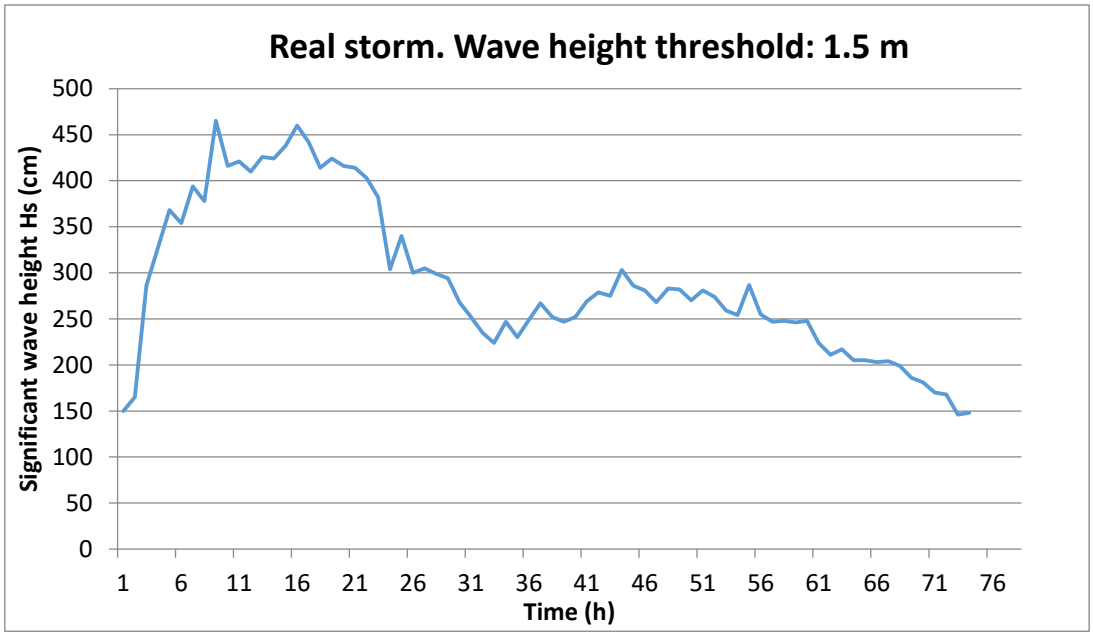


*Figure 26. Real storm profile.*

Considering the wave height threshold of 3 m, but also taking into account the wave height values near the threshold in the increasing branch and in the decreasing one, the profile of the real storm has a lower intrinsic duration and can be seen below:

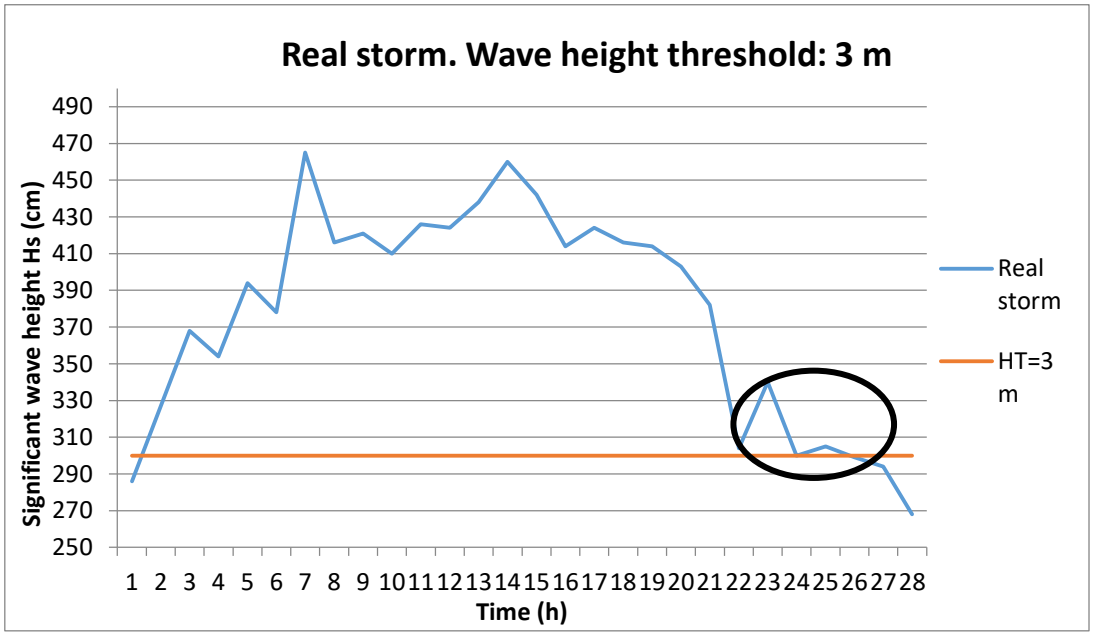


*Figure 27. Real storm profile with a wave height threshold of 3 m.*

Finally, if the short peak mentioned after the power of the storm has decreased considerably is neglected, the definitive profile of the storm becomes the following:

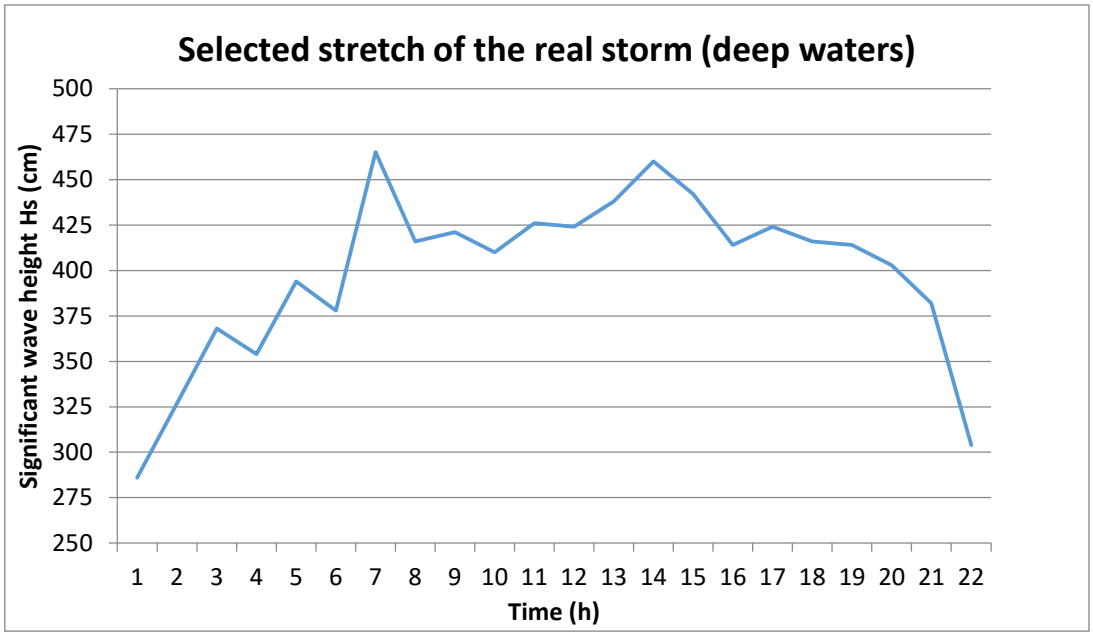


*Figure 28. Selected part of the real storm profile.*

This storm has a duration of 21 h, two significant wave height peaks (4.65 and 4.60 m) and a time interval between them of 7 h approximately.

Once the stretch of the real storm that is going to be used has been defined, and as the significant wave height values are obtained by a buy located at 65 m depth, these must be propagated until a depth of 24 m. With the propagation conditions, the peak of the storm will decrease until a value of 4.33 m.

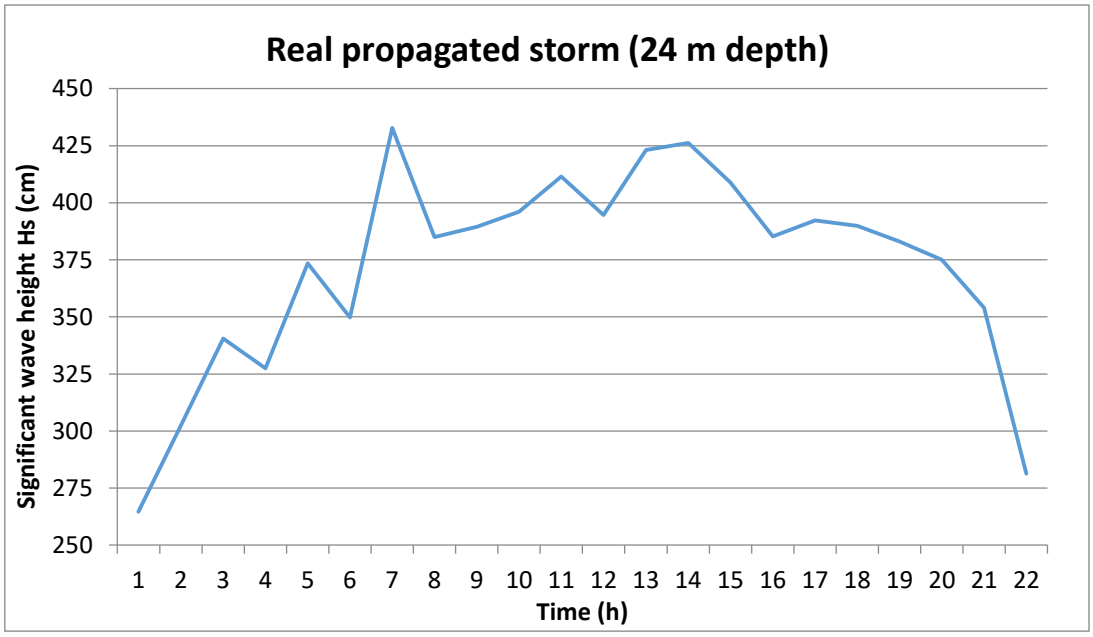


*Figure 29. Selected part of the real storm profile propagated at 24 m.*

### *3.2.2. Synthetic trapezoidal storm*

The synthetic model that is used to construct the synthetic storm is the Equivalent Magnitude Storm model (EMS) with a trapezium shape.

The first step consists on calculating the magnitude of the real storm, which is the energy associated to it and presented in previously. The energy can be assumed as the area below the series $H_s$-time and it is about **21.7 mh**. This energy must be the same that the associated to our synthetic storm.

If a triangular synthetic storm was used to represent the real storm history, the triangle base ($D^*_{triangle}$) would be found by making use of the expression of its area:

$$M_{triangle\ storm} = \frac{D^*_{triangle} * h_{max,eq}}{2} \quad (35)$$

$$D^*_{triangle} = \frac{2 * M_{triangle\ storm}}{h_{max,eq}} \quad (36)$$

The energy of this triangular synthetic storm ($M_{triangle\ storm}$) should be the same as the energy of the rea storm (21.5 mh) and the $H_{max,eq}$ (1.65 m) would be the height of the triangle. With those known parameters, the triangle base would be found as it follows:

$$D^*_{triangle} = \frac{2 * 21.7mh}{1.65m} = 26.3\ h$$

The next image compare the real storm and the synthetic storm if the model used were a triangular shaped one.

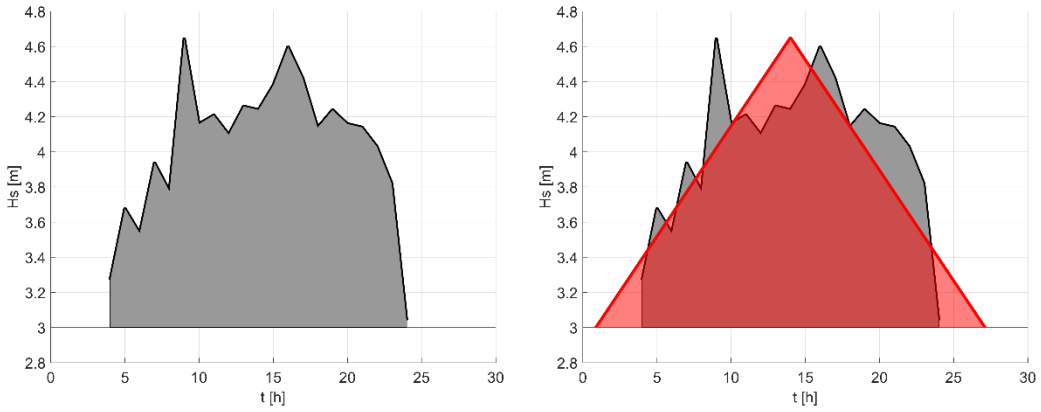


*Figure 30. Real storm profile and corresponding synthetic storm with triangular shape (Marzeddu et al., 2017).*

In conclusion, a triangular pattern to represent the evolution of the storm would be found, having a duration of 26.3 h instead of the 21 h that last our real storm.

As our model tries to represent the evolution of the real storm with a trapezium shape, the formula of the area used is the following:

$$M = \frac{1}{2} * (b_L + b_S) * h \quad (37)$$

Where $M$ is the energy of the synthetic trapezoidal storm (known), $h$ is the height of the trapezium, which is the same as the maximum significant wave height observed in the real storm, and the coefficients $b_L$, $b_S$ are the unknown trapezium bases (representing the time).

As both unknowns are in the same equation, it is needed first of all an escalation of the real storm. This escalation will generate a dimensionless storm with the axes 'x' and 'y' going from 0 to 1.

Knowing the $H_s$ and the time of each step of the real storm, the corresponding paired data of the escalated storm are shown in the next table:

| $D$(h) | $Hs$ (cm) | $Hs, eq.$ (cm) |
|---|---|---|
| 1 | 327 | 27 |
| 2 | 368 | 68 |
| 3 | 354 | 54 |
| 4 | 394 | 94 |
| 5 | 378 | 78 |
| 6 | 465 | 165 |
| 7 | 416 | 116 |
| 8 | 421 | 121 |
| 9 | 410 | 110 |
| 10 | 426 | 126 |
| 11 | 424 | 124 |
| 12 | 438 | 138 |
| 13 | 460 | 160 |
| 14 | 442 | 142 |
| 15 | 414 | 114 |
| 16 | 424 | 124 |
| 17 | 416 | 116 |
| 18 | 414 | 114 |
| 19 | 403 | 103 |
| 20 | 382 | 82 |
| 21 | 304 | 4 |

Escalation

| $Di/Dtotal$ | $Hs, eq./Hs, eq. peak$ |
|---|---|
| 0.048 | 0.164 |
| 0.095 | 0.412 |
| 0.143 | 0.327 |
| 0.190 | 0.570 |
| 0.238 | 0.473 |
| 0.286 | 1.000 |
| 0.333 | 0.703 |
| 0.381 | 0.733 |
| 0.429 | 0.667 |
| 0.476 | 0.764 |
| 0.524 | 0.752 |
| 0.571 | 0.836 |
| 0.619 | 0.970 |
| 0.667 | 0.861 |
| 0.714 | 0.691 |
| 0.762 | 0.752 |
| 0.810 | 0.703 |
| 0.857 | 0.691 |
| 0.905 | 0.624 |
| 0.952 | 0.497 |
| 1.000 | 0.024 |

*Figure 31. Escalation of the real storm.*

If the escalated values are plotted, it is obtained a graphic with the same evolution pattern of the significant wave height over the time but with dimensionless axes.

- Axis x: $\frac{D_i}{D_{total}}$
- Axis y: $\frac{H_{s,equiv.}}{H_{s,equiv.peak}}$

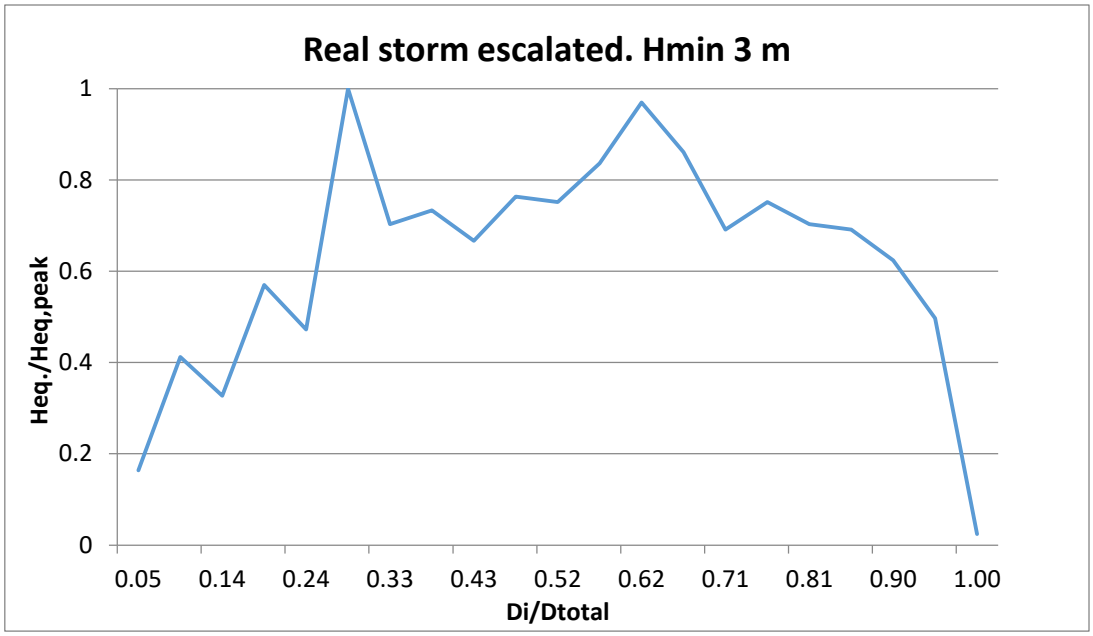


*Figure 32. Real storm scaled with dimensionless axes..*

With this new transformed storm, the same formula of the trapezium area is used, but now with only one unknown. The larger base ($b_L$) is now equal to one, the height is also 1 and the energy associated below this curve ($M_{escalated}$) can be calculated with the Matlab software:

$$\boldsymbol{M_{escalated}} = 0.6247\ mh$$

Now the formula of the trapezium area can be applied, and the smallest base ($b_S$) can be obtained. The expression resulting of isolating this parameter from the expression of the trapezium area is shown below:

$$b_S = \frac{M_{escalated} * 2}{h} - b_L = \frac{0.6247 * 2}{1} - 1 = 0.2494\ m \qquad (38)$$

Once it is known the last needed value, the duration of our trapezoidal storm ($D_{trapez.}$) is found by making use of the following formula:

$$M_{real} = \frac{1}{2} * (1 + b) * H_{equiv.peak} * D_{trapez.} \qquad (39)$$

The $M_{real}$ (21.7 mh), the parameter $b$(0.2494 m) and the peak equivalent wave height (1.65 m) are known values, so the $D_{trapez.}$ can be calculated, giving as a result:

$$D_{trapez.} = 21.05\ h \approx \boldsymbol{21\ h}$$

The duration of the trapezoidal synthetic storm is practically the same as the duration of the real storm. The final step is to see the duration between both peaks ($d_{peaks}$), which is found with the general equation of the trapezium area.

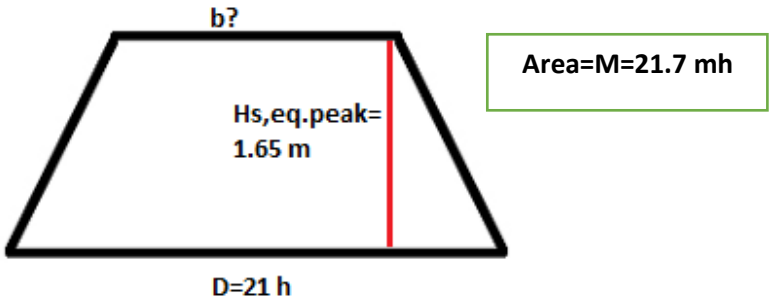


*Figure 33. Trapezium scheme and corresponding necessary values.*

$$M = \frac{(a+b)}{2} * h = \frac{\left(D_{trapez.} + d_{peaks}\right)}{2} * Hs, eq.peak \qquad (40)$$

$$d_{peaks} = \mathbf{5.3\ h}$$

The time interval between both peaks of the storm, unlike what it was seen with the duration, is smaller for the trapezoidal storm that for the real storm. While the time interval with the first is 5.3 h, the time between peaks in the real storm was 7 h approximately, with the 1st peak 6 h after the beginning of the storm and the 2nd peak after 13 h. Although both peaks in the real storm have not associated the same significant wave height (4.65 m and 4.60 m), in the trapezoidal storm are supposed to have the same wave height because the trapezium shape implies parallelism between both bases.

In addition, in order to create the evolution of the synthetic storm and attaining the conditions of the trapezoidal synthetic model, the shape of it must be symmetric. Therefore, the slope must be the same for the increasing and for the decreasing branch. Consequently, the small base (interval between peaks) is located in the middle of the total duration.

This synthetic storm evolution can be seen in the next figure. Note that the peak of this storm is the same as the real storm (4.33 m) and it will last 5 h.

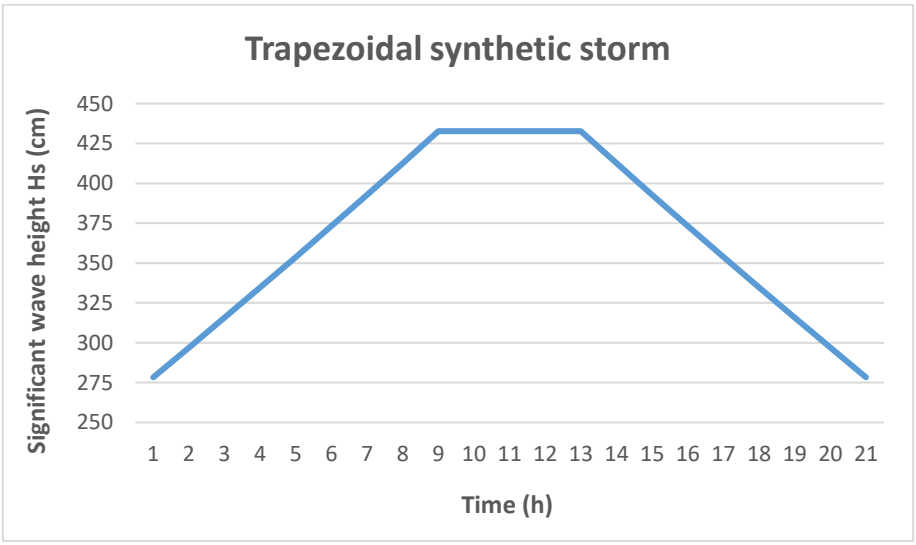


*Figure 34. Trapezoidal synthetic storm.*

### *3.2.3. Wave steepness and peak period*

Once the total duration, the time between peaks and the specific wave height of the storm peak are obtained for the synthetic trapezoidal storm, the must be divided in steps of the same duration (1h in the prototype scale) to be introduced in the program. Each of these 21 steps are defined with a significant wave height ($H_s$), a peak period ($T_p$) and a total number of waves ($N_z$).

As it has been introduced before, with the information provided in the works of Martín Soldevilla *et al.* (2015) and Martín-Hidalgo *et al.* (2014), the peak period can be obtained from the significant wave height by making use of the wave steepness expression:

$$s_p = \frac{2\pi * H_s}{g * T_p^2} \qquad (41)$$

The equation ( 41 ) can be used because the wave steepness is considered to be constant during the entire real storm. The chosen value for $s_p$ is 0.02 and is used to compute the wave periods associated to all the significant wave heights of the different steps. This chosen value of wave steepness is typically associated to storm conditions, normally ranging between 0.02 and 0.06.

Then, knowing all the variables of the equation, the peak period for each step can be isolated and calculated as it follows:

$$T_p = \sqrt{\frac{2\pi * H_s}{g * s_p}} \qquad (42)$$

The last variable that has to be set to later be entered with the others in the program is the number of waves of each step. As the peak wave period and the total duration of the storm are already known, this value is easily obtained by making use of the following equation:

$$N_z = \frac{D * 3600/21}{T_p * \sqrt{80}} \qquad (43)$$

## 3.3. Programs of the storms

In this chapter, a brief introduction to the main aspects of the test plan configuration is done. Although the tested storm methodologies in this work have been two, concretely the synthetic storm with the trapezium shape and the real storm, the programs of other two methodologies are also presented. These are the test program of the classical testing method and the synthetic storm with the triangular shape. These two methods were tested previously in the same flume, providing results showed in the Chapter 4.

Before the test plans of the different storms are explained, a detailed introduction of the program used to insert the wave data and the way of generating waves in the flume is done.

### *3.3.1. Program CIEMGEN v1.2*

This program is developed to command the movement of the piston. The interface of this program is very handy and allows to introduce the data easily. The different aspects that must be selected or introduced in the main tab are:

- ***Wave type***: selected *Irregular* for this Thesis
- ***Wave height (m)***
- ***Wave period (s)***
- ***Number of waves***
- ***Wave spectrum characteristics:*** *variables used to create the correct wave spectrum, in this case the JONSWAP*
- ***Wave generation seeding number***

An illustration of the program interface is shown in the Figure 35.

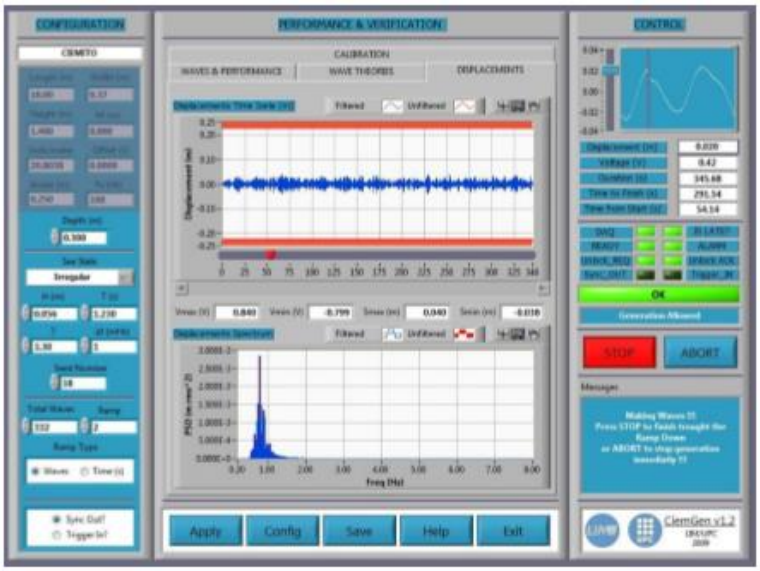


*Figure 35. Interface of the program CIEMWAVE v1.2.*

### *3.3.2. Generation of random waves*

For the generation of the waves in the flume, the JONSWAP spectrum is used. This is a kind of spectrum constructed with the significant wave height and peak period variables, with a frequency of discretization of 1 mHz. This frequency is directly related to the amplitude of the wave, which is translated to flume paddle.

With this pattern, a random phase is applied to every harmonic wave, leading to have for each of the frequencies a unique phase. The change in the wave generation seeding number (distribution of random starting phases) is used to create different orders in the phase alternation, affecting the association of phases with frequencies. If the seeding is not varied, the order of the phases does not change.

As the repeatability, the variability and the uncertainties in the breakwater damage processes are important aspects to take into account, the experiments have been performed by varying this wave generation seeding between tests. This variation is typical in small-scale model tests, when trying to reproduce the free surface elevation time series.

This variation of the seeding number in the tests tries to reproduce the variability of the storms in reality, because does not exist a specific seeding able to reproduce the exact temporal series. Although tests have been carried out using different seeding to compare breakwater damage with different wave patterns, some of them have been considered with the same seeding in order to compare the generation of the waves and to detect if the amplitudes and significant wave heights coincide.

### *3.3.3. Tests programs*

Real storm

The evolution of the real storm described in the Chapter 3.2.1 is reproduced in the flume model. As all the data of the real storm is tabulated in steps of 1 h, the evolution of the stretch selected of the propagated real storm can be deployed in terms of number steps, knowing that every step or test in the flume equals to 1h in the reality. The total number of steps to test all the storm are 22 and the significant wave heights of the two storm peaks are about 4.33 m and 4.25 m.

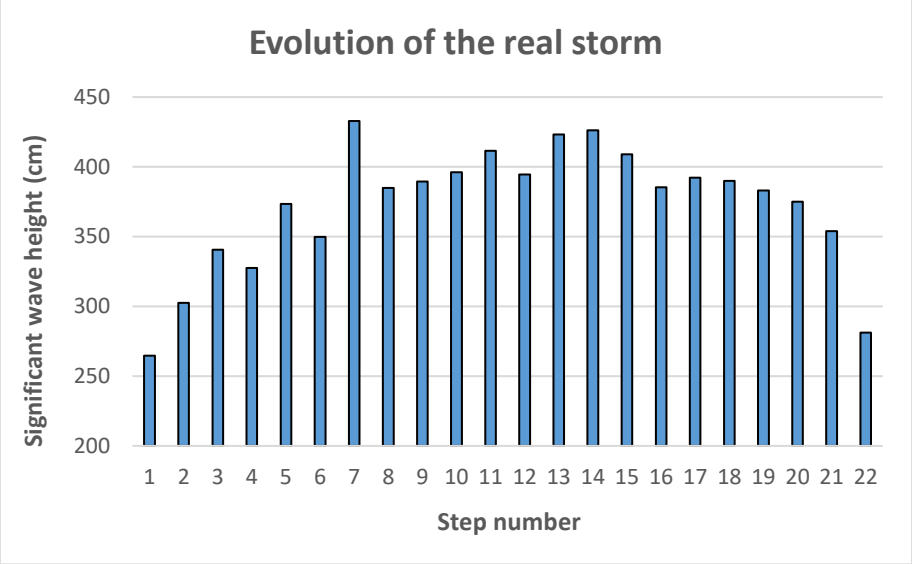


*Figure 36. Evolution of the real storm before the scaling of the wave data.*

The first step to do before the test plan of the real storm is escalate the main parameters of the storm. The propagated significant wave heights are divided by a factor of λ=80, so the corresponding target values to apply at the flume are the ones appearing in the following table. The significant wave heights corresponding at the two peaks of the real storm will be 5.41 cm and 5.33 cm respectively. These two peaks occur at the steps 7 and 14.

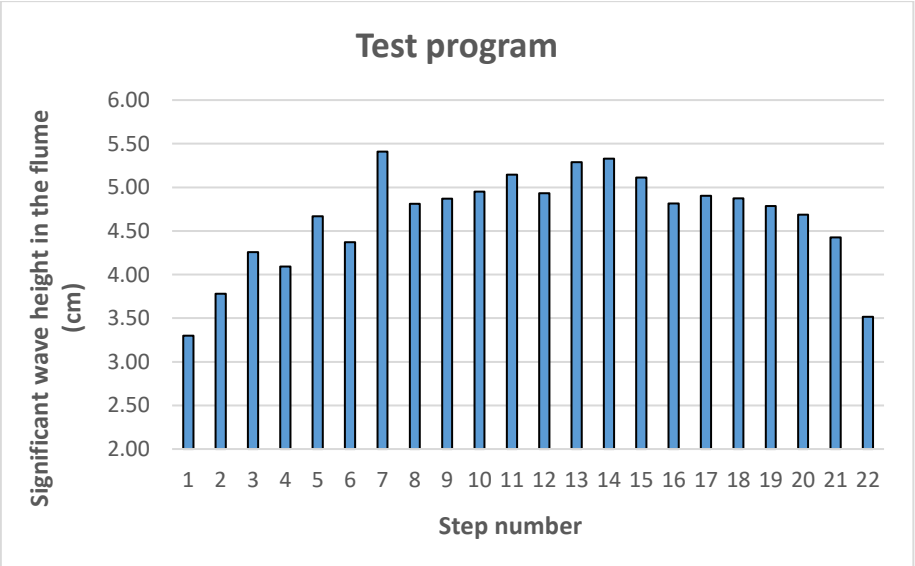


*Figure 37. Test program of the real storm.*

| *Step number* | *Significant wave height (cm)* | *Step number* | *Significant wave height (cm)* |
|---|---|---|---|
| 1 | 3.31 | 12 | 4.93 |
| 2 | 3.78 | 13 | 5.29 |
| 3 | 4.26 | 14 | 5.33 |
| 4 | 4.09 | 15 | 5.11 |
| 5 | 4.67 | 16 | 4.82 |
| 6 | 4.37 | 17 | 4.90 |
| 7 | 5.41 | 18 | 4.87 |
| 8 | 4.81 | 19 | 4.79 |
| 9 | 4.87 | 20 | 4.69 |
| 10 | 4.95 | 21 | 4.42 |
| 11 | 5.14 | 22 | 3.52 |

*Table 4. Wave data applied in the flume for the real storm.*

Concerning the wave period, for the real storm the peak period associated to the different significant wave height is used. Then, these values of $T_p$, as they are temporal variables, are escalated with a scaling factor of $\sqrt{\lambda}$ ($\sqrt{80}$) seen in the Chapter 3.1.3. To know the number of waves associated to each step number (1 h), the expression ( 43 ) must be used. On average, the test steps are composed of 320 waves and the peak period is about 1.26 s. The total number of waves of each test is 7.040 waves.

This test program for the real storm is executed 5 times in the flume for this work. Other 10 tests were carried out previously by other master students.

### Trapezoidal storm

The real storm is transformed in a synthetic storm defined with a trapezium shape. This transformation has already been deeply explained in the Chapter 3.2.2. Using the same criterion as in the real storm, the test program for this synthetic storm is also divided in steps that represent each one 1 h in the reality. The total number of steps is 21 and the significant wave height at the peak, 4.33 m. This wave height is maintained at that level during an interval of 5 h.

For the synthetic storm, the steepness is chosen constant and equal to 0.02, although in the wave climate analyses, the wave steepness normally decreases after the peak.

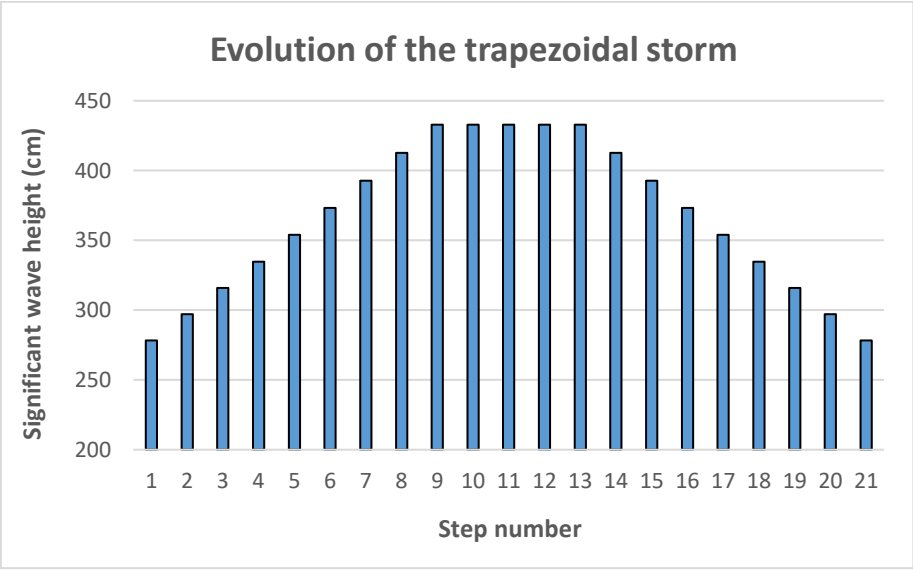


*Figure 38. Evolution of the trapezoidal storm before the scaling of the wave data.*

As it is done with the real storm, and in order to create the test plan used in the flume, these values of wave heights must be scaled down with a factor of λ=80. The evolution of the significant wave heights in the flume scale is shown in the next figure. The peak of the storm is maintained from the step 9 to the step 13.

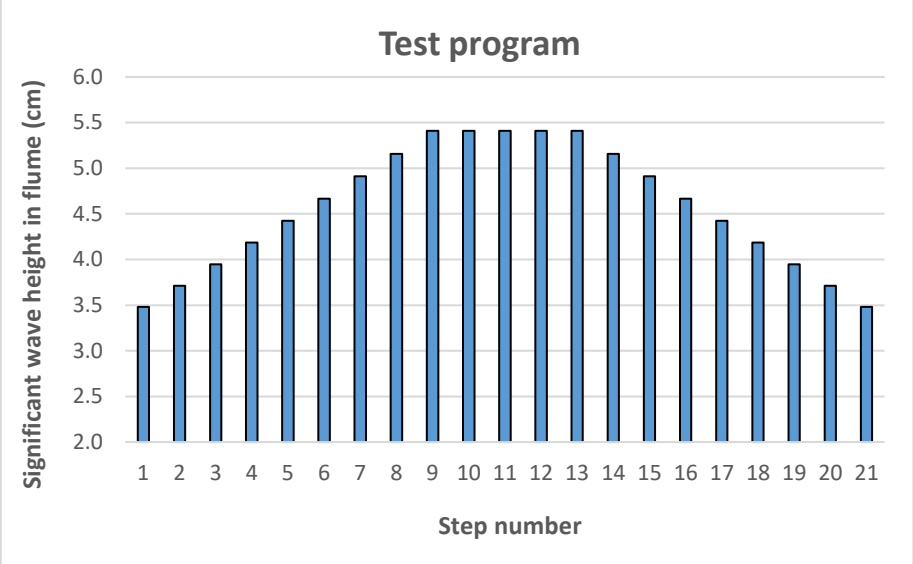


*Figure 39. Test program of the trapezoidal storm.*

| *Step number* | *Significant wave height (cm)* |
|---|---|
| 1 | 3.48 |
| 2 | 3.71 |
| 3 | 3.95 |
| 4 | 4.18 |
| 5 | 4.42 |
| 6 | 4.67 |
| 7 | 4.91 |
| 8 | 5.16 |
| 9 | 5.41 |
| 10 | 5.41 |
| 11 | 5.41 |

| *Step number* | *Significant wave height (cm)* |
|---|---|
| 12 | 5.41 |
| 13 | 5.41 |
| 14 | 5.16 |
| 15 | 4.91 |
| 16 | 4.67 |
| 17 | 4.42 |
| 18 | 4.18 |
| 19 | 3.95 |
| 20 | 3.71 |
| 21 | 3.48 |

*Table 5. Wave data applied in the flume for the trapezoidal storm.*

Regarding the peak period and the number of waves of each step, they are calculated by the same way than for real storm. On average, the test steps are composed of 337 waves and the peak period is about 1.20 s. The total number of waves of each test is 7.084 waves.

This test program for the trapezoidal storm is executed 10 times for this work, from which 6 of them have the same wave seeding for the random generation of the wave pattern. Unlike the real storm and the other tests that are going to be explained in the following lines other storms, this one has been developed exclusively by the author.

### Other tests

Triangular storm

The real storm is transformed into a synthetic one with triangular shape with the EMS model explained in the Chapter 2.3.2. Each step in which the test program corresponding to this storm is divided is equal to 1 h duration in the reality. To obtain the same magnitude for this synthetic storm than for the real one, and knowing that the significant wave height peak is the same (4.33 m) for both the synthetic and the real storm, the total number of steps should be approximately 28. Although this total number, it was checked that after the 23th step, the water did not cause damage anymore. Therefore, the total number of steps introduced in the flume is 23.

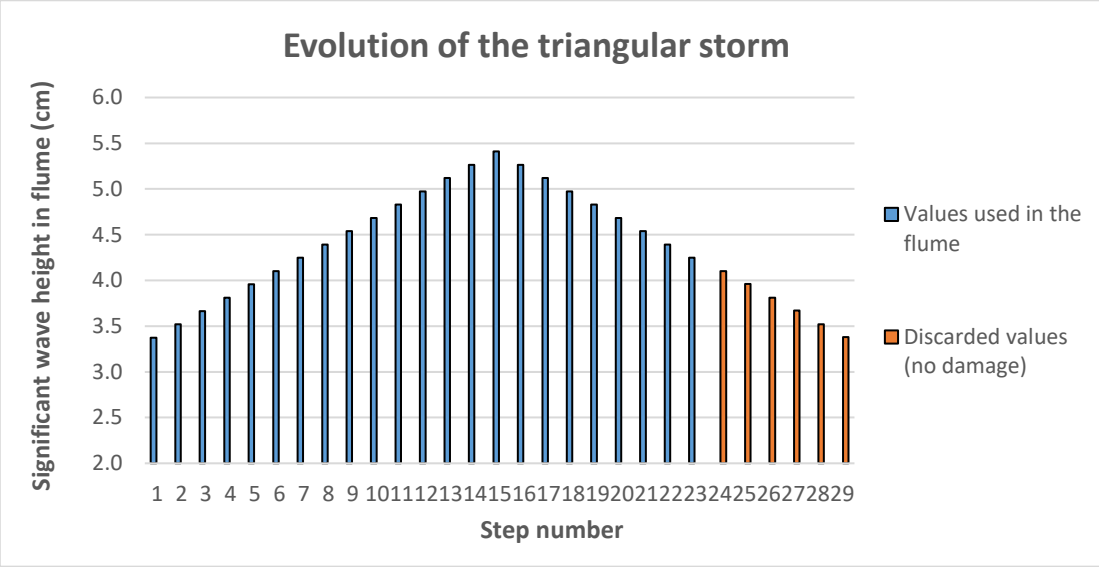


*Figure 40. Evolution of the triangular storm before the scaling of the wave data.*

The wave steepness is also chosen constant and equal to 0.02 as for the other test methodologies. The significant wave height of the peak in this synthetic storm is the same as in the real storm, 4.33 m, which corresponds to a significant wave height of 5.41 cm in the flume. The period associated to this peak is 11.8 s and it is achieved at the step 15.

The following graphic shows the wave data values introduced in the flume without taking into account the steps going from 24 to 28 because of the non-observed damage.

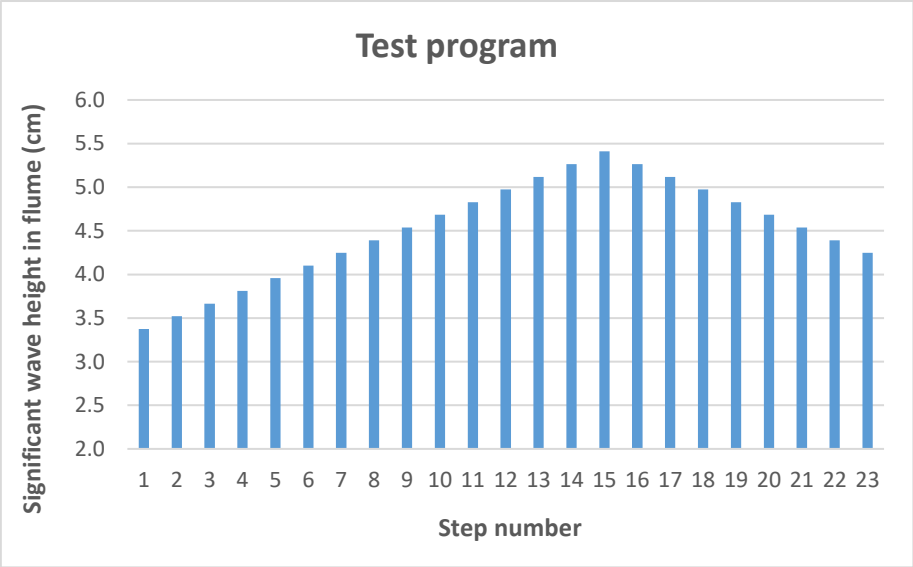


*Figure 41. Test program of the triangular storm.*

| *Step number* | *Significant wave height (cm)* |
|---|---|
| 1 | 3.38 |
| 2 | 3.52 |
| 3 | 3.67 |
| 4 | 3.81 |
| 5 | 3.96 |
| 6 | 4.10 |
| 7 | 4.25 |
| 8 | 4.39 |
| 9 | 4.54 |
| 10 | 4.68 |
| 11 | 4.83 |
| 12 | 4.97 |

| *Step number* | *Significant wave height (cm)* |
|---|---|
| 13 | 5.12 |
| 14 | 5.26 |
| 15 | 5.41 |
| 16 | 5.26 |
| 17 | 5.12 |
| 18 | 4.97 |
| 19 | 4.83 |
| 20 | 4.68 |
| 21 | 4.54 |
| 22 | 4.39 |
| 23 | 4.25 |

*Table 6. Wave data applied in the flume for the triangular storm.*

Once the peak period and the number of waves of each steps are obtained with the same formulation as for the other storms, it can be conclude that on average, the test steps are composed of 355 waves and the peak period is about 1.16 s. The total number of waves of each test is 8.170 waves.

Unlike the real and trapezoidal storm, it has been not tested for the work of this Thesis, but the data available of the experiments with this synthetic triangular storm done previously (10 in total) are exposed to have a general overview of the damage.

Classical testing method

In the classical testing method proposed by Owen and Allsop (1984), the breakwater must be subjected to the action of the waves with an increasing of the significant wave height from the 60% of the significant wave height of the storm peak until the 120% of it, passing through the 80% and 100%.

A typical number of waves used in this kind of experiments for every test is about 1000 waves. Unfortunately, due to the large number of waves per step (1000 waves per hour in reality does

not happen), the $H_{s,target}$ is not the same as the produced by the flume. In order to overcome this problem, the testing method is adapted accordingly to maintain a comparable level of damage with the other kind of storms. The result is to split these 1000 waves in 3 steps of 330 waves for each significant wave height. Since this total duration after the change is the same, the errors observed are similar and only the number of waves is decreased. The important point is that wave generation seeding must be different in the 3 steps in order to ensure different wave patterns.

Due to the propagation of the storm until a depth of 24 m, the storm peak becomes 4.33 m and the associated peak period is 11.8 s. The target values used in the flume for this peak are, after the escalation, equal to 5.41 cm and 1.32 s. The wave periods used will be the peak periods associated to the four values of the significant wave height. The wave steepness is considered constant in order to ensure the increase of the wave period with the increase of the wave height.

The representative tables of both classical testing method with 1000 waves and 3x330 waves used are presented below. These tables are constructed with the $H_s$(cm), $T_p$(s) and $N_z$. The total number of waves of the complete tests is 4000 waves for one and 3960 for the other, so practically the same.

| Name | | $H_s$ (cm) | $T_p$ (s) | $N_z$ (-) |
|---|---|---|---|---|
| **60% $H_{s,peak}$** | Step 1 | 3.24 | 1 | 1000 |
| **80% $H_{s,peak}$** | Step 2 | 4.32 | 1.16 | 1000 |
| **$H_{s,peak}$** | Step 3 | 5.41 | 1.32 | 1000 |
| **120% $H_{s,peak}$** | Step 4 | 6.48 | 1.42 | 1000 |

*Table 7. Wave data applied in the flume for classical method with 1000 waves.*

| Name | | $H_s$ (cm) | $T_p$ (s) | $N_z$ (-) |
|---|---|---|---|---|
| **60% $H_{s,peak}$** | Step 1 | 3.24 | 1 | 330 |
| | Step 2 | 3.24 | 1 | 330 |
| | Step 3 | 3.24 | 1 | 330 |
| **80% $H_{s,peak}$** | Step 4 | 4.32 | 1.16 | 330 |
| | Step 5 | 4.32 | 1.16 | 330 |
| | Step 6 | 4.32 | 1.16 | 330 |
| **$H_{s,peak}$** | Step 7 | 5.41 | 1.32 | 330 |
| | Step 8 | 5.41 | 1.32 | 330 |
| | Step 9 | 5.41 | 1.32 | 330 |
| **$H_{s,peak}$** | Step 10 | 6.48 | 1.42 | 330 |
| | Step 11 | 6.48 | 1.42 | 330 |
| | Step 12 | 6.48 | 1.42 | 330 |

*Table 8. Wave data applied in the flume for classical method with 3x330 waves.*

The total steps of the test plan for the classical testing method are 4, with 1000 waves each test, while for the method with 3x330 waves the total steps are 12. From this 12 steps, the first three are related to the first significant wave height (60% of the $H_{s,peak}$), the next three to the second one and so on.

These evolutions can also be represented in visual graphics.

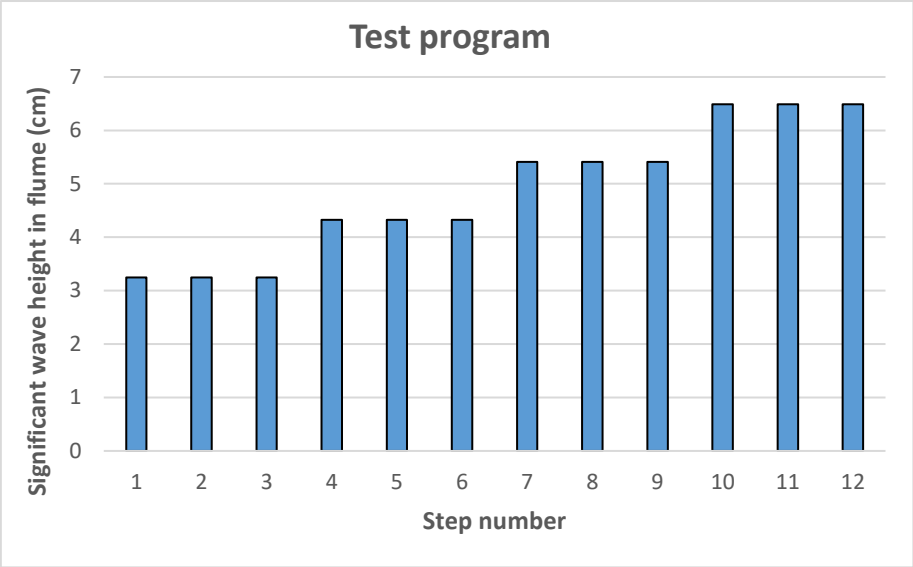


*Figure 42. Test program of the classical testing method with 3x330 waves.*

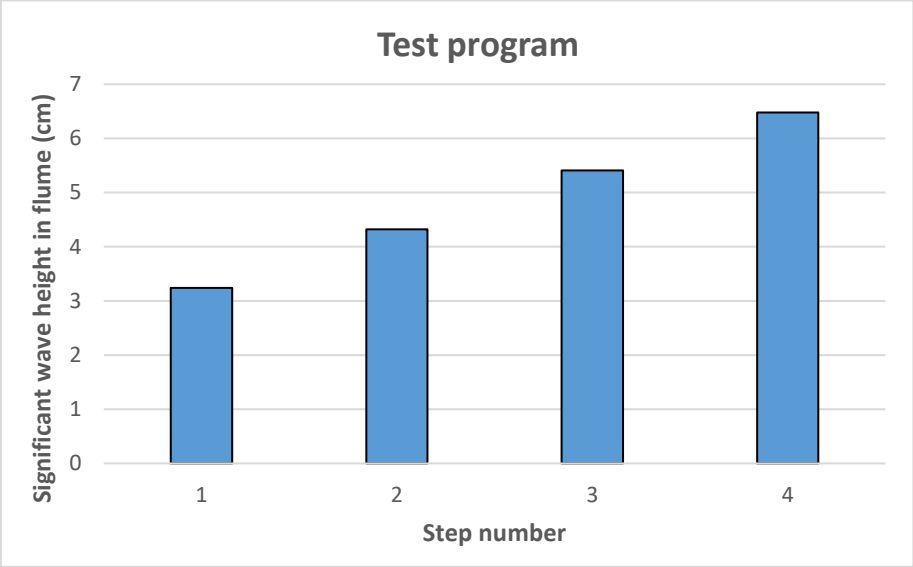


*Figure 43. Test program of the classical testing method with 1000 waves.*

As it happened with the triangular synthetic storm, these test programs were executed many times before this work (5 tests of the classical 1000 and 10 for the classical 3x330), so the damage results obtained are presented with the other test methodologies carried out in this Thesis. Due to that fact, it has been considered important to define how is this classical method structured.

## 3.4. Data analysis

This section of the Thesis explains how the required data is gathered before, during and after the flume testes, and how it is transformed to useful data. This post-processed data will be essential to later assess the damage in the breakwater. In addition, it is described the process of wave data registering in the CIEMGEN v1.2 for each step of each test.

### *3.4.1. Damage quantification*

The quantification of the damage is done with the basic visual counting method. The cubes that have moved more than a distance equal to one nominal diameter are summed up ($N_o$) and then, the relative damage $N_{od}$ is obtained. This parameter, coming from the $N_o$ is obtained after the pre-process and post-process of the data available, explained in the next lines.

As each individual cube is well marked with a unique number in all of its sides, is easy to detect the displacement of each one after every step with the pictures taken by the fixed GoPro (parallel to the breakwater slope).

As summary, the damage is quantified with the parameters:

- Number of armour units moved more than one nominal diameter ($N_o$)
- $N_{od}$

The higher these parameters are, the higher the damage in the breakwater become.

### *3.4.2. Data analysis procedure*

Before having useful data to be process with different software and methodologies in the computer, this must be gathered during the tests, which is called the pre-process. As for all the tests in the flume the actuations are the same, the steps in which the pre-process is divided are only explained for one general case. If there are variations for specific steps, these will be commented while explaining all the process.

#### Gathering data (Pre-process)

The steps to gather the raw data are listed below.

Before the test run

1. *Pictures to later obtain a 3D model of the filter layer*
   Take between 80 and 100 pictures of the filter layer from different angles and positions with the GoPro camera.
2. *Pictures to later obtain a 3D model of the initial armour (2 layers)*
   Take between 80 and 100 pictures of the armour layer from different angles and positions with the GoPro camera.
3. *Capture the initial position of the armour cubes*
   Take 1 picture with the fixed GoPro in a perpendicular direction to the slope of the breakwater structure.
4. *Calibrate the wave gauges*
   Once the water depth in the flume is equal to 30 cm, the different wave gauges must be calibrated in order to be able to register the wave pattern in the flume.

During the test run

5. *Capture the position of the armour cubes after each step*
   Take 1 picture with the fixed GoPro in a perpendicular direction to the slope of the breakwater structure. With all these pictures, an evolution of the cubes movements will be determined.
6. *Pictures to later obtain 3D models of specific steps during a test*
   Take between 80 and 100 pictures of the armour layer from different angles and positions with the GoPro camera after the steps that are control points during the tests, as the peaks of the storm (1 or 2 depending the case) and the final step.
7. *Registration of wave gauge measurements*
   For each test run, the evolution of the wave height measured by the wave gauges must be registered to later use the data.

After the test run

8. *Capture the final position of the armour cubes*
   Take 1 picture with the fixed GoPro in a perpendicular direction to the slope of the breakwater structure.
9. *Pictures to later obtain a 3D model of the final state of the armour layer*
   Take between 80 and 100 pictures of the armour layer from different angles and positions with the GoPro camera.

### Post-processing of the data

Once all the data necessary to evaluate the damage is gathered, this must be processed in the computer. All this processing procedure will give us a quantitative description of the damage, which is interesting for the posterior analysis and comparative. In addition, it can be obtained quantitative data regarding the armour layer thickness in the initial state of all the sets and the evolution of the wave heights measured by the wave gauges in the flume.

This procedure can be divided in ordered steps that are described below with the same structure than the pre-processing. First of all, the steps to generate the 3D models from the pictures taken before and during the test are listed. Then, there is explained how to get the essential parameters to describe the damage.

#### Creation of 3D models

1. *Compile the pictures to create a 3D model*
   The pictures taken in the steps 1,2, 6 and 8 of the pre-processing are uploaded to the website in a free software of the AutoCAD firm called Autodesk Recap 360. This software uses all this pictures to construct a 3D model.
2. *Same scale and orientation of all the 3D models*
   The file '.obj' must be downloaded from the software and the constructed model must be scaled. The control points (4 in total) must be inserted with the exact coordinates in order to reference the model.
3. *Conversion of the '.obj' file to a '.xyz' file*
   With this conversion, it is guaranteed that the Matlab program will be able to read this new extension of the files generated. Matlab will be an indispensable tool to generate all the data related to the damage.

4. *Obtain 3D model or matrix with only the armour layer*
   Subtract the filter layer from the armour layer model (which englobes all the structure) in order to have a representative model only containing the armour layer. This can be done in the steps where pictures have been taken to create a 3D model.

Damage parameters

1. *Select pictures taken with the fixed GoPro of the steps with 3D model*
   The pictures taken with the fixed GoPro in the step 5 of the pre-processing in the steps where a 3D model is created (generally the peak/s of the storm and the final step) are selected. The first picture taken after the armour layer construction (step 3 of the pre-processing) also will be used as an initial reference.
2. *Open the initial armour layer picture with the Photoshop program*
   The first picture taken perpendicular to the breakwater slope of each step is open with the Photoshop format.
3. *Number the cubes*
   The blocks of the initial armour layer are numbered using the Photoshop tools by texting each number in the centre of the cubes position.
4. *Follow the tracks of the moved cubes*
   Using the reference of the initial armour layer picture, the second selected picture is open with Photoshop and the texts with the number of the cubes that have been displaced are moved until they are located once again in the respective centres. This procedure is done successively with the other pictures, always taking as a reference the previous ones.
5. *Conversion of Photoshop files to '.txt' files and read files with Matlab*
   The Photoshop files are converted to '.txt.' files called '*GetLayers*', which express the positions of all the armour layer cubes with the coordinates with respect to a fixed referenced point. The extension '.txt' is readable by Matlab, being able to give use results of the number of blocks displaced and therefore, results of the necessary relative damage $N_{od}$ .

Wave gauge measurements

1. *Compilation of registrations in the server*
   The files with the registrations of the wave height measurements done by the wave gauges are transferred from the computer connected to the flume to the server. These are files with extension '.dat'.
2. *Conversion of registration files to '.txt' and read files with Matlab*
   The files are converted to text files in order to be readable by Matlab.

## Processing results

### 3D models

The 3D models are constructed with the compilation of several pictures taken with GoPro from different angles and positions of the structure. With a minimum of 60-70 pictures the results of the generated 3D model can be accurate enough, but if more pictures are taken (in the case of this Thesis around 100) the AutoCAD software has more input data to create a better version of the 3D. In addition, if some pictures have problems of shadows or low resolution quality, these can be deleted without affecting too much at the total number of pictures, which remains high enough.

After that, these pictures are uploaded to the Autodesk Recap 360, which is a cloud based 3D modelling software. Even with limited options with respect the paying Recap 360 software, it still gives us a point cloud detailed and accurate enough, which enable us to assess the damage in the breakwater. The final 3D model is produced after approximate 2 h of processing. This model, which is shown in the Figure 44, can be downloaded as an object file.

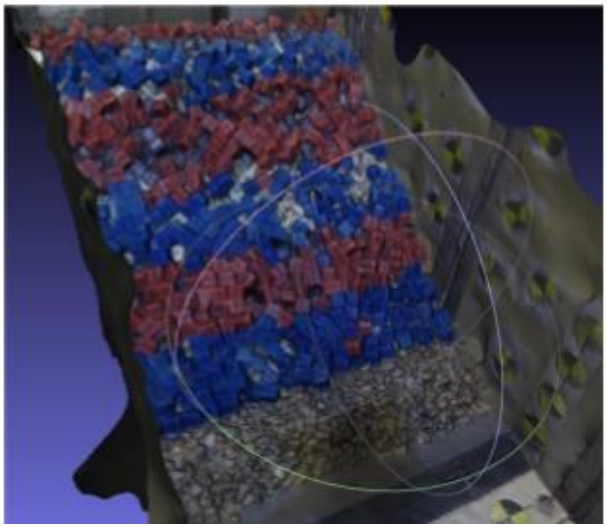

*Figure 44. Example of 3D model generated with the AutoCAD software.*

This 3D model is not in the real scale and also is not yet in the correct position. In order to scale and reference it, 4 markers with black and yellow colours are placed 2 in the top of the coronation and 2 in the front of the toe. These locations are fixed for all the experiments.

The exact coordinates of the different markers are determined with respect to one of them, which serves as the origin. The coordinates of the four reference points in (x,y,x) format in mm are:

- (0,0,0)
- (229.5,0,0)
- (0,712,227.5)
- (222,712,227.5)

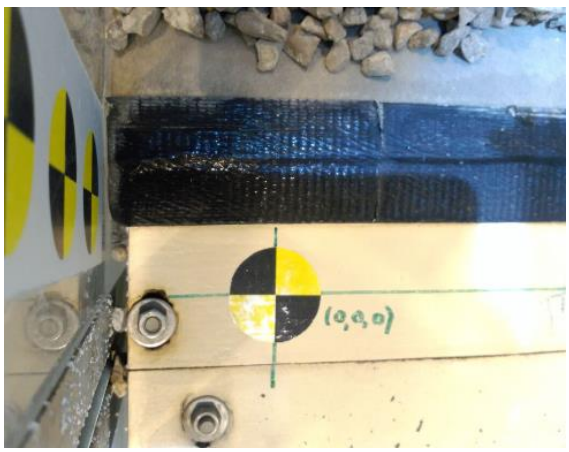


*Figure 45. Marker with the coordinates (0,0,0) of the models.*


*Figure 46. Reference points of the 3D model.*

The errors induced by inaccurate precision when selecting the four points at the screen are given by the program in a text file and can be used later for different calculations.

As the object file created by AutoCAD cannot be read by Matlab, this must be transformed into a '.xyz' file, which is another kind of extension. For each test run in the flume, regardless of the test methodology, the models of the filter layer (step 1 of the pre-processing) and the initial state of the armour layer (step 2 of the pre-processing) are always generated. What respect the 3D models after specific steps, these can vary depending on the test methodology.

The '.xyz' file created by Matlab generates a figure as the one showed in the Figure 47. In addition, and by subtracting the filter layer from the armour layer, another model with only the irregularities of the armour layer is obtained and showed in the right position of the same figure. In this new model, with the same extension '.xyz', the slope of the breakwater is presented in a horizontal way.

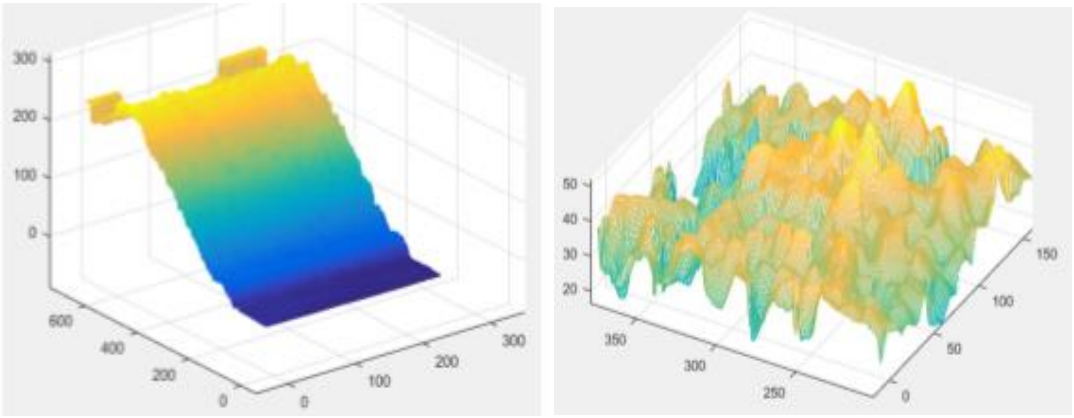


*Figure 47. '.xyz' model of the filter layer in Matlab and '.xyz' model with only the armour layer variation.*

While the first '.xyz' file is used to see the variation in the filter layer and the armour layer along the slope of the breakwater, the second '.xyz' file is necessary to calculate the average thickness of the armour layer. With this thickness value, which depends always on the cubes placement, it can be checked the porosity of the structure.

This average thickness value of the initial state of the armour layer will be computed for each step of each kind of storm. A specific script of Matlab will be defined in order to get these values.

Damage parameters

First of all, the pictures taken with the fixed GoPro in the steps where a 3D is created are selected. Taking as an example the real storm, the pictures needed are the one of the initial state of the armour layer (always, regardless the test methodology), the one of the 1st peak, the one of the 2nd peak and the one of the final step.

The picture of the initial state is opened with the Photoshop program and the numbers are texted in the centre position of each block. Then, with the following picture, and using as reference the first one, the movement of each single cube can be tracked down just moving the written number until the centre of the new position. This procedure is done with all the pictures, taking always as a reference the previous one in order to have smaller movements.

The following two images represent the first picture selected of the armour layer (initial state) with the numbers positioned in the centre of the blocks and the second selected picture (related to the 1st peak) with some blocks displaced, leading to have numbers not in the centre of the blocks.

As each block is defined with a unique number, it can be clearly seen the initial position and its position in the specific state considered.

*Figure 48. Numbered cubes in the initial state of the armour layer and after a specific step.*

From all the movements observed of the cubes comparing the numbers position between two pictures, the ones that will count to the final damage are those cubes that have moved more than one nominal diameter. As it cannot be assessed visually, the positions of the numbers must be determined exactly from a reference point.

To do that, and after having all the selected pictures saved in the Photoshop format, these files are converted to '.txt' files, where all the positions of the cubes are described with coordinates x, y and z with respect to the mentioned reference point.

130217_01_GetLayers.txt

| | | | | | | | | | |
|---|---|---|---|---|---|---|---|---|---|
| 1 | 460 | 2773 | cm | 1976 | cm | 2817 | cm | 1996 | cm |
| 2 | 578 | 2681 | cm | 1999 | cm | 2723 | cm | 2019 | cm |
| 3 | 445 | 2594 | cm | 2015 | cm | 2637 | cm | 2035 | cm |
| 4 | 580 | 2498 | cm | 2006 | cm | 2541 | cm | 2026 | cm |
| 5 | 559 | 2405 | cm | 2008 | cm | 2448 | cm | 2028 | cm |
| 6 | 612 | 2306 | cm | 2026 | cm | 2349 | cm | 2046 | cm |
| 7 | 442 | 2213 | cm | 2002 | cm | 2257 | cm | 2022 | cm |
| 8 | 485 | 2110 | cm | 2032 | cm | 2153 | cm | 2052 | cm |
| 9 | 650 | 2028 | cm | 2039 | cm | 2071 | cm | 2059 | cm |
| 10 | 647 | 1927 | cm | 2059 | cm | 1970 | cm | 2079 | cm |
| 11 | 603 | 1823 | cm | 2072 | cm | 1865 | cm | 2092 | cm |
| 12 | 505 | 1725 | cm | 2049 | cm | 1767 | cm | 2069 | cm |
| 13 | 589 | 1642 | cm | 2041 | cm | 1685 | cm | 2061 | cm |
| 14 | 583 | 1563 | cm | 2046 | cm | 1605 | cm | 2066 | cm |
| 15 | 628 | 1456 | cm | 2060 | cm | 1499 | cm | 2080 | cm |
| 16 | 510 | 1364 | cm | 2035 | cm | 1407 | cm | 2055 | cm |
| 17 | 617 | 1280 | cm | 2061 | cm | 1323 | cm | 2081 | cm |
| 18 | 638 | 1279 | cm | 1981 | cm | 1322 | cm | 2001 | cm |
| 19 | 515 | 1365 | cm | 1962 | cm | 1407 | cm | 1982 | cm |
| 20 | 573 | 1439 | cm | 1953 | cm | 1480 | cm | 1973 | cm |

130217_8_GetLayers.txt

| | | | | | | | | | |
|---|---|---|---|---|---|---|---|---|---|
| 1 | 460 | 2775 | cm | 1986 | cm | 2819 | cm | 2006 | cm |
| 2 | 578 | 2694 | cm | 2035 | cm | 2736 | cm | 2055 | cm |
| 3 | 445 | 2593 | cm | 2016 | cm | 2636 | cm | 2036 | cm |
| 4 | 580 | 2497 | cm | 2019 | cm | 2540 | cm | 2039 | cm |
| 5 | 559 | 2404 | cm | 2009 | cm | 2447 | cm | 2029 | cm |
| 6 | 612 | 2305 | cm | 2027 | cm | 2348 | cm | 2047 | cm |
| 7 | 442 | 2212 | cm | 2003 | cm | 2256 | cm | 2023 | cm |
| 8 | 485 | 2109 | cm | 2033 | cm | 2152 | cm | 2053 | cm |
| 9 | 650 | 2027 | cm | 2040 | cm | 2070 | cm | 2060 | cm |
| 10 | 647 | 1926 | cm | 2060 | cm | 1969 | cm | 2080 | cm |
| 11 | 603 | 1829 | cm | 2080 | cm | 1871 | cm | 2100 | cm |
| 12 | 505 | 1724 | cm | 2050 | cm | 1766 | cm | 2070 | cm |
| 13 | 589 | 1641 | cm | 2042 | cm | 1684 | cm | 2062 | cm |
| 14 | 583 | 1562 | cm | 2047 | cm | 1604 | cm | 2067 | cm |
| 15 | 628 | 1455 | cm | 2061 | cm | 1498 | cm | 2081 | cm |
| 16 | 510 | 1363 | cm | 2036 | cm | 1406 | cm | 2056 | cm |
| 17 | 617 | 1277 | cm | 2073 | cm | 1320 | cm | 2093 | cm |
| 18 | 638 | 1278 | cm | 1982 | cm | 1321 | cm | 2002 | cm |
| 19 | 515 | 1364 | cm | 1976 | cm | 1406 | cm | 1996 | cm |
| 20 | 573 | 1427 | cm | 1966 | cm | 1468 | cm | 1986 | cm |

*Figure 49. Positions of the cubes in the initial state and after a specific step of a test.*

These files can now be read by Matlab, which with one script will construct a path tracking of all the cubes moved more than one diameter Figure 50.

This Matlab script draws an arrow between two specified locations of the same cube based in the work done with the pictures taken by the fixed GoPro with the Photoshop program and the '.txt' files. These arrows will only be drawn if the distance between both locations for each cube is more than a fixed threshold equal to one nominal diameter. The number of arrows determine the number of displaced blocks ($N_o$) and therefore, the parameter $N_{od}$ can be determined directly with the formulas presented in the Chapter 2.2.2.

An example of path tracking can be observed in the following pictures.

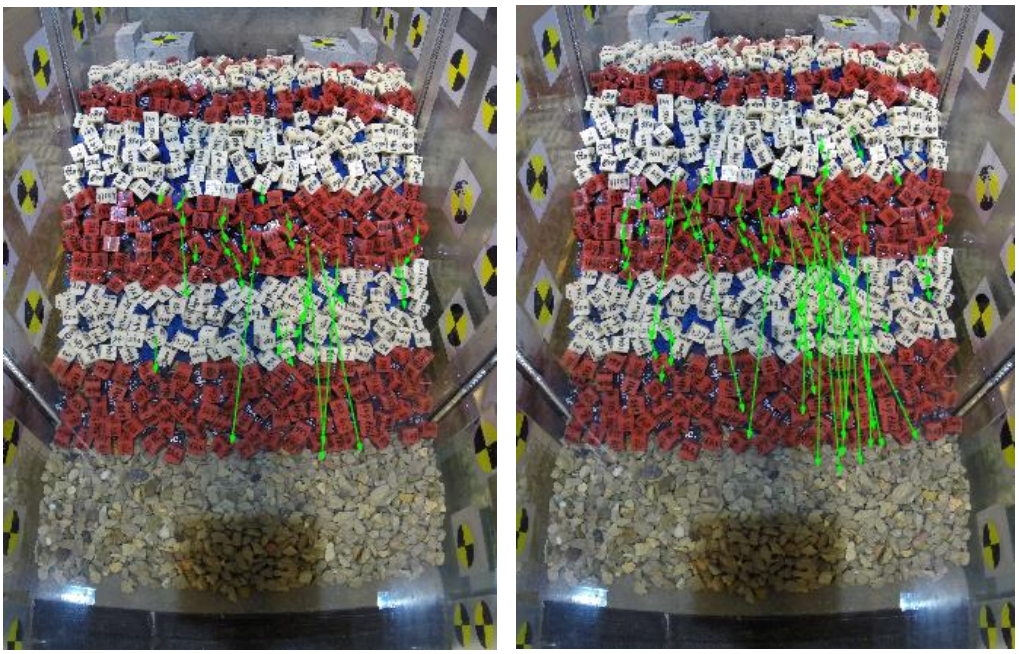

*Figure 50. Tracking map of the cubes moved more than one diameter until the 1st peak and the 2nd peak for the trapezoidal storm.*

In these figures can be noticed that lots of arrows are created, indicating that a great number of blocks in the armour layer have been displaced more than one nominal diameter. The more arrows are generated, the higher is the damage in the structure.

The damage parameters are given after the run as it is seen in the Figure 51.

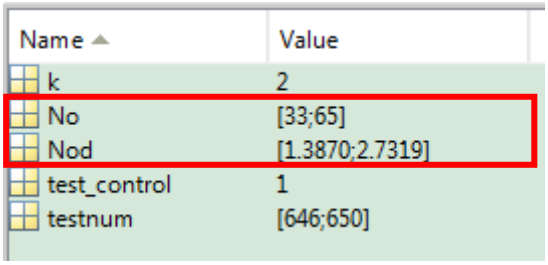


*Figure 51. Visual result of damage parameters $N_o$ and $N_{od}$ .*

### *3.4.3. Obtained data*

The data used for this report come from the following storms reproduced in the flume:

- ***Real storm***
- ***Synthetic storm (trapezium)***
- ***Synthetic storm (triangle)***
- ***Classical method***
  - 3x330 waves
  - 1000 waves

The synthetic storm with the trapezium shape is tested exclusively for this Thesis. In addition, some tests of the real storm have been carried out in order to complement some that were developed. On the other hand, the other storm methodologies have not been reproduced in the flume for this Thesis. However, what concerns the post-process to obtain the damage data, it has been executed for all the test methodologies presented.

For each test, the data is collected in a UPC server. The tests plans, the output wave data and the pictures with the fixed GoPro after each step of every test are saved.

The 3D models required for each kind of storm are the ones of the filter layer, the initial state of the armour layer and the final state of the armour layer. Some other 3D are constructed in specific intermediate control points of the storm (peaks).

In relation with the 3D models, the damage values $N_o$ and $N_{od}$ are also obtained for the peaks of the storms (at the 100% $H_{s,peak}$ and 120% $H_{s,peak}$ steps when talking about classical testing method) and at the final step. In addition, for 1 test of each storm, $N_o$ and $N_{od}$ are obtained for every single step

The total experiments carried out for each storm are listed below:

- ***Real storm***
  15 experiments from set 1 to set 15. The last 5 are the ones reproduced during this work.
- ***Synthetic storm (trapezium)***
  10 experiments fro set 1 to set 10 (all reproduced during this work).
- ***Synthetic storm (triangle)***
  10 experiments from set 1 to set 10.

- ***Classical method 3x330 waves***
  10 experiments from set 1 to set 11. The 8th experiment is not valid due to problems with pictures.
- ***Classical method 1000 waves***
  5 experiments from set 1 to set 5.

In the next tables are marked with a cross the steps where $N_o$ and $N_{od}$ are available.

| Real storm | | | |
|---|---|---|---|
| Step number | 1rst peak | 2nd peak | Final |
| | 7 | 14 | 22 |
| Set 1 | x | x | x |
| Set 2 | x | x | x |
| Set 3 | x | x | x |
| Set 4 | x | x | x |
| Set 5 | x | x | x |
| Set 6 | x | x | x |
| Set 7 | x | x | x |
| Set 8 | x | x | x |
| Set 9 | x | x | x |
| Set 10 | x | x | x |
| Set 11 | x | x | x |
| Set 12 | x | x | x |
| Set 13 | x | x | x |
| Set 14 | x | x | x |
| Set 15 | x | x | x |

| Triangle storm | | |
|---|---|---|
| Step number | Peak | Final |
| | 15 | 23 |
| Set 1 | x | x |
| Set 2 | x | x |
| Set 3 | x | x |
| Set 4 | x | x |
| Set 5 | x | x |
| Set 6 | x | x |
| Set 7 | x | x |
| Set 8 | x | x |
| Set 9 | x | x |
| Set 10 | x | x |

| Trapezium storm | | | |
|---|---|---|---|
| Step number | 1rst peak | 2nd peak | Final |
| | 9 | 13 | 21 |
| Set 1 | x | x | x |
| Set 2 | x | x | x |
| Set 3 | x | x | x |
| Set 4 | x | x | x |
| Set 5 | x | x | x |
| Set 6 | x | x | x |
| Set 7 | x | x | x |
| Set 8 | x | x | x |
| Set 9 | x | x | x |
| Set 10 | x | x | x |

| Classical 3x330 | | |
|---|---|---|
| Step number | 100% Hs,peak | 120% Hs,peak |
| | 9 | 12 |
| Set 1 | x | x |
| Set 2 | x | x |
| Set 3 | x | x |
| Set 4 | x | |
| Set 5 | x | |
| Set 6 | x | x |
| Set 7 | x | x |
| Set 8 | x | x |
| Set 9 | x | x |
| Set 10 | x | x |

| Classical 1000 | | |
|---|---|---|
| Step number | 100% Hs,peak | 120% Hs,peak |
| | 3 | 4 |
| Set 1 | x | x |
| Set 2 | x | x |
| Set 3 | x | x |
| Set 4 | x | x |
| Set 5 | x | x |

*Table 9. For each test methodology, steps where $N_o$ and $N_{od}$ are obtained.*

This lack of data in some steps is due to the end of the test before the test pan is completed. This happens with the classical testing method with 3x330 waves (set 4 and 5), where after the step with the 100% of the significant wave height at the peak ($H_{s,peak}$), the damage observed was so high that was not considered representative to get these damage parameters.

### *3.4.4. Steps for the test preparation*

The general steps for the preparation of any test in the CIEMito channel are the ones numbered below.

1. The filter layer of the breakwater is prepared to have the fixed slope of the tests (3:2), which profile boundary is drawn in the lateral glass wall serving as a reference. This is done with a wooden plate, leading also to avoid the surface irregularities.
2. Take 80-100 pictures of the filter layer with the GoPro to later create the 3D model.
3. Construction of the armour layer. The cubes of the first layer (black and blue colours) are placed alternating 5 rows of each colour and then 2 rows of each one, when arriving at the top. The construction of the second armour layer follows the same pattern but with red and white cubes, beginning with 5 rows of the red ones. All the rows contain 17 cubes, leading to have the porosity fixed by knowing the flume width.
4. Take 80-100 pictures of the initial state of the armour layer with the GoPro to later create the 3D model.
5. Flume is filled up by auctioning the pump until the water depth has reached 30 cm. This is controlled visually with a marked ruler in the flume glass.
6. Calibration of the wave gauges.
7. First picture with the fixed GoPro of the initial state of the armour layer.
8. Introduction of the wave data (significant wave height, wave period, number of waves…) in the CIEMGEN v1.2 program of the first step of the tested storm.
9. Initiation of the test (duration of 5-6 minutes) with the corresponding registration of the measurements in the computer. The registration is done for about 7 minutes, always with more time than the test duration.
10. When the first step is finished, a picture of the armour layer is taken. This is done after each step until the final one to document the damage progression for each storm.
11. Depending of the need of 3D model…
    a. Repetition of the steps 8,9 and 10 with the following steps of the tests when no 3D model is needed for the step.
    b. If 3D model is needed, the flume is emptied by gravity, 80-100 pictures are taken of the armour layer state of the specific step to later construct the 3D model and finally the flume is filled up until a water depth of 30 cm. Then, the actions of the steps 8, 9 and 10 are executed.
12. After the last step of the experiment, the flume is emptied.
13. Take 80-100 pictures of the final state of the armour layer to later create the 3D model.
14. The armour layer cubes are taken apart of the breakwater.

# 4. RESULTS

This section of the Thesis explains how the analysis of the results is performed. Once the data obtained from the developed experiments are processed, results are obtained and depicted to find similarities and differences between the test methodologies (focusing on real storm and trapezoidal storm).

First of all, the measurements of the wave heights registered by a specific wave gauge in the flume are analysed. The steps for each storm are divided in two groups, the ones with the same wave generation seeding and the ones with different seeding. An important factor that is studied in this chapter is the repeatability of the wave gauge registrations in the cases with the same seeding.

Then, an analysis of the breakwater damage for the different test methodologies is done. With the relative damage $N_{od}$ found from the number of displaced cubes ($N_o$), a quantitative comparison between the trapezoidal storm and real storm is done basing on final damage but also on intermediate representative steps as the peaks.

## 4.1. Checking of wave gauges measurements

To assess the repeatability of the measurements of a specific wave gauge (WG3) for the steps with same wave generation seeding, the existing differences between the respective significant wave heights measured must be done. As tests with the same seeding are generated with the same wave sequences and the procedure to register the water elevation is always the same, the expected significant wave heights should be practically the same. To see that, the average wave height measured for these sets and the standard deviation of these measurements are calculated.

On the other hand, and attaining to tests with different seeding, an analysis of the differences of the significant wave height measured will also be developed. These registered values are compared with the target value to see with how much error are the wave gauges working.

As checking 8 different wave gauges is hard to do and takes lot of time, this process has only be done for the wave gauge 3 (WG3), which is located near the generation paddle. The results obtained for this wave gauge are considered representatively of all the rest, excluding the wave gauges that are out of order for technical problems and need to be repaired for future experiments.

### *4.1.1. Real storm*

For the real storm, the measurements of the significant wave height registered by the WG 3 are saved for the 10 experiments done, including 5 executed previously to this work and the 5 carried out by the author for this work.

Studying the sets with same wave generation seeding (seeding number 7), which are the 1, 2, 3, 4, 5 and 9; the evolution of the significant wave height measured for each of them can be plotted in a graphic like the following.

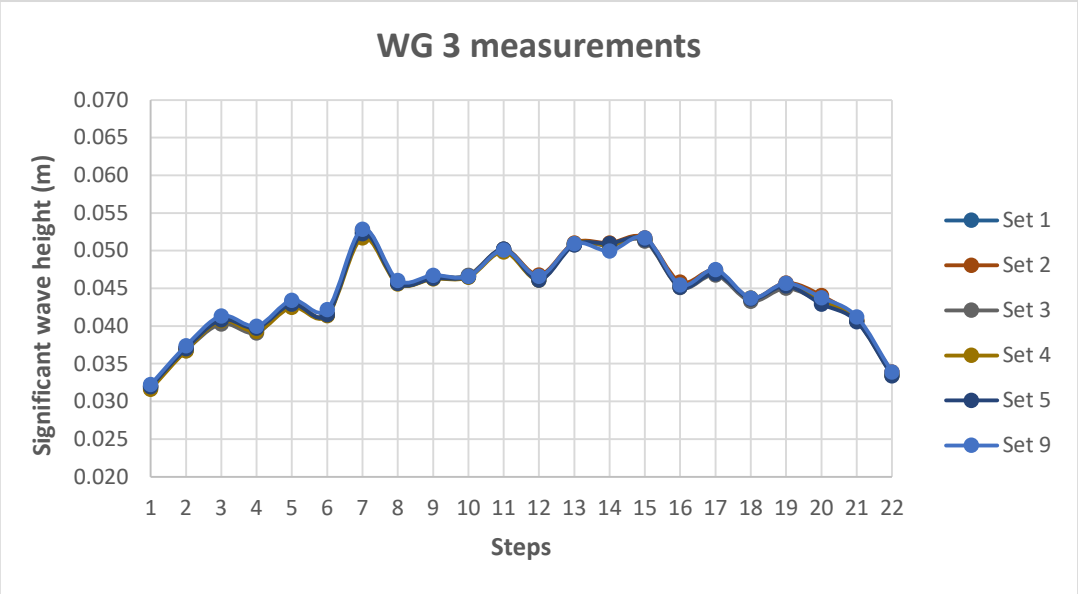


*Figure 52. Evolution of the significant wave height measurements (WG3) for sets with same seeding (Real storm).*

From the graphic it can be affirmed what it was expected: the wave height measurements are practically identic when evaluating sets with the same pattern of wave random generation. There is no remarkable difference between the measurements, allowing us to prove that the wave gauge 3 works properly when the initial conditions of wave generation are the same.

This small variation between measurements can be also represented quantitatively with the standard deviation by knowing the arithmetic mean of the six evolutions.

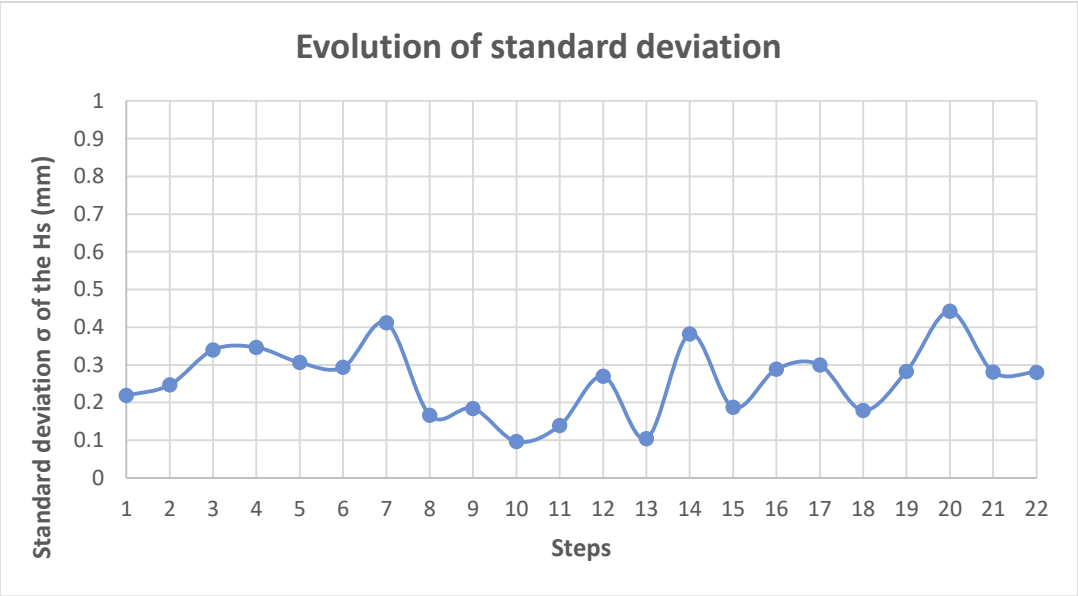


*Figure 53. Standard deviation evolution of the significant wave height measurements of the sets with same seeding for all the steps (Real storm).*

It can be observed that the standard deviation from the measurements of the steps with the same seeding respect the mean is negligible, being 0.4 mm the highest value.

| | |
|---|---|
| **Average standard deviation [mm]** | 0.261 |
| **Maximum standard deviation [mm]** | 0.442 |

The second step is to compare the evolution of the significant wave heights measured by the wave gauge for the tests with different seeding (4 in total) and the evolution of the significant wave height target in the program. It can be observed in the following graphic.

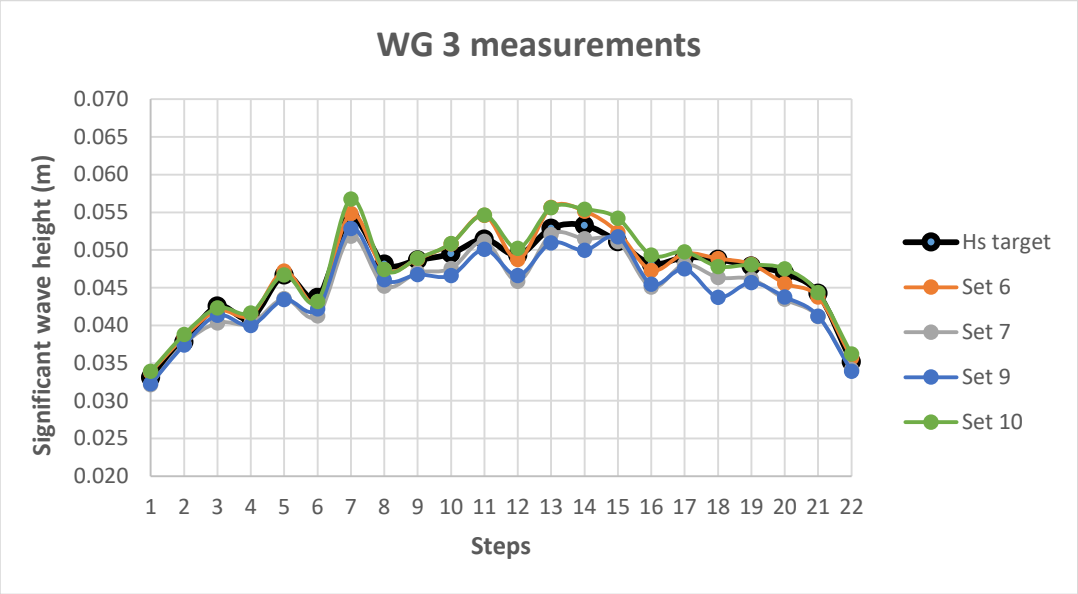


*Figure 54. Evolution of the significant wave height measurements (WG3) for sets with different seeding (Real storm).*

It can be noticed that some measurements are in general higher than the target value, while others are below. This variety in the measurements is due to the different wave generation seeding between the 4 steps. These sets are created with different sequence of waves, leading to different generation processes.

As the sequence of phases are different, the wave gauge registers different water surface evolutions and then, when calculating the significant wave height as a statistical parameter, differences between sets appear.

### *4.1.2. Trapezoidal storm*

The process is the same that for the real storm. The wave gauge registrations done by the WG 3 of the significant wave heights are saved and compared. The total sets evaluated are also 10, being all completed during the work on this Thesis.

Firstly, the measurements of the sets with the same seeding are gathered and plotted to compare them from the step 1 to the step 21. For the trapezoidal storm, the sets 2, 6, 7, 8, 9 and 10 are those with the same seeding (seeding number 2).

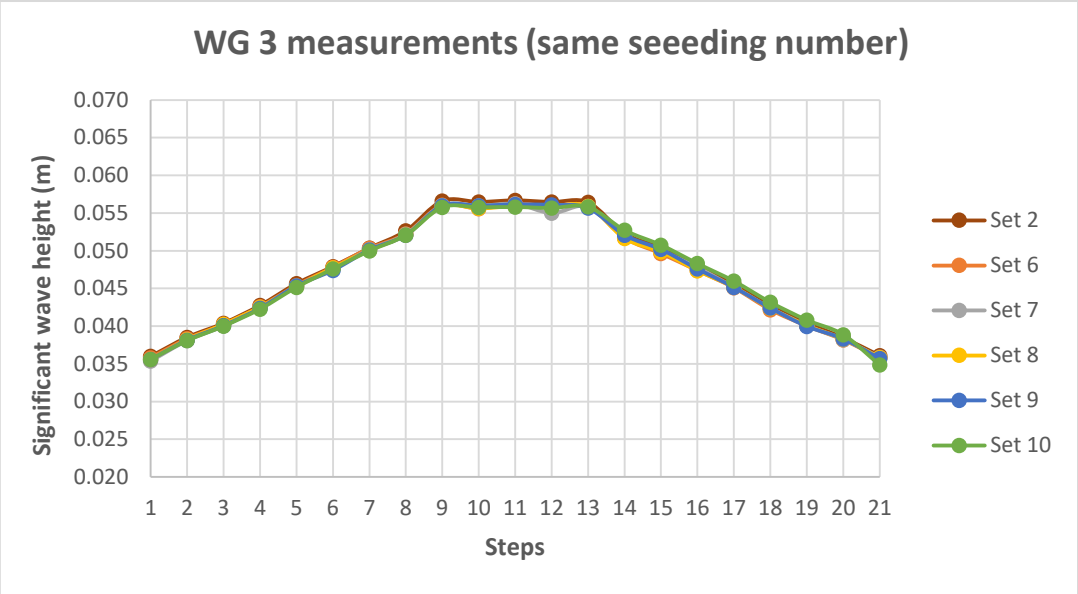


*Figure 55. Evolution of the significant wave height measurements (WG3) for sets with same seeding (Trapezoidal storm).*

As happened with the real storm, and proved by the graphic, the evolutions of the measurements for this six sets are practically identic. Due to the same wave pattern generation that have these sets, the WG 3 registers more less the same evolution of the water surface. Only the measures of the set 2 from the step 9 to 13, which are those composing the peak, are slightly different to the others.

If the arithmetic mean of these 6 evolutions is computed and then the respective standard deviation, the result of the evolution of this variable can be seen in the next graphic.

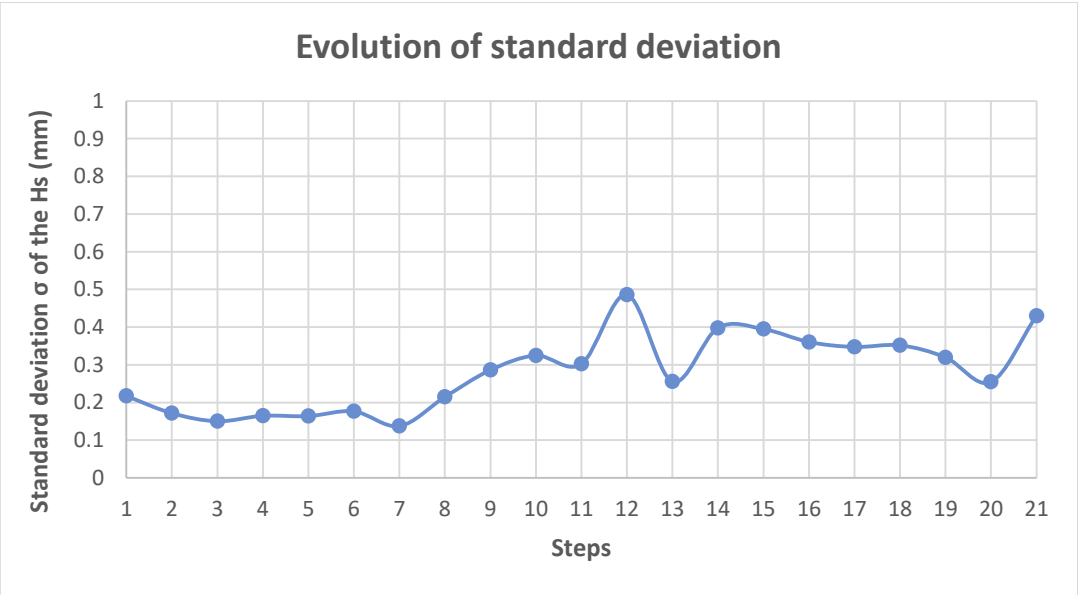


*Figure 56. Standard deviation evolution of the significant wave height measurements of the sets with same seeding for all the steps (Trapezoidal storm).*

It can be noticed that the standard deviation from the measurements of the steps with the same seeding respect the mean is negligible, being 0.48 mm the highest value. This maximum value of the deviation is very similar to the one found in the real storm.

| | |
|---|---|
| **Average standard deviation [mm]** | 0.281 |
| **Maximum standard deviation [mm]** | 0.486 |

Once the sets with same seeding have been assessed, it is time to compare the evolution of the significant wave heights measured by the wave gauge for the tests with different seeding (5 in total) and the evolution of the significant wave height target introduced into the program.

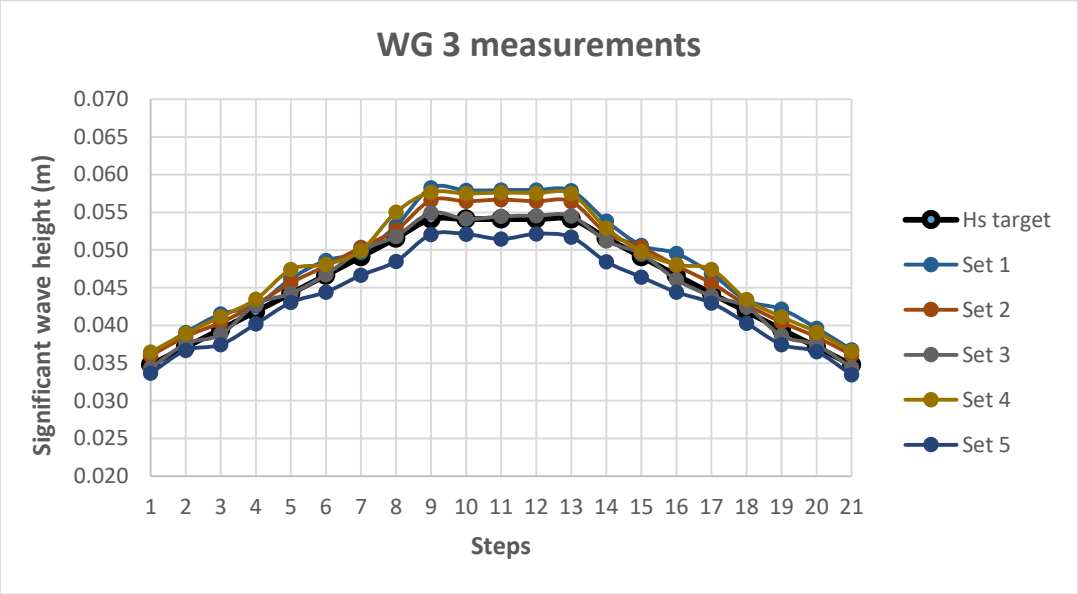


*Figure 57. Evolution of the significant wave height measurements (WG3) for sets with different seeding (Trapezoidal storm).*

For sets with different seeding, the measurements are visually distanced from the target value, being some of them higher than the target value of significant wave height, while others are below.

### *4.1.3. Other tests*

For the triangular storm, the classical testing method with 1000 waves and the classical testing method for the 3x330 waves, the same results are plotted.

Triangular storm

The evolutions of the significant wave height measured for the WG 3 for each set of the triangular storm (10 sets) are analysed and compared, depending on the seeding of each one.

Repeating the process from the other storms, the first graphic includes the evolution of the wave height measurements done for the sets with same seeding, which are the sets 6,7,8,9 and 10.


*Figure 58. Evolution of the significant wave height measurements (WG3) for sets with same seeding (Triangular storm).*

With the exception of the measured significant wave height value in the step 13 of the storm for the set 10, the evolution of the wave height measurements for the sets with the same seeding is practically the same. To show this small variability with numerical values, an evolution of the standard deviation of the evolution with respect the mean can also be plotted.

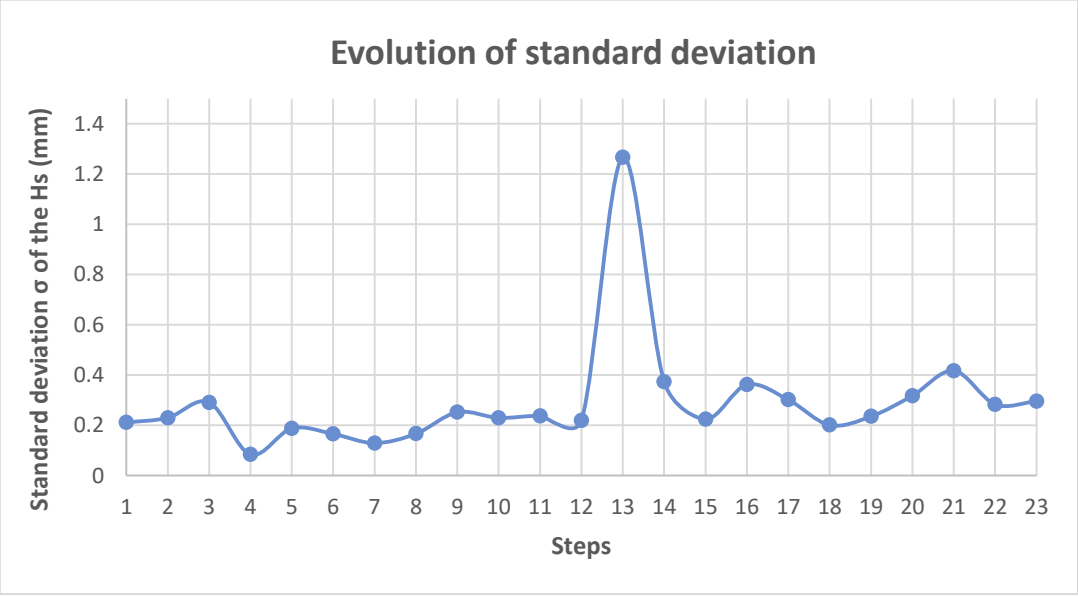


*Figure 59. Standard deviation evolution of the significant wave height measurements of the sets with same seeding for all the steps (Triangular storm).*

The situation seen in the Figure 58 is also seen in this one. The measure in the step 13 of the set 10 is the one that makes that the standard deviation in the same step reaches a higher value in comparison with the others.

| | |
|---|---|
| **Average standard deviation [mm]** | 0.291 |
| **Maximum standard deviation [mm]** | 1.267 |

Regarding the sets with the same seeding (5 in total), the evolutions of the significant wave height measurements with respect the evolution of the target value are observed in the following graphic.

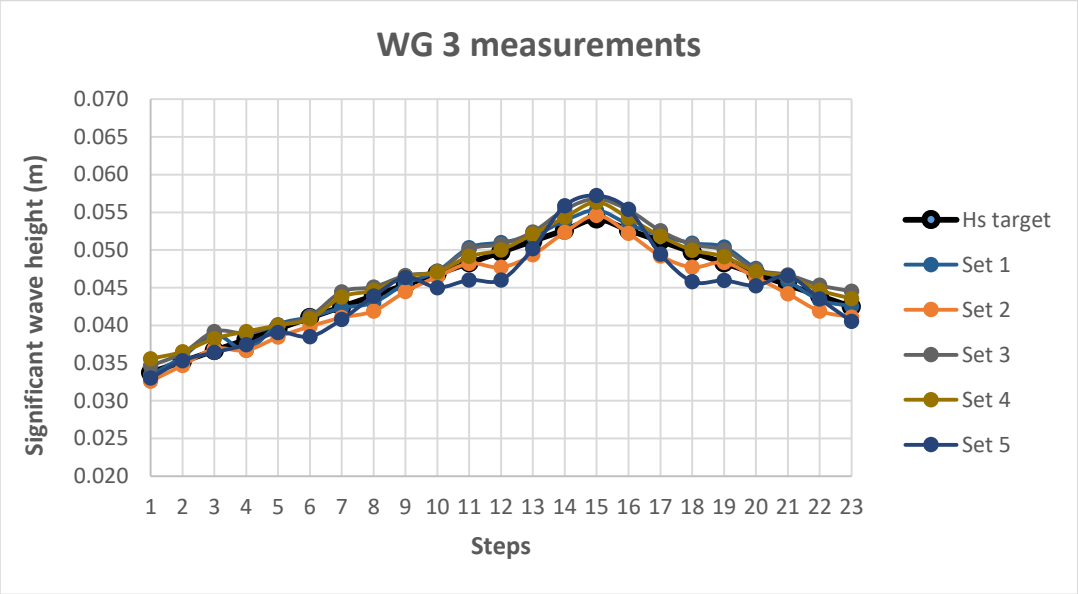


*Figure 60. Evolution of the significant wave height measurements (WG3) for sets with different seeding (Triangular storm).*

The variability between measurements can be clearly observed, differing from the target values due to the generation of waves with different sequences of phases. In particular, the measurements of the set 5 are the ones that follow a more different and irregular tendency with respect the black line, which is the one of the target values.

### Classical testing method 1000 waves

This testing method is the only one that has only been carried 5 times. Unlike the other storms, for this method all the sets have different seeding. Therefore, the analysis of the significant wave height measurements is only done in terms of comparing them with the evolution of the target value.

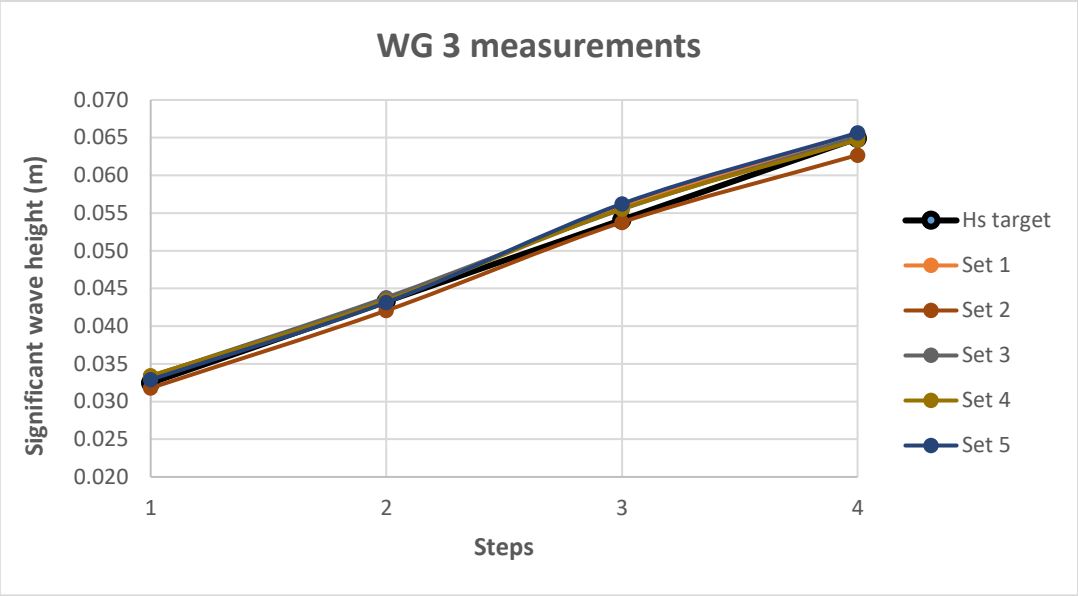


*Figure 61. Evolution of the significant wave height measurements (WG3) for sets with different seeding (Classical testing method 1000 waves).*

The results observed have the same structure than for the other storms when working with sets with different seeding. There is a slightly deviation from the different measurements respect the progression of the target value.

### Classical testing method with 3x330 waves

This classical testing method has been tested 10 times as the real, trapezoidal and triangular storm. In addition, 6 from these 10 sets have the same seeding number sequence. The main difference of this storm from the others is that the seeding number is not unique for each global set. As the test is composed of 12 steps, but with groups of 3 steps with the same wave height target value (60%, 80%, 100% or 120% of the $H_{s,peak}$), the seeding is different between the sets of each group of 3, but the same sequence of seeding between groups.

To illustrate this seeding sequence, an example of a specific set is presented in the Table 10.

| Steps | Seeding number | $H_{s,target}$(m) |
|---|---|---|
| 1 | 19 | 0.032 |
| 2 | 20 | 0.032 |
| 3 | 21 | 0.032 |
| 4 | 19 | 0.043 |
| 5 | 20 | 0.043 |
| 6 | 21 | 0.043 |
| 7 | 19 | 0.054 |
| 8 | 20 | 0.054 |
| 9 | 21 | 0.054 |
| 10 | 19 | 0.065 |
| 11 | 20 | 0.065 |
| 12 | 21 | 0.065 |

*Table 10. Example of seeding sequence for a classical testing method with 3x330 waves set.*

Firstly, the wave height measurements registered for the sets with same seeding sequence (sets 1,6,7,8,9 and 10) along all the 12 steps are analysed.


*Figure 62. Evolution of the significant wave height measurements (WG3) for sets with same seeding (Classical testing method 3x330 waves).*

The results observed are the same with respect all the rest of the storms, confirming with all of them the practically coincidence in the evolutions of the significant wave height measured by the WG 3, when comparing sets with the same seeding.

The evolution of the standard deviation with respect the arithmetic mean of the 6 evolutions along the 12 steps is plotted in the next graphic.

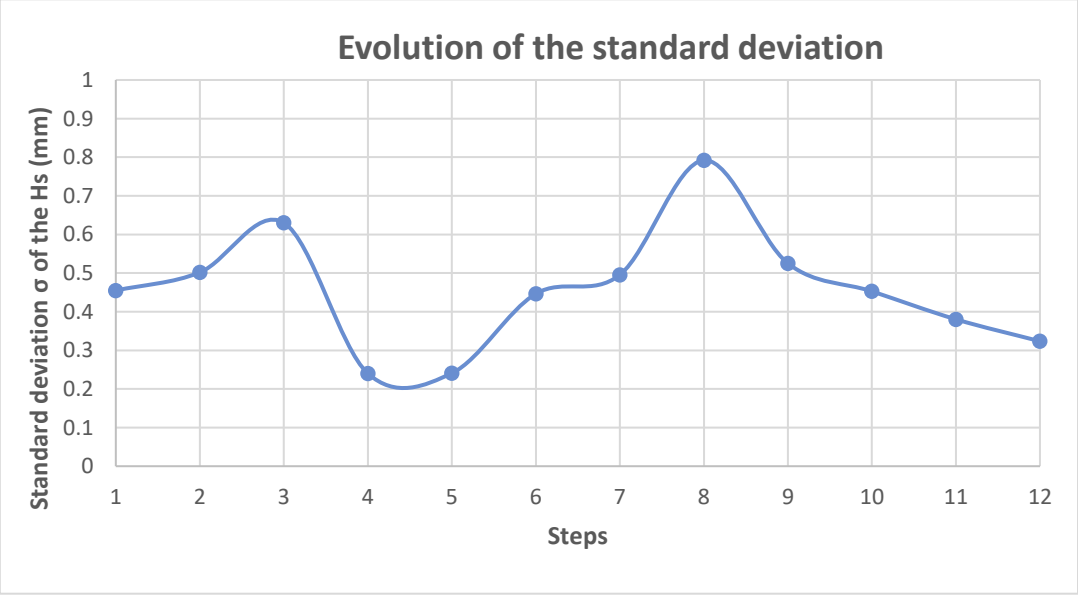


*Figure 63. Standard deviation evolution of the significant wave height measurements of the sets with same seeding for all the steps (Classical testing method 3x330 waves).*

The results of the average and maximum standard deviation of the wave height measurements with same seeding of all the steps are presented in the next table:

| | |
|---|---|
| **Average standard deviation [mm]** | 0.457 |
| **Maximum standard deviation [mm]** | 0.792 |

The average value is near a half mm and the maximum is also less than 1.

If now are picked the evolutions of the 4 sets with different seeding it will be seen the great variability with respect the target values.

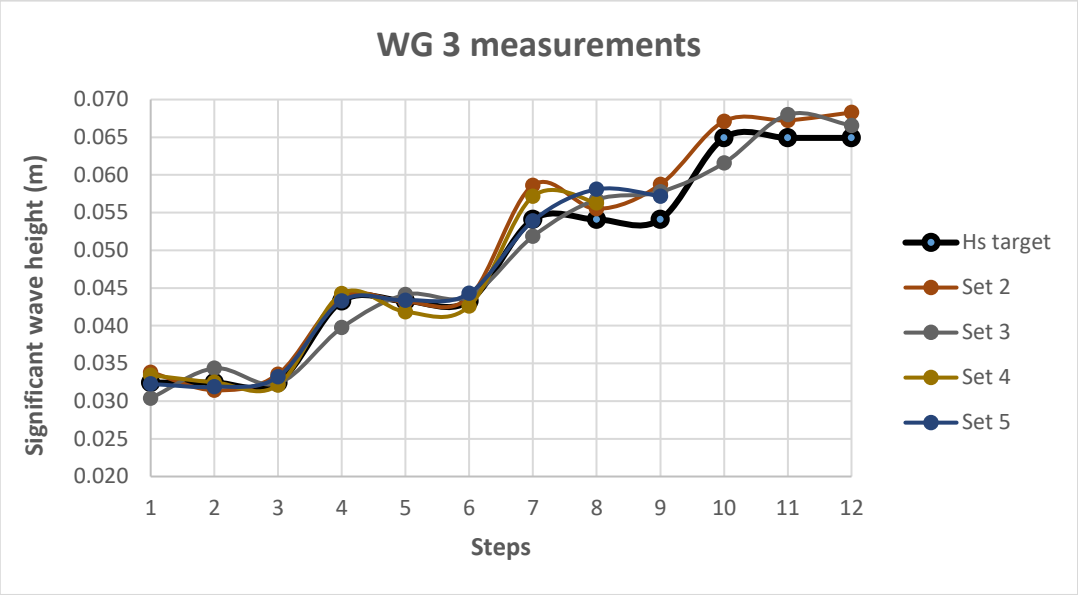


*Figure 64. Evolution of the significant wave height measurements (WG3) for sets with different seeding (Classical testing method 3x330 waves).*

### *4.1.4. Summary of the measurements*

In this chapter the dispersion of the wave height measurements for sets with same seeding of the different storms are compiled and compared.

| | Real | Trapezoidal | Triangular | Classical 3x330 |
|---|---|---|---|---|
| **Average standard deviation [mm]** | 0.261 | 0.281 | 0.291 | 0.457 |
| **Maximum standard deviation [mm]** | 0.442 | 0.486 | 1.267 | 0.792 |

*Table 11. Average and maximum standard deviations of significant wave height measurements of sets with same seeding for the different storms.*

It can be observed that in any case the average standard deviation for all the steps of any storm is higher than a half mm. In fact, the values are around 0.25 and 0.3 mm with the exception of the classical 3x300, which has a little more of difference between the significant wave height measurements of sets with same seeding.

Regarding the maximum values, with the exception of one particular step in the set 10 of the triangular storm that leads to have more than 1 mm of maximum standard deviation, the others are below 1 mm.

In any case, the results show the reliability in the wave gauge 3 measurements when generating tests with the same sequence of waves along all the registered spectrum.

When evaluating sets with different seeding, it has been noticed a slight difference between the evolutions of the wave height measurements of these sets and the target values. Nevertheless, this variability is intrinsic in a laboratory process, where the conditions from one set to the other vary a lot.

## 4.2. Evaluation of relative damage

In this chapter an evaluation of the damage progression for all the test methodologies is done. This damage can be assessed once it is quantified, and the parameters that characterize it are $N_o$ and $N_{od}$. This last value is the most used in the literature.

The values for the parameters $N_o$ and $N_{od}$ are obtained for the steps marked with a cross in the Chapter 3.4.3. To have an ideal characterization of the damage evolution, the optimum would be to compute these values for all the steps of each test. Unfortunately, this would be a very costly process in terms of time spent, so the values $N_o$ and $N_{od}$ have been obtained for every step only for one set of each test methodology. In general, the main comparisons of the damage evolution between test methodologies are done for crucial steps.

These significant steps are the 1st peak, the 2nd peak and the final step for the real storm and trapezoidal storm, the peak and the final step for the triangular storm and the steps with a wave attack of 100% and 120% of the significant wave height of the peak ($H_{s,peak}$) for the classical methodology.

Among all the storms, only for the trapezoidal and the real storm (storms tested by the author), the damage is deeply assessed. In addition, essential results regarding the damage from the others is also be presented to have an overview. The results of the $N_{od}$ parameters of the storms are plotted for all the storms in combination with interesting parameters than influence their values as the number of accumulated waves ($N_z$) and the stability number seen in the literature ($N_s = \frac{Hs}{\Delta D_{n50}}$).

Regarding only the trapezoidal and real storm, it is analysed the progression of the damage for one specific set. The influence of the seeding and the operator in charge of the construction on the results is also analysed. Regarding the construction process, three people have taken part in this project in the CIEMito flume: Jordi de Leau, a student from Netherlands; Alexander Mathijs, a student from Belgium, and the author.

### *4.2.1. Trapezoidal storm*

The trapezoidal storm has been reproduced 10 times in the flume installations. All these experiments have been carried by the author during the last months of this work.

#### Overview of the results

The results of $N_o$ and $N_{od}$ obtained after the post-process of the data for the 10 sets are expressed in the Table 12. The seeding number of each set is also represented for further analysis.

| Nº set | Seed number | Trapezium storm | | | | | |
|---|---|---|---|---|---|---|---|
| | | No | | | Nod | | |
| | | 1rst peak | 2nd peak | Final | 1rst peak | 2nd peak | Final |
| 1 | 1 | 33 | 65 | 83 | 1.39 | 2.73 | 3.49 |
| 2 | 2 | 37 | 59 | 62 | 1.56 | 2.48 | 2.61 |
| 3 | 3 | 32 | 73 | 81 | 1.34 | 3.07 | 3.4 |
| 4 | 4 | 27 | 40 | 45 | 1.13 | 1.68 | 1.89 |
| 5 | 5 | 37 | 63 | 65 | 1.6 | 2.65 | 2.73 |
| 6 | 2 | 19 | 31 | 34 | 0.8 | 1.3 | 1.43 |
| 7 | 2 | 6 | 7 | 8 | 0.25 | 0.29 | 0.34 |
| 8 | 2 | 43 | 51 | 51 | 1.81 | 2.14 | 2.14 |
| 9 | 2 | 8 | 20 | 22 | 0.34 | 0.84 | 0.92 |
| 10 | 2 | 13 | 20 | 21 | 0.55 | 0.84 | 0.88 |

*Table 12. Summary of the $N_o$ and $N_{od}$ values (Trapezoidal storm).*

Although with the $N_o$ values is easier to imagine the damage caused by the storm to the breakwater, all the damage results from works focusing on that topic, as Van der Meer (1999), use the values of $N_{od}$ to plot the progression of the damage.

First of all, these $N_{od}$ values are plotted in a graphic with respect the stability number ($N_s$) in the 'y' axis, where the $H_s$ refers to the measured wave height, and the number of accumulated waves. This last value is represented with different colours depending on the point that this damage parameter is measured (1st peak, 2nd peak and final step).

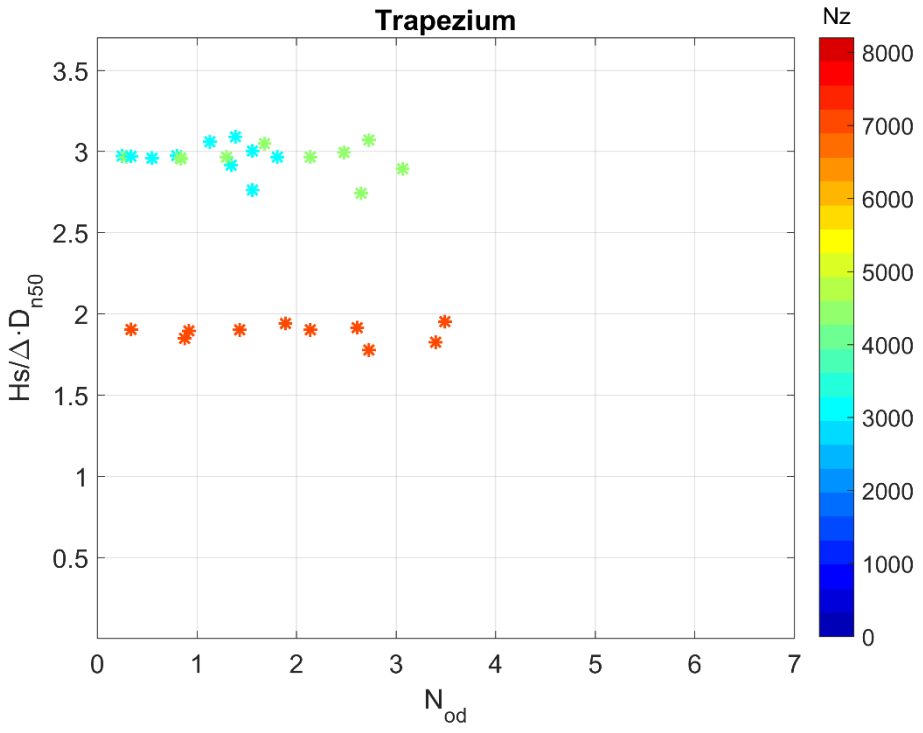


*Figure 65. Damage parameter $N_{od}$ in terms of stability number and number of accumulated waves (Trapezoidal storm).*

In this graphic are represented the 10 sets of the trapezoidal storm. As all the 10 experiments have been carried out by the author, there is no differentiation in the point marks between operators in charge of the construction, as it will be seen for the following testing methodologies.

The blue marks are the $N_{od}$ values corresponding to the 1st peak, while the green ones are the ones obtained in the 2nd peak of the storm. By last, the 10 values in red colour are the ones of the final step. These 3 main cluster of points have approximately the same distribution and form in the space. This concept shows us that the evolution of the damage between sets does not suffer essential variations for this storm.

The values of the 1st peak and 2nd peak are located in the same stability number range (approximate 3), because the significant wave height measured by the wave gauges is practically the same. For this storm, both peaks have the same significant wave height, so the 1st peak and 2nd peak marks must be near between them when looking at the stability number than they will be for the real storm, where 2nd peak has a smaller significant wave height.

The great difference in the area occupied by both groups of points comes when looking at the 'x' axis and in the colour bar. Although there are $N_{od}$ values higher for the 1st peak than for the second, the 2nd peak marks have on average higher $N_{od}$ values. In general, the relative damage ($N_{od}$) for the 2nd peak is higher than for the 1st peak, because the number of accumulated waves at this point is higher (4305 vs. 3084) and the maximum significant wave height is maintained from both peaks.

Concerning the final step, the values are painted in red, because the total number of accumulated waves is higher than in the intermediate peak steps and approximate 7000. In comparison with the results of the 2nd peak, no significant differences of relative damage can be observed. Therefore, the damage does not practically increase once the storm has exceed the 2nd peak and begins to decrease in terms of wave height. The maximum values of $N_{od}$ observed at the final steps are around 3.5.

In the Figure 66, the points represented in the previous figure are connected to understand easier the progression of the damage.

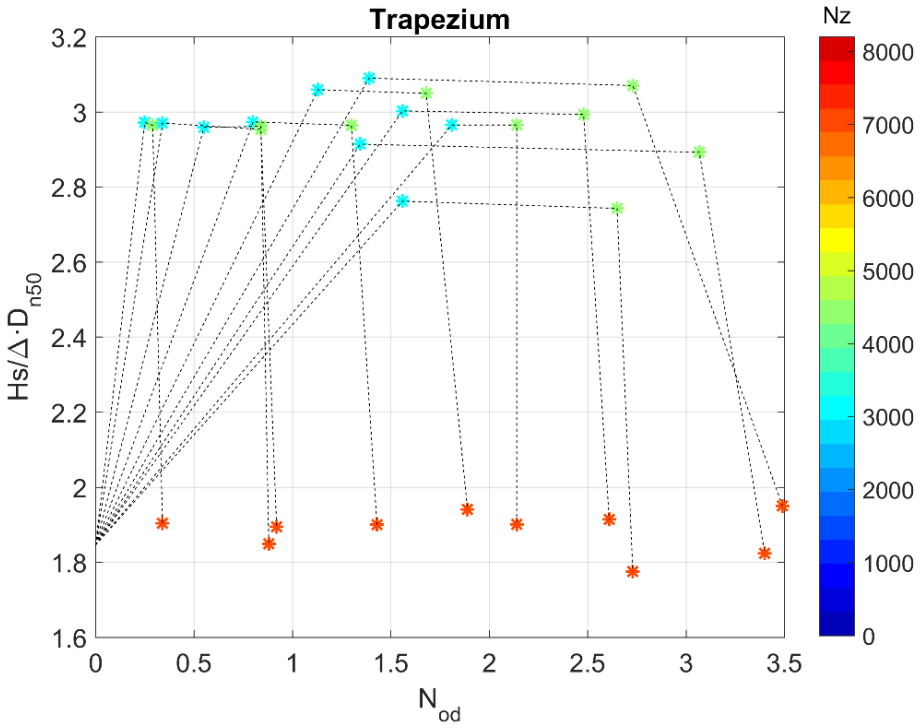


*Figure 66. Damage progression with the stability number and the accumulated number of waves (Trapezoidal storm).*

In this figure, the points representing $N_{od}$ values for each set are linked between them and the clear progression of the damage with the evolution of the trapezoidal storm can be clearly observed.

Starting from a position with the significant wave height measured in the first step, where almost any damage can be observed, there is an increasing in the significant wave height and the relative damage until it is achieved the 1st peak, which is marked in colour blue. In this 1st peak the stability number is always about 3 and the number of waves is approximate 3000. Then, the measured significant wave height is maintained constant while the damage continue increasing until values of $N_{od}$ around 2-3 when it is achieved the 2nd peak, marked in colour green (approximate 4300 number of accumulate waves). After this 2nd peak there is a decreasing of the significant wave height and consequently of the stability number. During the interval from the 2nd peak to the final step, for the majority of the sets the damage is not practically increased.

The results of both previous graphics also allow identifying the marks with same seeding and different one. The values related to the sets with same seeding are located in the same horizontal line, because the $H_s$ measured that appears in the stability number is the same for all of them. This has been already proved in the Chapter 4.1. This influence of the seeding in the damage results will be later analysed.

### Progression of damage for all the steps

The damage for all the sets is characterized only in the 1st peak, 2nd peak and the final step, because are the most representative of the storm evolution. In addition, doing all the post-process related to these parameters for all the steps represent a long process. Nevertheless, and in order to see the real evolution through all the 21 steps of the damage, the parameters $N_o$ and $N_{od}$ have been obtained for all the steps for one specific representative set (set 3).

The progression of the damage in terms of $N_{od}$ with respect the number of accumulated waves ($N_z$), which is directly related with the step number, is represented in the Figure 67. All the data necessary to construct this evolution, with the addition of the number of displaced blocks ($N_o$) is also presented in the Table 13.

| Set 3 | | | |
|---|---|---|---|
| **Step** | **Nz** | **No** | **Nod** |
| 1 | 387 | 6 | 0.25 |
| 2 | 760 | 8 | 0.34 |
| 3 | 1122 | 10 | 0.42 |
| 4 | 1473 | 10 | 0.42 |
| 5 | 1814 | 13 | 0.55 |
| 6 | 2145 | 18 | 0.76 |
| 7 | 2466 | 21 | 0.88 |
| 8 | 2779 | 21 | 0.88 |
| 9 | 3084 | 32 | 1.34 |
| 10 | 3389 | 50 | 2.10 |
| 11 | 3694 | 62 | 2.61 |

| Set 3 | | | |
|---|---|---|---|
| **Step** | **Nz** | **No** | **Nod** |
| 12 | 4000 | 63 | 2.65 |
| 13 | 4305 | 73 | 3.07 |
| 14 | 4618 | 78 | 3.28 |
| 15 | 4939 | 78 | 3.28 |
| 16 | 5269 | 78 | 3.28 |
| 17 | 5611 | 79 | 3.32 |
| 18 | 5962 | 81 | 3.40 |
| 19 | 6324 | 81 | 3.40 |
| 20 | 6697 | 81 | 3.40 |
| 21 | 7084 | 81 | 3.40 |

*Table 13. Damage parameters $N_o$ and $N_{od}$ for the different steps of the set 3.*

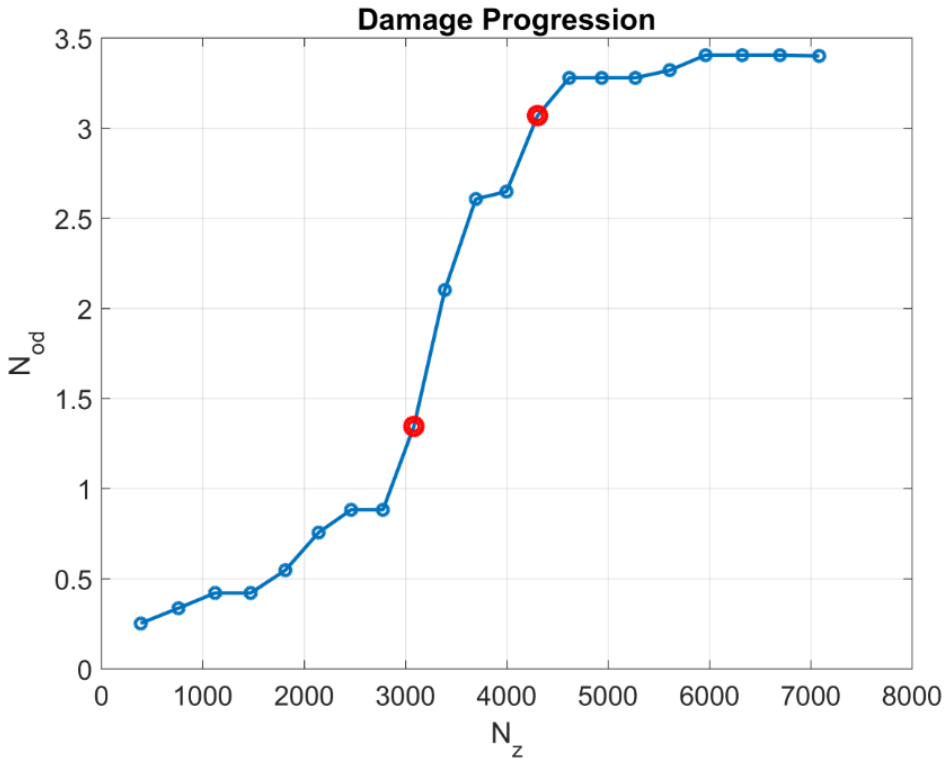


*Figure 67. Damage progression ($N_{od}$) respect the total number of accumulated waves ($Nz$) for the set 3. In red circles, the 1st peak and 2nd peak of the storm.*

From this picture, it can be seen that the damage at the first steps increases slowly, even staying the same between two consecutive steps as for example steps 3 and 4. Once the 3000 waves are exceeded, and coinciding with the final of the 1st peak (red circle), the slope of the curve becomes much steeper, so the damage increases considerably with few steps.

This clear rise of the relative damage, which is increased from 1 to 3 with only 5 steps, finishes when the 2nd peak (red circle) of the storm arrives. At this moment, the number of accumulated waves is about 4300. Therefore, in comparison with the small increment of 1300 waves from the 1st peak to the 2nd one, the damage produced between both peaks is really high. This is due to the constant maximum significant wave height applied in the flume during these 5 steps.

Finally, and taking a look from the 2nd peak to the final, the damage does not practically grow. The increment in this last part of the evolution, which includes 8 steps, represents more less only a 9% of the total final damage.

Although this is a specific progression for the set 3 of this storm, the relative damage observed can be generalized to the other sets without being too far.

### *4.2.2. Real storm*

The real storm has been reproduced 15 times in the flume facility. The experiments going from 1 to 5 were carried out by Jordi de Leau, the ones from 6 to 10 by Alexander Mathijs and the final 5 have been done by the author during the last months.

#### Overview of the results

The results of $N_o$ and $N_{od}$ obtained after the post-process of the data for the 15 sets are expressed in the Table 14. The seeding number of each set is also represented.

| Nº set | Seed number | Real Storm | | | | | |
|---|---|---|---|---|---|---|---|
| | | No | | | Nod | | |
| | | 1rst peak | 2nd peak | Final | 1rst peak | 2nd peak | Final |
| 1 | 3 | 12 | 47 | 47 | 0.5 | 1.98 | 1.98 |
| 2 | 5 | 38 | 60 | 63 | 1.6 | 2.52 | 2.65 |
| 3 | 6 | 25 | 32 | 32 | 1.05 | 1.35 | 1.35 |
| 4 | 7 | 30 | 54 | 55 | 1.26 | 2.24 | 2.31 |
| 5 | 8 | 8 | 33 | 33 | 0.34 | 1.39 | 1.39 |
| 6 | 7 | 64 | 112 | 112 | 2.69 | 4.71 | 4.71 |
| 7 | 7 | 59 | 84 | 91 | 2.48 | 3.53 | 3.82 |
| 8 | 7 | 47 | 82 | 84 | 1.98 | 3.45 | 3.53 |
| 9 | 7 | 64 | 86 | 91 | 2.69 | 3.61 | 3.82 |
| 10 | 7 | 46 | 65 | 75 | 1.93 | 2.73 | 3.15 |
| 11 | 3 | 3 | 23 | 26 | 0.13 | 0.97 | 1.09 |
| 12 | 5 | 25 | 35 | 42 | 1.05 | 1.47 | 1.77 |
| 13 | 5 | 23 | 41 | 42 | 0.97 | 1.72 | 1.77 |
| 14 | 7 | 14 | 34 | 39 | 0.59 | 1.43 | 1.64 |
| 15 | 8 | 19 | 35 | 51 | 0.8 | 1.51 | 2.14 |

*Table 14. Summary of the $N_o$ and $N_{od}$ values (Real storm).*

As it has been done for the trapezoidal storm, the $N_{od}$ values are plotted in a graphic with the same characteristics. The steps were these values have been calculated are the same that in the trapezoidal storm (1st peak, 2nd peak and final step). The difference now lies in the fact that the 15 sets have been done by 3 different operators, so a comparison of the damage depending on this operator who constructs the breakwater can be done.

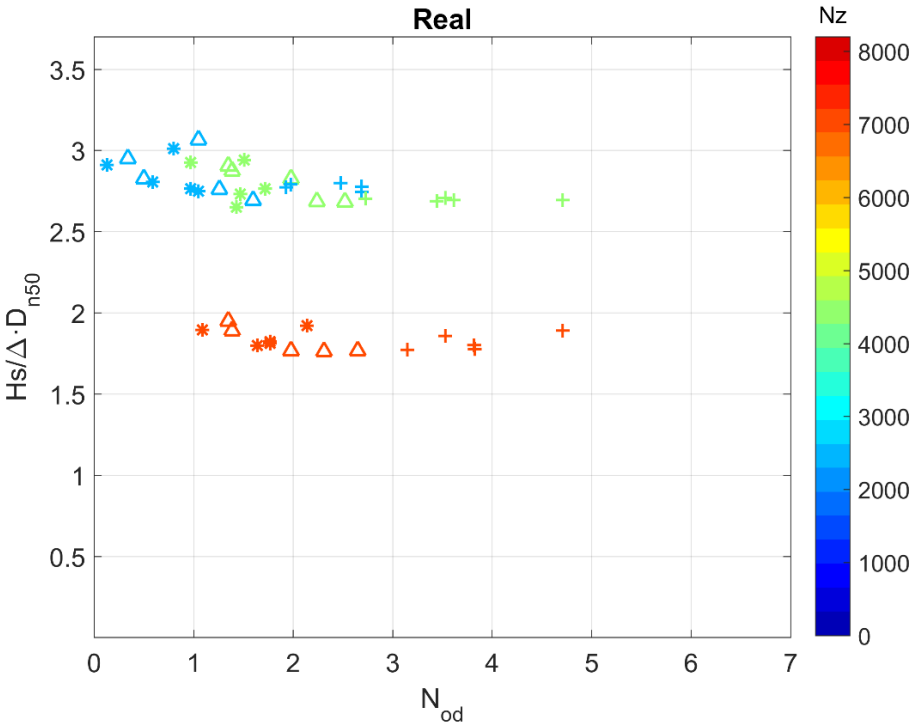


*Figure 68. Damage parameter $N_{od}$ in terms of stability number and number of accumulated waves (Real storm).*

In this graphic are represented the 15 sets of the real storm. The asterisk marks refer to the author sets, the triangle marks to Jordi's sets and plus marks are the results obtained with the Alexander's experiments.

The representation with colours is the same that for the real storm. The blue marks are the $N_{od}$ values corresponding to the 1st peak, the green ones are the obtained in the 2nd peak of the storm and the 15 values in red colour are the ones of the final step.

The values of the 1st peak and 2nd peak have similar values of the stability number ($N_s$), as the ones for the trapezoidal storm. Nevertheless, the wave height values in the 2nd peak are on average lower than the ones of the 1st peak, as it happens with the peaks propagated in the real scale (4.33 m vs. 4.26 m). Therefore, the values of the 2nd peak are slightly lower in terms of stability number than for the trapezoidal storm.

Regarding the relative damage ('x' axis), there is an important increasing of the $N_{od}$ values from 1st peak to the 2nd peak, as it happened with the trapezoidal storm. At the 2nd peak, the points related to Alexander's sets clearly show a higher damage. The number of accumulated waves for the real storm plan at the 2nd peak point is 4429, while at the 1st peak 2341.

For the points marked in red it can be observed that, although the number of waves has increased from 4300 to 7000 waves from the 2nd peak to the final step, the damage has not increased too much.

The results of the graphic also give visual information about the measured significant wave heights in the experiment. Although not being differentiated the sets with the same seeding (seeding number 7) from the rest, the points related to these sets concerning the 3 main steps are easily identifiable, due to the fact that they have more less the same measured $H_s$ when looking at the 'y' axis.

### Progression of damage for all the steps

As it is done for the trapezoidal storm, and attaining at the moment to the real storm sets developed by the author, the parameters $N_o$ and $N_{od}$ have been obtained not only for the crucial steps, but also for all the steps of one specific representative set (set 12), which $N_{od}$ values in the peaks are near to the mean. With this quantitative characterization of the damage along all the steps, the evolution of it can be seen more clearly.

This progression of the damage in terms of $N_{od}$ with respect the number of accumulated waves ($N_z$) is represented in the Figure 69. The data to create this evolution is showed in the table below.

| Set 12 | | | |
|---|---|---|---|
| **Step** | **Nz** | **No** | **Nod** |
| 1 | 360 | 0 | 0 |
| 2 | 703 | 1 | 0 |
| 3 | 1063 | 3 | 0.1 |
| 4 | 1406 | 3 | 0.1 |
| 5 | 1676 | 5 | 0.21 |
| 6 | 2036 | 7 | 0.29 |
| 7 | 2341 | 25 | 1.05 |
| 8 | 2701 | 26 | 1.09 |
| 9 | 3044 | 26 | 1.09 |
| 10 | 3296 | 29 | 1.22 |
| 11 | 3548 | 32 | 1.34 |

| Set 12 | | | |
|---|---|---|---|
| **Step** | **Nz** | **No** | **Nod** |
| 12 | 3853 | 32 | 1.34 |
| 13 | 4105 | 35 | 1.47 |
| 14 | 4429 | 35 | 1.47 |
| 15 | 4772 | 39 | 1.64 |
| 16 | 5077 | 40 | 1.68 |
| 17 | 5420 | 41 | 1.72 |
| 18 | 5708 | 41 | 1.72 |
| 19 | 6051 | 41 | 1.72 |
| 20 | 6356 | 41 | 1.72 |
| 21 | 6680 | 41 | 1.72 |
| 22 | 7040 | 42 | 1.77 |

*Table 15. Damage parameters $N_o$ and $N_{od}$ for the different steps of the set 12.*

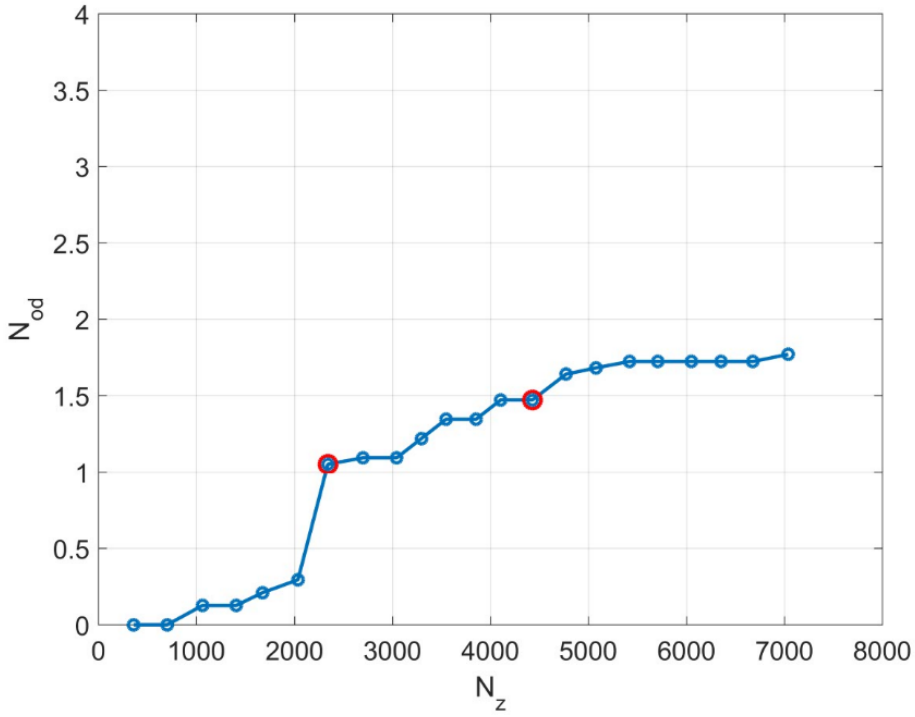


*Figure 69. Damage progression ($N_{od}$) respect the total number of accumulated waves ($N_z$) for the set 12. In red circles, the 1st peak and 2nd peak of the storm.*

From the graphic, it can be observed that the damage at the first steps increases slowly, even without increasing between two consecutive steps. The change in this dynamic is produced when analysing the damage after the run of the 1st peak (from the 6th step to the step with the red circle), where it is produced an abrupt increment of $N_{od}$.

Before both peaks, the damage is not increased too much, going from a $N_{od}$ value of 1.05 to a value of 1.47 (45% of the total damage) , which means an increment lower than 0.5. This evolution of the damage between peaks, knowing that the significant wave height is maintained with high values during 7 steps, is not as high as it might be supposed.

Finally, and looking from the 2nd peak to the final step, the damage does not practically grow. The contribution of the tail of the storm to the final damage is about the 15%.

This damage progression of the author representative set is compared in the next chapter with the evolution of one set carried out by other 2 operators in charge of the breakwater construction: Jordi and Alexander. This comparison will enable to see the differences of damage depending on the breakwater operator.

### *4.2.3. Other tests*

For the triangular storm and the classical testing methods with 1000 waves and 3x330 waves it has not been done such an extensive analysis of the damage progression as the previous two storm methodologies, because they are not executed directly by the author in the flume. Nevertheless, and as the post-processing procedure has also been done for these storms in this work, the parameters obtained and the figures created with them are also exposed.

### Triangular storm

The triangular storm has been reproduced 10 times in the flume installations. The first 5 experiments were carried out by Alexander Mathijs and the other 5 by Jordi de Leau.

The results of $N_o$ and $N_{od}$ obtained after the post-process of the data for the 10 sets are expressed in the next table. The seeding number of each set is also represented.

| Nº set | Seed number | Triangular storm | | | |
|---|---|---|---|---|---|
| | | No | | Nod | |
| | | Peak | Final | Peak | Final |
| 1 | 14 | 25 | 31 | 1.05 | 1.3 |
| 2 | 15 | 43 | 53 | 1.81 | 2.23 |
| 3 | 16 | 62 | 73 | 2.61 | 3.07 |
| 4 | 17 | 31 | 40 | 1.3 | 1.68 |
| 5 | 18 | 27 | 45 | 1.13 | 1.89 |
| 6 | 15 | 55 | 63 | 2.31 | 2.65 |
| 7 | 15 | 15 | 18 | 0.63 | 0.76 |
| 8 | 15 | 99 | 116 | 4.16 | 4.88 |
| 9 | 15 | 54 | 55 | 2.27 | 2.31 |
| 10 | 15 | 14 | 16 | 0.59 | 0.67 |

*Table 16. Summary of the $N_o$ and $N_{od}$ values (Triangular storm).*

The results of the $N_{od}$ parameter are plotted for the peak step and the final step. These are coloured depending on the accumulated waves in the flume in the specific step.

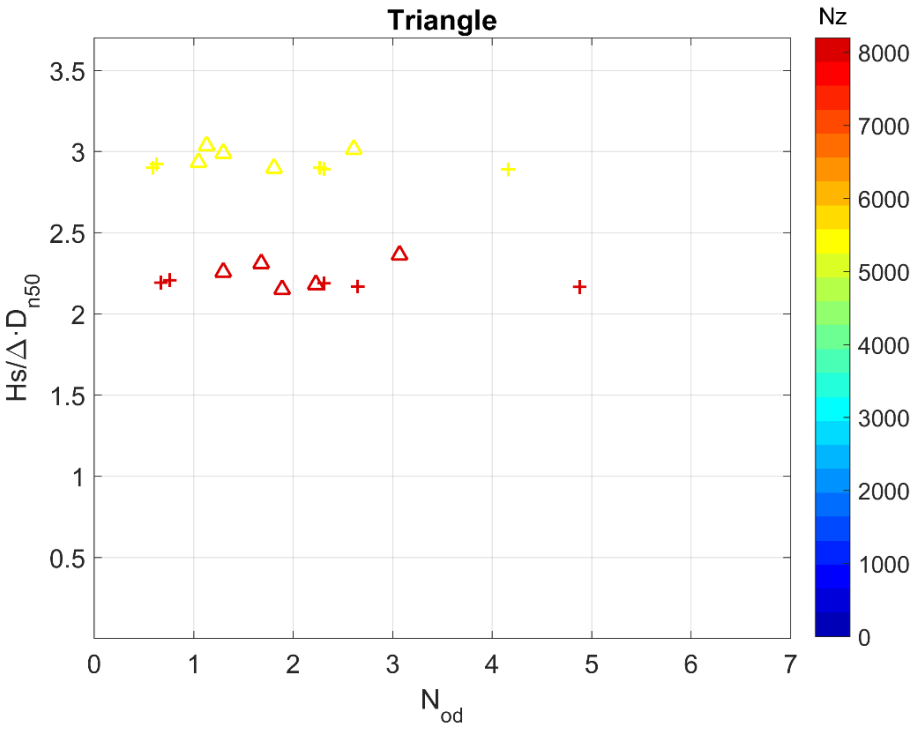


*Figure 70. Damage parameter $N_{od}$ in terms of stability number and number of accumulated waves (Triangular storm).*

The plus marks refer to Alexander sets and the triangle marks are the results obtained with the Jordi experiments.

For this storm there are only values marked with 2 colours, because unlike the other two, the triangular storm has only one peak. Then, the yellow marks are the $N_{od}$ values corresponding to the peak and the values in red colour are the ones of the final step.

The 2 main cluster of points have approximately the same distribution and form in the space. This concept shows us that the evolution of the damage between steps does not suffer essential variations in this kind of storm. I addition, and with the exception of one specific step, which has the two values clearly higher than the others, there is not a substantial variability of the damage between sets. The final $N_{od}$ values are ranged approximately between 1 and 3 and they do not differ so much from those of the peak.

For this storm, as the peak arrives later than the 2nd peak for the real and trapezoidal storm (15th step vs. 14th and 13th respectively), the total accumulated number of waves is higher than the other two storms (5412 vs. 4429 and 4305). Regarding the final step, as the total number of waves is also higher than for the real storm and trapezoidal storm, the marks have a deeper red colour.

As the peak significant wave height is the same than for the real and trapezoidal storm, the peak values have a stability number also around 3. The sets with the same seeding can be easy identified, by looking at the 5 plus marks which are aligned in the same horizontal line. This confirms that the wave gauge is measuring practically the same significant weave height in the flume.

### Classical testing method with 1000 waves

The classical method with 1000 waves has been reproduced 5 times in the flume installations, all of them carried out by Alexander. The results of the number of blocks displaced ($N_o$) and the $N_{od}$ parameters are presented in the next table.

| Nº set | Seed number | Classical 1000 | | | |
|---|---|---|---|---|---|
| | | No | | Nod | |
| | | 100% Hs,peak | 120% Hs,peak | 100% Hs,peak | 120% Hs,peak |
| 1 | 9 | 68 | 115 | 2.86 | 4.83 |
| 2 | 10 | 82 | 115 | 3.45 | 4.83 |
| 3 | 11 | 134 | 169 | 5.63 | 7.1 |
| 4 | 12 | 93 | 133 | 3.91 | 5.59 |
| 5 | 13 | 12 | 42 | 0.5 | 1.77 |

*Table 17. Summary of the $N_o$ and $N_{od}$ values (Classical testing method with 1000 waves).*

The same type of graphic than for the other storms is created with the $N_{od}$ values.

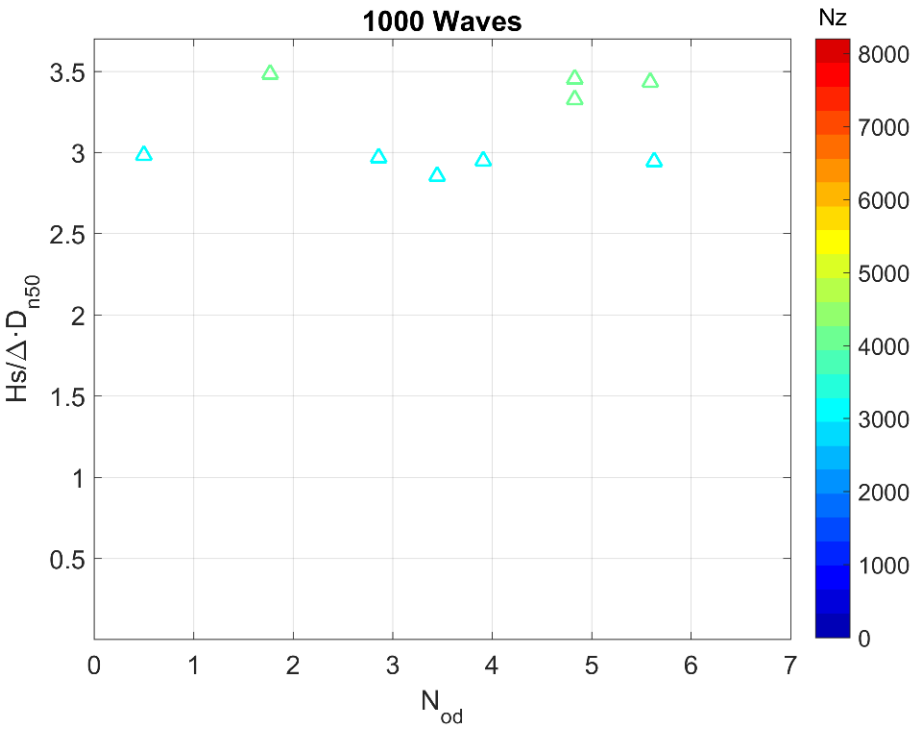


*Figure 71. Damage parameter $N_{od}$ in terms of stability number and number of accumulated waves (Classical testing method with 1000 waves).*

When working with the classical method, the evolution of the experiments does not follow the tendency of the others to increase significant wave height until a peak (or two) and then decrease it until the end. For this experiment, the wave height is always increased and the interesting steps where $N_{od}$ value have been evaluated are the ones with a wave height of 100% and 120% of the $H_{s,peak}$.

The $N_{od}$ values regarding the step with 100% of the $H_{s,peak}$ are those marked with blue colour (3000 accumulated number of waves). As the significant wave height measured must be the same as the significant wave height of the peak for the real storm, the trapezoidal storm and the triangular storm, the stability number values are around 3. Observing the horizontal axis ($N_{od}$ values), the damage noticed is higher than for the other storms, achieving for one step a relative damage of 6 and on average more than 3.

With respect the steps with 120% of the $H_{s,peak}$, the results are those depicted with green colour (4000 accumulated number of waves). For this step, there is an increment of 1 cm in the significant wave height applied at the flume. Therefore, the stability number related to the results also increments until values around 3.5. On average, the damage in the breakwater in terms of $N_{od}$ is increased in 1.5 points, when comparing with the steps with the 100% of $H_{s,peak}$.

### Classical testing method with 3x330 waves

This classical method with 3x330 waves has been reproduced 10 times in the flume installations. The first 5 experiments were carried out by Alexander Mathijs and the other 5 by Jordi de Leau. The results of the number of blocks displaced ($N_o$) and the $N_{od}$ parameters are presented in the next table.

| Nº set | Seed number | Classical 3x330 | | | |
|---|---|---|---|---|---|
| | | No | | Nod | |
| | | 100% Hs,peak | 120% Hs,peak | 100% Hs,peak | 120% Hs,peak |
| 1 | 21 | 26 | 60 | 1.09 | 2.52 |
| 2 | 24 | 65 | 132 | 2.73 | 5.55 |
| 3 | 27 | 23 | 60 | 0.97 | 2.52 |
| 4 | 29 | 90 | - | 3.78 | - |
| 5 | 33 | 75 | - | 3.15 | - |
| 6 | 21 | 77 | 121 | 3.24 | 5.09 |
| 7 | 21 | 53 | 94 | 2.23 | 3.95 |
| 8 | 21 | 28 | 77 | 1.18 | 3.24 |
| 9 | 21 | 49 | 75 | 2.06 | 3.15 |
| 10 | 21 | 77 | 157 | 3.24 | 6.6 |

*Table 18. Summary of the $N_o$ and $N_{od}$ values (Classical testing method with 3x330 waves).*

As it can be seen, for the sets 4 and 5 in the step with 120% of the $H_{s,peak}$, no values could be obtained. As in the step of 100% of the $H_{s,peak}$ the damage observed for both sets was very high, probably with such an increment until 120%, the total failure might succeeded and it was impossible to analyse a real progression of this damage.

The graphic with the damage parameter $N_{od}$ is the following:

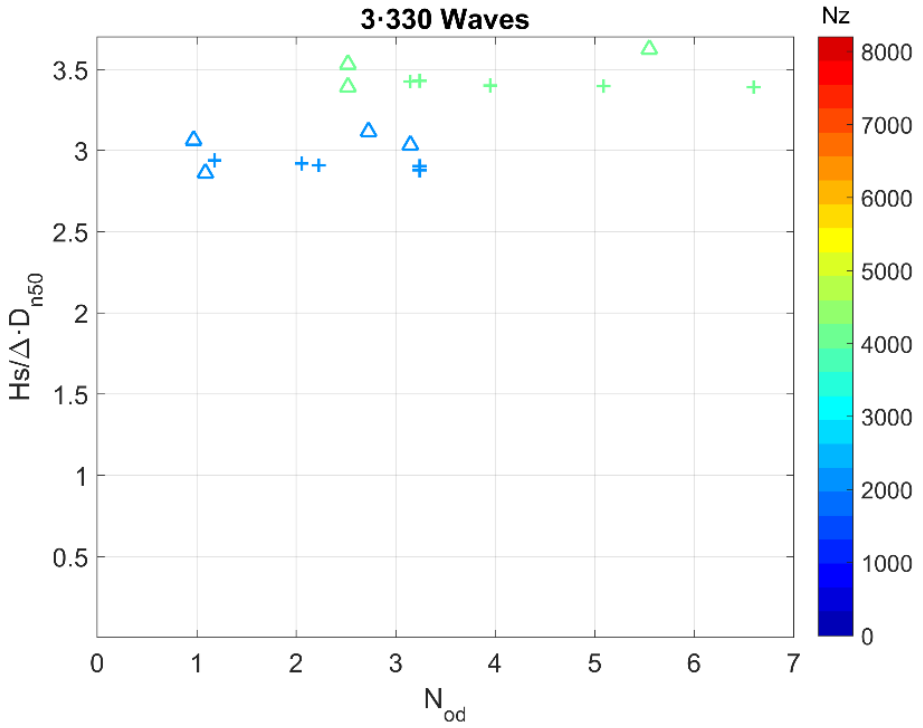


*Figure 72. Damage parameter $N_{od}$ in terms of stability number and number of accumulated waves (Classical testing method with 3x330 waves).*

The plus marks refer to Alexander's sets and the triangle marks are the results obtained with the Jordi experiments.

The characteristics of this testing method are similar with the previous one. The two steps where $N_{od}$ values are obtained are also for 100% and 120% of the $H_{s,peak}$, and the number of

accumulated waves at those steps is the same that for the classical testing method with 1000 waves. The difference is that for the previous one the $N_{od}$ for the 100% of the $H_{s,peak}$ was obtained after 3 steps of 1000 waves (60%, 80% and 100%), while with this testing method, the $N_{od}$ values have been obtained after 12 steps (3x60%, 3x80% and 3x100%). This separation of the same number of waves in more steps is more representative of the reality duration of a storm and lead to have less damage in the breakwater at the same point that the classical testing method with 100 waves.

### *4.2.4. Variability in damage results*

In this chapter the influence of different variables on the relative damage is analysed. As the effect of each variable is evaluated independently, the other variables will be not taken into account in order to not affect the conclusions obtained for each one.

The main variables analysed are:

- ***Test methodology***
- ***Operator in charge of the breakwater construction***
- ***Wave generation seeding***

The first one, the test methodology, is related to the kind of storm that is tested in the flume. By studying the figures of the overview of the results for the different test methodologies, it can be appreciated a real difference in terms of relative damage between them. Although the results are available for all the storms, the comparison is done only for the trapezoidal and the real storm, which are the ones related to this work.

In addition, it is studied the influence of the operator, which is referred to the person who is in charge of the breakwater amour layer construction, and the wave generation seeding applied to the flume program.

#### Influence of the test methodology. Trapezoidal storm vs. Real storm

To see the real differences in the damage generated by both types of storm, the other variables that can affect this damage must be removed and should not be taken into account.

In other words, to compare the trapezoidal and the real storm, the sets selected from each one must be the ones carried out by the author, being the unique person who has tested the trapezoidal storm among the three different operators. Therefore, the number of sets of the real storm are 5, while for the trapezoidal storm are 10.

This comparison between both test methodologies has been done by fitting the $N_{od}$ parameters with normal distributions. Probability density functions will be generated for the 1st peak, 2nd peak and final step.

Firstly, it was thought to compare only 5 sets of the trapeziums storm to have the same sets for both storms. To do that, there were generated multiple random combinations (more than 1000) of 5 sets without repetition among the 10 sets available of the trapezoidal and a normal distribution with these 5 $N_{od}$ values of each combination was generated.

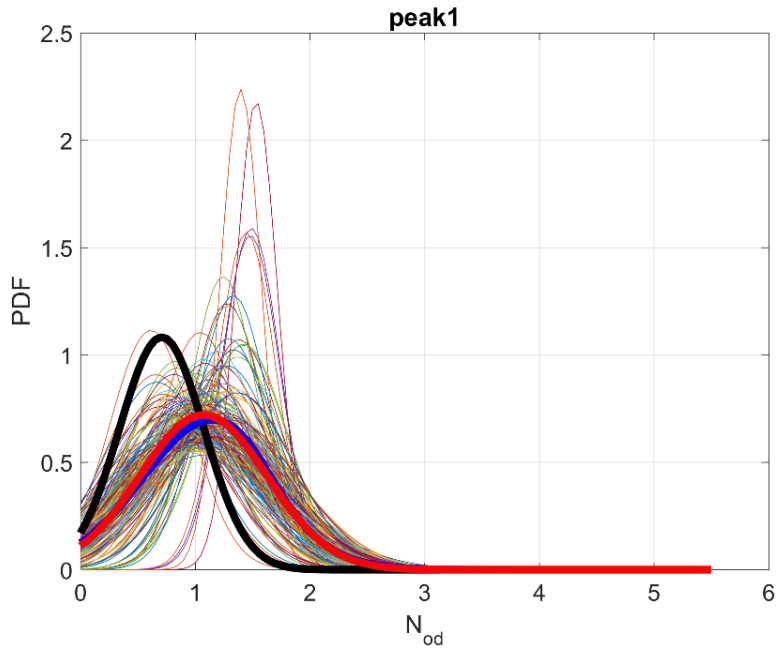


*Figure 73. PDF's of $N_{od}$ values regarding the 5 sets of real storm (black curve), the 10 of the trapezoidal (red curve) and the mean of the multiple combinations of 5 sets of the trapezoidal (blue curve).*

With these functions depicted, it was noticed that the average of all these normal distributions (blue curve) was also a normal one and practically identic to the normal distribution generated with the 10 $N_{od}$ values of all the trapezoidal sets (blue line). Therefore, it was concluded that the damage comparison could be done working with the 10 sets of the trapezoidal and the 5 of the real storm. This new comparison for the 1st peak, 2nd peak and final step is shown below:

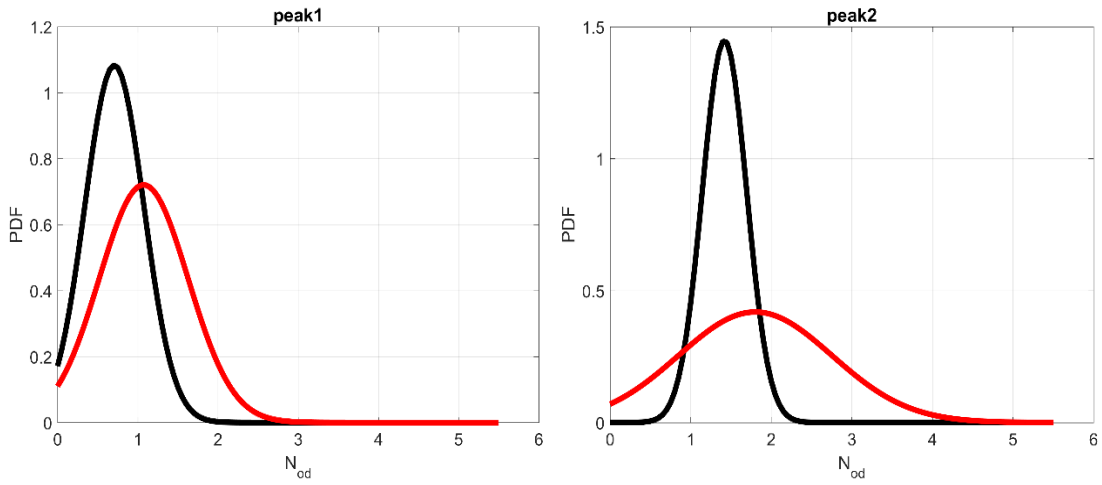

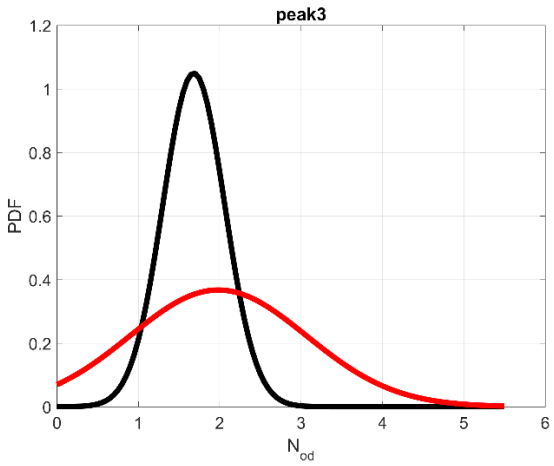


*Figure 74. PDF's comparison between real storm sets (black curve) and trapezoidal storm sets (red curve) carried out by the author for crucial steps.*

A general observation by looking at the graphics of the Figure 74 is that the damage caused by the trapezoidal storm is higher than the real storm. The trapezoidal storm causes on average a 52% more damage that the real storm in the 1st peak, 27% in the 2nd peak and 17% at the final, where the results become more comparable

The results obtained show what it was concluded in the work of Martín Soldevilla *et al.* (2015), where the use of trapezium shape resulted in causing more damage than the other synthetic storms and the real one when analysing them analytically. The explanation is that the storm peak in the trapezoidal storm is maintained during hours, while in the reality, although two similar storm peaks can exist, the storm power is not always the maximum between them.

In addition to the average higher damage for the trapezoidal storm, the deviation of the $N_{od}$ data for this kind of storm is also higher than the real storm. It means that the $N_{od}$ values obtained from the 5 sets of the real storm when the breakwater operator has been the author, are very near between them, without existing remarkable differences.

The results of the average and standard deviation of the $N_{od}$ values for the three steps and for the trapezoidal and real storm are exposed in the Table 19.

| | $\mu_N$ | | | $\sigma_N$ | | |
|---|---|---|---|---|---|---|
| | **1st peak** | **2nd peak** | **Final step** | **1st peak** | **2nd peak** | **Final step** |
| **Trapezoidal** | 1.08 | 1.80 | 1.96 | 0.557 | 0.953 | 1.052 |
| **Real** | 0.71 | 1.42 | 1.68 | 0.368 | 0.275 | 0.380 |

*Table 19. Average and standard deviation of $N_{od}$ values of the 1st peak, 2nd peak and final step for the real and trapezoidal storm (5 sets vs. 10 sets).*

The average $N_{od}$ value for both storms at the final step, when the breakwater has received all the accumulated damage caused by the wave attacks, is lower than 2.

If this damage assessment of the real storm and trapezoidal storm would have been done by comparing all the 15 sets of the real one (regardless of the breakwater operator) and the 10 sets of the trapezoidal, the results should have been these ones:

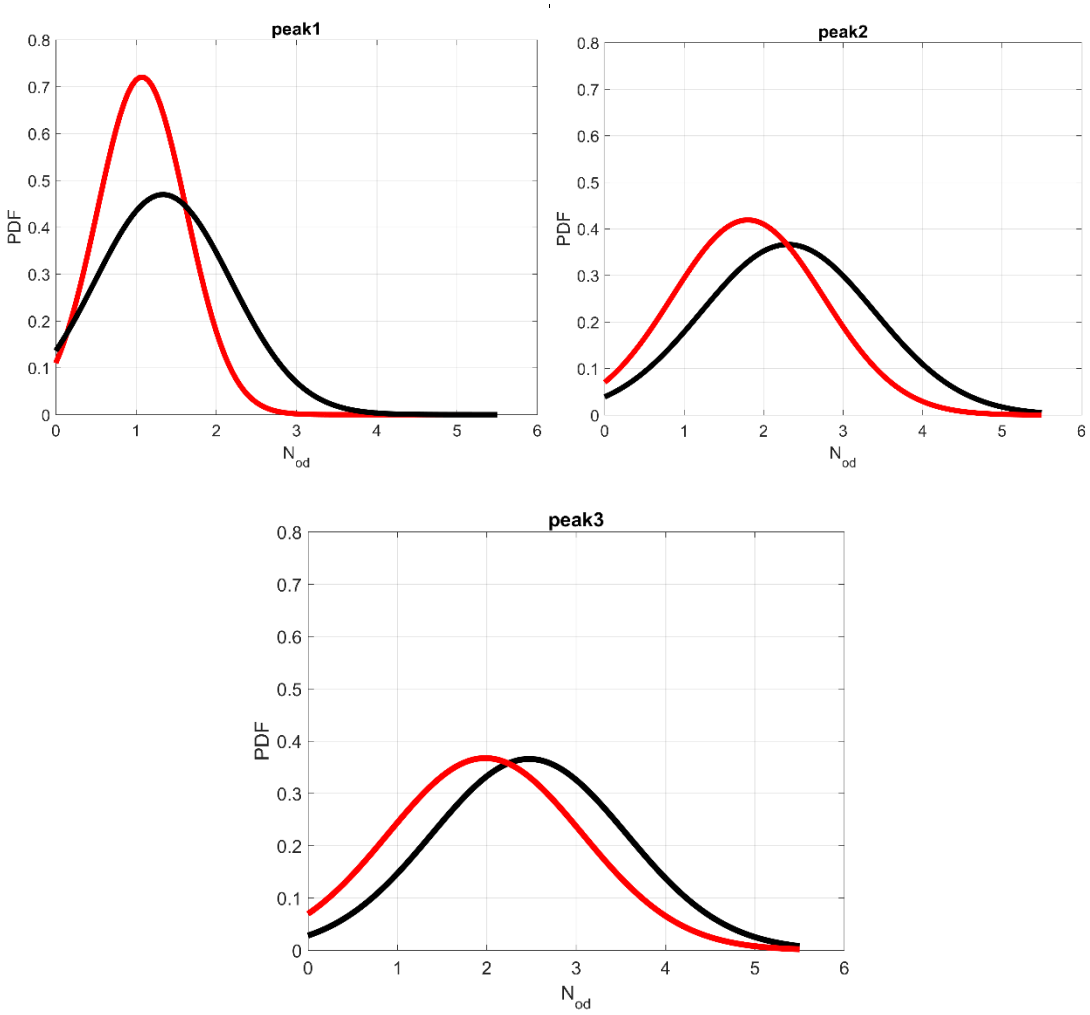


*Figure 75. PDF's comparison between real storm sets (black curve) and trapezoidal storm sets (red curve) regardless the breakwater operator for crucial steps.*

As now the $N_{od}$ values for the real storm come from sets where the breakwater construction has been carried out by three different operators, the variable of the operator is present in the analysis of the damage for the different storms. Therefore, the results differ considerably respect the previous graphics.

For this situation, it happens like a reversion of the results, being now the real storm that causes in average more damage than the trapezoidal one for any of the 3 steps deployed. This real storm causes in terms of $N_{od}$ approximately 25% more damage than the trapezoidal storm regardless the step analysed. Studying the values of the standard deviation of the data presented in the Table 20, the real storm shows a higher dispersion than the trapezoidal storm. Nevertheless, for the analysis of the previous results attaining only at the author constructions, the dispersion of the real storm $N_{od}$ values was notable lower than the one for the trapezoidal.

| | $\mu_N$ | | | $\sigma_N$ | | |
|---|---|---|---|---|---|---|
| | **1st peak** | **2nd peak** | **Final step** | **1st peak** | **2nd peak** | **Final step** |
| **Trapezoidal** | 1.08 | 1.80 | 1.96 | 0.557 | 0.953 | 1.052 |
| **Real** | 1.34 | 2.31 | 2.47 | 0.850 | 1.089 | 1.091 |

*Table 20. Average and standard deviation of $N_{od}$ values of the 1st peak, 2nd peak and final step for the real and trapezoidal storm (15 sets vs. 10 sets).*

This general change in the damage results, having higher $N_{od}$ values the trapezoidal storm when attaining at the author constructions, but being higher this damage for the real storm when using a database of all the operators, can only be explained due to the importance of how each cube is placed in the breakwater.

This influence of the operator is deeply analysed in the next lines.

### Influence of the operator in charge of the breakwater construction

With the results stated in the last subchapter and looking at the Figure 68, it can be appreciate a difference in terms of damage between the results of the author experiments and the ones carried out by two other operators: Jordi and Alexander. Although the construction methodology is fixed and presented in the Chapter 3.1.7, this difference is due to a variability that exists during the positioning of the cubes during construction process of the armour layer. In that process, the placement of the cubes can be more regular or irregular depending on how the operator drops the cubes in the breakwater.

This difference can be firstly observed with a comparison of pictures from the initial position of the armour layer. In the Figure 76 it can be observed that the author construction of the armour layer (left picture) is done more regular than the Alexander one (right picture), where the cubes are normally touching the filter with their vertices and not with their sides.

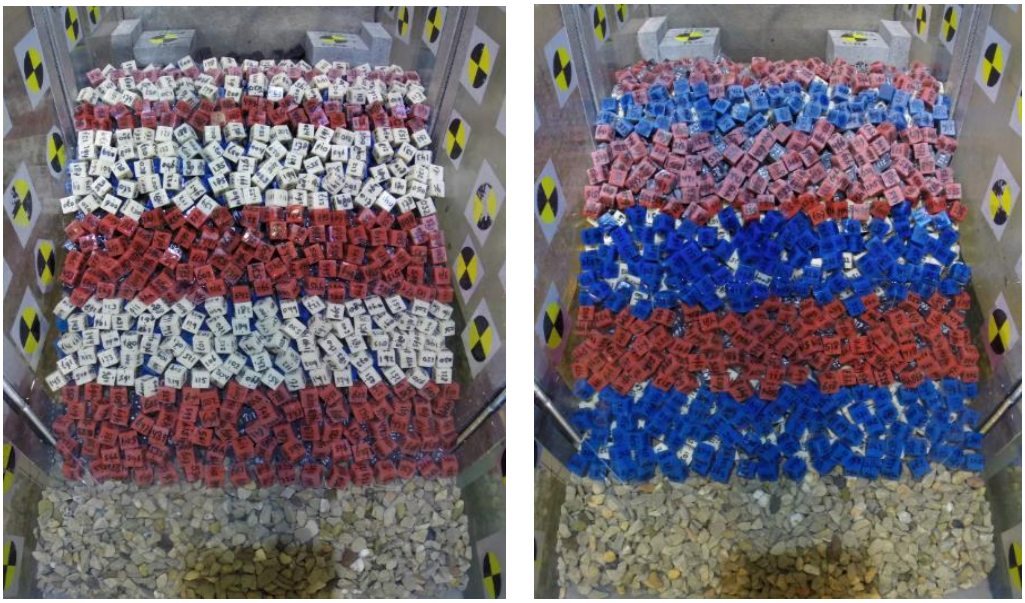

*Figure 76. Example of an initial state of the armour layer constructed by the author (left) and by Alexander (right).*

This difference in the damage can be represented quantitatively by studying the progression of the parameter $N_{od}$ for a representative set of each operator in charge of the construction of the breakwater armour layer. In addition to the damage progression of the author set (Figure 69 of the previous chapter), the calculation of $N_{od}$ for each step is also done for one of Jordi's sets (set 4) and for one of Alexander (set 8). These two sets are also representative of the group of sets that has carried out everyone.

Using the same structure than in the Figure 69, the progression of the damage in terms of $N_{od}$ with respect the number of accumulated waves ($N_z$) is represented in the next figure.

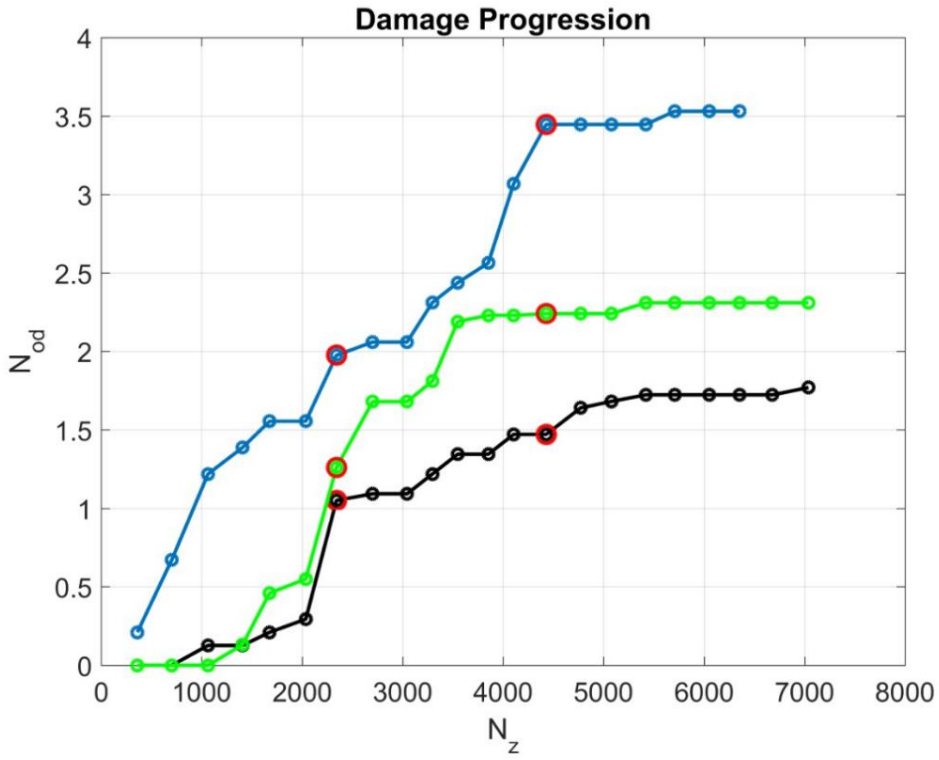


*Figure 77. Damage progression ($N_{od}$) respect $N_z$ for a set of Jordi (green), Alexander (blue) and the author (black). In red circles, the 1st peak and 2nd peak of the storm.*

From the picture is seen that the set with more damage regardless of the step is the Alexander one. The relative damage for the Alexander set is in the 1st peak 80% higher than the one observed for the Jordi set, while approximately the double when being compared to the author one. Regarding the 2nd peak, this difference becomes more noticeable with the author set, but the difference respect the Alexander set is decreased to a 60%. From 2nd peak to the final, the damage is does not practically increase ore for any set, which can be generalized for all the sets of the real storm.

If it is compared the damage of the author set (black line) and the Jordi's set (green one), the values of $N_{od}$ differ less between them than they do when comparing with the Alexander set. In fact, this difference in the 1st peak is practically negligible. Therefore, it can be assumed that although the differences in these 2 specific sets, Jordi's constructions and he author ones give similar results of damage. This situation is assessed later, when comparing the relative damage results with the normal distributions.

In order to see a comparison of the damage evolution rate between the same 3 sets, the $N_{od}$ values can be normalized with respect the maximum one, having as a result the following graphic.

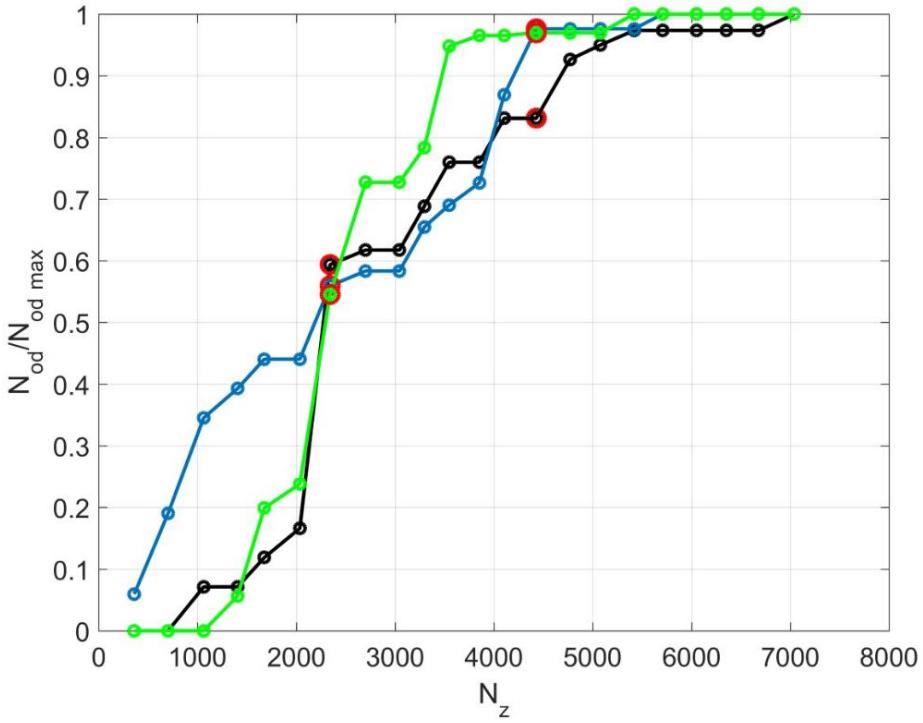


*Figure 78. Damage rate ($N_{od}/N_{od\_max}$) respect $N_z$ for a set of Jordi (green), Alexander (blue) and the author (black). In red circles, the 1st peak and 2nd peak of the storm.*

With this normalization, it can be affirmed that the set with more damage seen with the previous graphic (Alexander set in colour blue) is also the one with a higher relative damage in the first steps before arriving at the 1st peak. This sudden increment of the damage can be understood as a compaction process of the cubes, due to the opened distribution of them in Alexander breakwater constructions.

The author set and Jordi's one have a similar rate of damage at the beginning, but from the 1st peak to the 2nd one, the relative damage of the Jordi set is substantially higher than the author set. In fact, the relative damage between peaks of Jordi's set is the highest.

By looking and the three evolutions, it can be clearly seen that the damage rate at the 1st peak is practically the same, having each set the same relative damage when comparing to the corresponding final $N_{od}$. With the 2nd peak, this situation is not the same, because although the Jordi and Alexander sets have the same normalized damage, the damage rate of the author set is considerably lower. Consequently, and as it has been also analysed in the previous chapter, the damage increment of the author set between peaks is much lower than for the other sets, being recovered this damage rate after this 2nd peak.

Statistical comparison

This comparison between one specific real storm set of each operator in charge of the breakwater construction helps to know in advance, who causes at the end more damage. Nevertheless, to have a better comparative between the damage regarding the construction process, the $N_{od}$ values from the 5 sets of each operator for all the steps should be taken into account. If not, although being representative the sets drawn in the Figure 77 and Figure 78, statistical parameters as the mean ($\mu_N$) and standard deviation ($\sigma_N$) cannot be known.

These $N_{od}$ values for each operator (5 sets for each one) are fitted with a normal distribution. Therefore, for the 1st peak a normal distribution for the $N_{od}$ values of Alex, another for Jordi's values and another for the author values is created. The same happens for the 2nd peak and final step.

The comparative graphic that is used in the analysis is the one with the normal distributions of the final step.

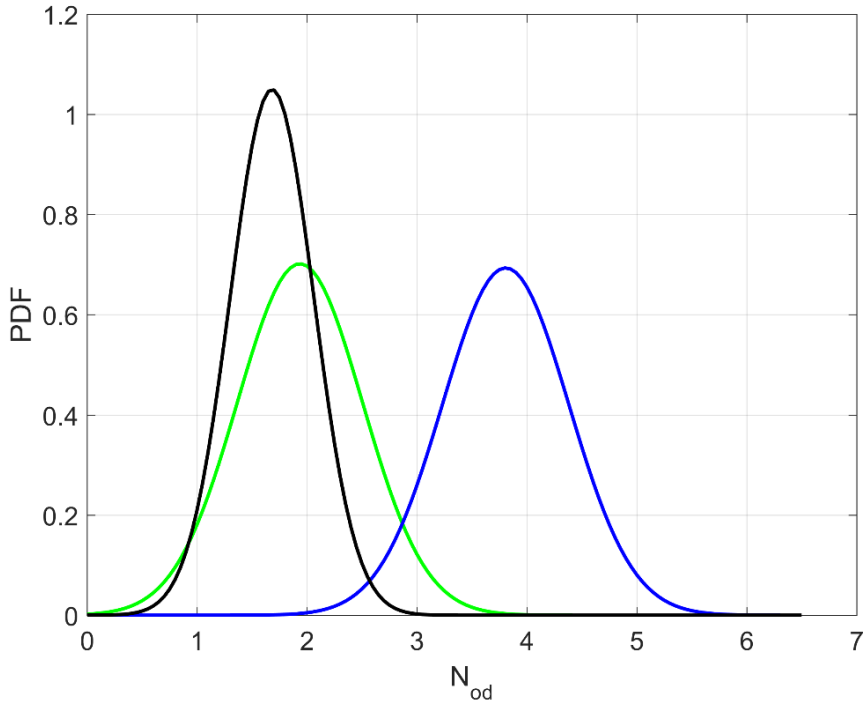


*Figure 79. PDF's of $N_{od}$ values referred to the final step for constructions done by Alex (blue), Jordi (green) and the author (black).*

These normal distributions are depicted in a graphic where the 'y' axis represents the probability density function and the 'x' axis the $N_{od}$ values.

The author and Jordi distributions are overlapped, showing then similar range of $N_{od}$ values in the final step. Therefore, the differences in the breakwater constructions are not decisive when evaluating the final damage. Nevertheless, the average damage and the standard deviation of the values is higher for Jordi's sets.

What respect the Alex normal distribution, it can be seen that is totally differenced from the other two, only with a minimum overlapping. Although it explain also that the damage caused when looking at his sets is higher than for the others (Figure 77), this remarkable difference in the distributions curves is quite unreal, because the damage results cannot have such this sensibility when only changing the operator of the breakwater.

The mean and the standard deviation extracted from the normal distributions of the final step are presented in the next table:

| | $\mu_N$ | $\sigma_N$ |
|---|---|---|
| **Jordi** | 1.94 | 0.569 |
| **Alexander** | 3.81 | 0.575 |
| **Eduard** | 1.68 | 0.380 |

*Table 21. Average and standard deviation of $N_{od}$ of the final step and depending on the operator.*

### Influence of the wave generation seeding

The objective of this chapter is to try to see if there are important differences in the damage results when changing the wave generation seeding. This influence of the seeding can only be done focusing on the same test methodology and the same operator, because the base conditions before doing this comparison must be the same.

Taking into account the previous requirements, this comparative is done for the trapezoidal storm, which has only been carried out by the author. It cannot be also done for the real storm, because there are no enough sets available done by only one operator to be separated in two groups of same seeding and different seeding.

The 10 sets of the trapezoidal storm are separated in two different samples:

- ***Sample 1 (Different seeding)***: Sets 1, 2, 3, 4 and 5.
- ***Sample 2 (Same seeding)***: Sets 6, 7, 8, 9 and 10.

The comparison of the damage between both groups is done by creating a normal distribution with the $N_{od}$ data available for both samples for the 1st peak, 2nd peak and final step. These distributions will show the average damage and the dispersion of the data for both groups separated.

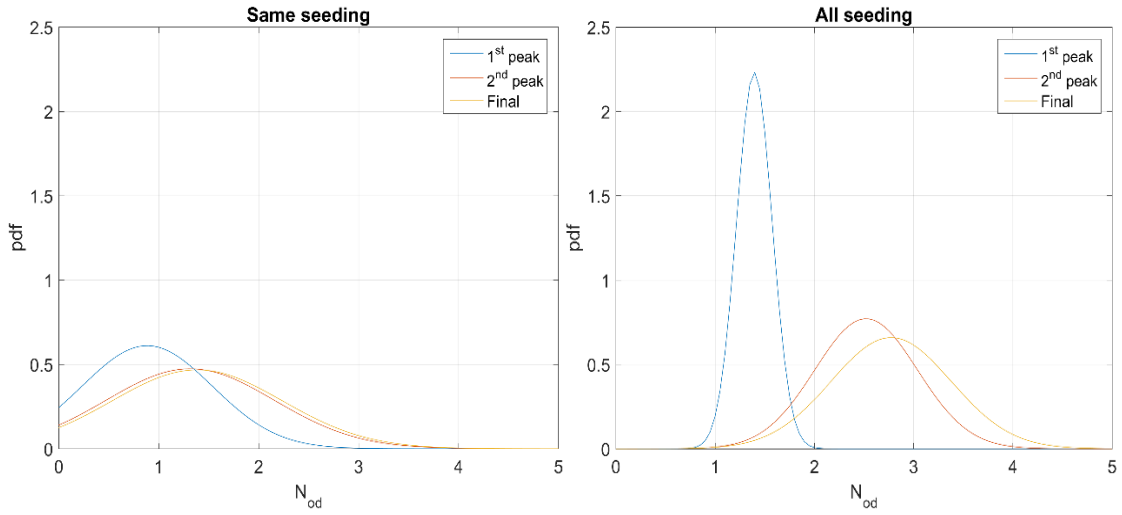


*Figure 80. PDF's of sets with same seeding (left) and different seeding (right) for the 1st peak, 2nd peak and final step $N_{od}$ values.*

Comparing both graphics, the results do not show what it could be logical to think. As the sets with the same seeding have the same sequence in the waves generation and the significant wave height is the same between them, it might be expected a smaller deviation of the $N_{od}$ data with respect the average. Nevertheless, the dispersion of the damage results regardless the step for the sets with the same seeding is higher than for the sets with different seeding. This difference is even higher in the 1st peak.

As the situation observed does not follow a logical reasoning, it can be concluded that the changing of the seeding do not influence final damage results.

# 5. CONCLUSIONS AND RECOMMENDATIONS

The aim of this work is to improve the knowledge on the process of design/verification of a breakwater armour layer. A series of tests have been carried out in a small-scale wave flume and the stability of a breakwater with an armour layer composed by two layers of cubic blocks has been assessed by the use of the relative damage $N_{od}$. A real storm measured by a buoy in the Catalan coast of the Mediterranean Sea has been scaled down and tested fifteen times and the observed relative damage has been used to create a benchmark for the evaluation of new methodologies based on different synthetic storms.

Ten repetitions of three different synthetic storms have been compared with the benchmark case starting from the so-called "classical methodology" and followed by two Equivalent Magnitude Storms models with two different shapes, triangle and trapezium. Only the latter and the real storm have been tested by the author. The results associated to the other methodologies were already available from previous experiments carried out in the same facility.

The parameters used for the definition of the synthetic storms were derived from the real storm. In particular, the pair wave height ($H_s$), peak period ($T_p$) associated to the peak of the storm and the Magnitude, which is an identifier of the energy of the storm. All the tested storms have been discretized insteps of 1h at prototype scale.

The generation of these storms in the flume has always followed the same procedure, with the only change of the random generation of wave sequences (seeding). This repetitive procedure aims to guarantee that the difference in results obtained are due to the intrinsic variability of the phenomenon and to ensure that at least, no error has been introduced.

The damage assessment has been done in terms of the $N_{od}$ parameter (relative damage). For each test methodology, the $N_{od}$ of the significant steps has been obtained. In addition, for a representative test of each test methodology, the relative damage has been calculated for all the steps.

In this research, the author only studied the comparison between the trapezoidal and the real storm through the relative damage parameter $N_{od}$. This comparison has been mainly focused on the final $N_{od}$ values, because is the only point in which the energy delivered to the system (magnitude) is comparable between storms. Nevertheless, damage in intermediate steps (1$^{st}$ peak and 2$^{nd}$ peak) has also been compared to have a control of the damage progression.

The number of repetitions were not enough for performing a best fitting procedure on a series of parametric statistical distribution and it has been decided to use normal distributions to fit the $N_{od}$ values. The average and the standard deviation of these distributions have been the statistical variables used to make this comparison.

In addition, the influence of other variables as the operator in charge of the breakwater construction and the wave generation seeding has been assessed. For the first analysis, only the results associated to the real storm has been taken into account since it was the only one in which three different operators built the breakwater following the same construction methodology. Moreover, comparing results only through the real storm takes away the variability of the test methodology. For the second, only the results associated to the trapezoidal synthetic storm have been taken into account since it was the only test methodology for which

only one operator (the author) built the breakwater. Thus, the variability associated to the operator is removed.

The first noticeable aspect seen is that the most contribution to the final damage happens from the first steps until the 2nd peak. What respect the decreasing branch of the storm, the damage practically does not increase.

To illustrate it by numbers, the accumulated damage in the 2nd peak of the real storm represents on average approximately the 85% of the final damage, while for the trapezoidal storm it is even higher, near 91%. Therefore, the damage caused by the tail of the storm corresponds only to the 15% and 9% respectively.

From the comparison between $N_{od}$ values for the real storm and trapezoidal storm carried out by the author, the probability density functions of the normal distributions highlight that the damage caused by the trapezoidal storm is on average higher than the real storm. The damage caused by the trapezoidal storm is 52% higher than the observed for the real storm in the 1st peak, 27% at the 2nd peak and 17% at the final step. Regarding the standard deviation of the $N_{od}$ data respect the average value, the one of trapezoidal storm is revealed to be 50% higher than the noticed for the real storm in the 1st peak, but it becomes almost the triple in the final step.

After this analysis, it was suggested to compare the same test methodologies but taking into account all the results of the dataset obtained not only with the author tests, but also with previous experiments. This implies adding $N_{od}$ values for 10 more real storm tests to the 5 used in the previous comparison. The results of this new comparison put in evidence the effect that the operator has in the final damage. For this situation, is now the real storm that results in having on average more damage than the trapezoidal one. The average damage of the real storm is 25% higher than the trapezoidal storm and this difference is maintained constant from the 1st peak to the final step.

Although having different damage results between the real and trapezoidal storm when introducing the variable operator, the probability density functions of both test methodologies are overlapped for all the representative steps. This gives an idea of the similar damage caused by both testing methodologies.

The manifestation of the operator's dependency in the damage results has led to compare for the same test methodology (real storm) the damage results obtained from tests carried out by three different operators. The results show a clear overlapping between the probability density functions of $N_{od}$ results for the final step for two operators (including the author). Nevertheless, the probability density function of the third operator is noticed to be much more distanced, with only a minimum overlap with the other two. This situation lead to have an average $N_{od}$ value for the third operator much higher than the obtained for the other two, which are similar. This difference is approximately the double.

The study of the possible effect of the wave generation seeding to the damage results has focused on a division in two groups of the trapezoidal storm tests. The results of relative damage ($N_{od}$) of the first group, tests with same seeding, have showed a higher dispersion of the $N_{od}$ data respect an average value than the one obtained for the tests with different seeding. Although this difference is practically not noticed in the final step, is more than the triple at the end of the storm.

From the results obtained, it can be concluded that for the real and trapezoidal storm, the contribution to the final damage of the decreasing branch of the storm (after the 2nd peak) is practically negligible. Therefore, this last part could be removed by cutting the storm evolution from the 2nd peak onwards. Then, the evolution of these test methodologies would be composed of two sections: an increasing branch and a part with significant wave heights near to the peak one (equal in case of trapezoidal storm) maintained during few hours.

Regarding the damage results from the comparison between the real and trapezoidal storm, the similarity between them could allow the synthetization in flume of the real storm by means of an Equivalent Magnitude Storm model composed of a trapezium shape. These results match with the conclusions extracted from the work of Martín Soldevilla *et al.* (2015), where it was highlighted that the EMS model was the model with best results when comparing with the real storm.

Although these comparable results between both testing methodologies, it is clearly noticed that the operator in charge of the breakwater construction is decisive in the final $N_{od}$ results.

The higher damage observed for the trapezoidal storm than for the real one when only the author tests are considered, is in line with the stated in the work of Martin Soldevilla *et al.* (2015). In this study it was proved analytically that the use of the trapezium shape resulted in an overestimation of the damage in all kind of storms. The reason is that the storm peak is maintained during few hours, while in the reality, it does not persist for so long.

The reversion of the situation when different operators are considered makes further investigations on this influence necessary. Although the construction methodology of the armour layer in the flume is fixed, it has been verified that the positioning of each cube in the armour layer reveals great importance when assessing the final damage results. This influence of the cubes placement was already stated in the work of Frens (2007).

The results obtained when assessing the possible influence of the wave generation seeding to the damage have been the opposite of the ones expected. To consider an affection of this variable to the damage, results should have shown a smaller dispersion of $N_{od}$ data for the tests with same seeding. Nevertheless, the normal distribution of the values for tests with different seeding provides a lower standard deviation than the one constructed with data of tests with same seeding. Therefore, and unlike the operator variable, the wave generation seeding has resulted in having no influence to the final damage.

For future works, the author suggest to exclude the decreasing branch from the planed test methodologies, included real and synthetic storms, because it practically does not contribute to the final relative damage. Once achieving the last peak, the relative damage at that point could be multiplied by a standardized factor slightly higher than one to know the final damage. With this, more tests could be carried out with the same time.

Furthermore, more research is needed focusing on the influence of the operator in charge of the breakwater construction. Probably, more control should be exercised when placing the cubes in the armour layer to ensure that the packing density is maintained uniform along all the breakwater. Regarding the wave generation seeding number, it should be removed of further damage sensitivity analysis due to the insignificant effect in the final damage results.

# 6. BIBLIOGRAPHY


1. Ali, A. M. & Al Sayed, I. D. (2014). Double layer armor breakwater stability (case study: El Dikheila Port, Alexandria, Egypt). *Ain Shams Engineering Journal, 5*(3), 681-689.
2. Autodesk Inc. (2016). Autodesk Recap 360. ***https://recap360.autodesk.com/***
3. Bocotti, P. (1997). A general theory of three-dimensional wave groups. Part I: The formal derivation. *Ocean Engineering, 24*(3), 265-280.
4. Boccotti, P. (2000). *Wave mechanics for ocean engineering* (Vol. 64). Elsevier Science.
5. Bolaños, R., Jordá, G., Cateura, J., Lopez, J., Puigdefabregas, J., Gómez, J. & Espino, M. (2009). The XIOM: 20 years of a regional coastal observatory in the Spanish Catalan coast. *Journal of Marine Systems, 77*(3), 237-260.
6. Borgman, L. E. (1970). Maximum wave height probabilities for a random number of random intensity storms. In *Coastal Engineering 1970* (pp. 53-64).
7. Corbella, S. & Strech, D. D. (2012). Predicting coastal erosion trends using non-stationary statistics and process-based models. *Coastal Engineering*, *70*, 40-49.
8. De Jong, R. J. (1996). *Wave transmissions at low-crested structures. Stability of tetrapods at front, crest and rear of a low-crested breakwater*. Master Thesis. TU Delft.
9. De Leau, Jordi (January 2017). *Laboratory experiments on the stability of concrete cubes; a comparison of testing methodologies*. Master Thesis. Universitat Politècnica de Catalunya (UPC), Barcelona, Spain.
10. De Michele, C., Salvadori, G., Passoni, G. & Vezzoli, R. (2007). A multivariate model of sea storms using copulas. *Coastal Engineering, 54*(10), 734-751.
11. Del Estado, P. (2015). Extremos máximos de oleaje (altura significante). Puertos del Estado
12. Engineers, U. A. C. O (1984). Shore protection manual. *Army Engineer Waterways Experiment Station, Vicksburg, MS. 2v*, 37-53.
13. Engineers, U. A. C. O. (2011). Chapter 5: Fundamentals of design. *Coastal Engineering Manual part VI.* pp. VI-5-94 until VI-5-98. Washington.
14. Favalli, M., Fornaciai, A., Isola, I., Tarquini, S. & Nannipieri, L. (2012). Multiview 3D reconstruction in geosciences. *Computers & Geosciences, 44*, 168-176.
15. Frens, A. B. (2007). *The impact of placement method of Antifer-block stability*. Master Thesis. TU Delft, Civil Engineering and Geosciences, Hydraulic Engineering.
16. Gómez-Martín, M. E. & Medina, J. R. (2007). Damage progression on cube armored breakwaters. In *Coastal Engineering 2006: (In 5 Volumes)* (pp. 5229-5240).
17. Gómez-Martín, M. E., & Medina, J. R. (2013). Heterogeneous packing and hydraulic stability of cube and Cubipod armor units. *Journal of Waterway, Port, Coastal and Ocean Engineering*, *140*(1), 100–108.
18. Hasselmann, K., Barnett, T. P., Bouws, E., Carlson, H., Cartwright, D. E., Enke, K.,…& Meerburg, A. (1973). *Measurements of wind-wave growth and swell decay during the joint North Sea wave project (JONSWAP)*. Deutches Hydrographisches Institut.

19. Hudson, R. Y. (Ed.) (1974). *Concrete armor units for protection against wave attack*. Waterways Experiment Station.
20. Hughes, S. A. (1993). *Physical models and laboratory techniques in coastal engineering* (Vol. 7). World Scientific.
21. Losada, M. A., Desiré, J. M. & Alejo, L. M. (1986). Stability of blocks as breakwater armor units. *Journal of Structural Engineering, 112*(11), 2392-2401.
22. Martín-Hidalgo, M., Martín-Soldevilla, M. J., Negro, V., Aberturas, P. & López-Gutiérrez, J. S. (2014). Storm evolution characterization for analysing stone armour damage progression. *Coastal Engineering, 85,* 1-11.
23. Martín-Soldevilla, M. J., Martín-Hidalgo, M., Negro, V., López-Gutiérrez, J. S. & Aberturas, P. (2015). Improvement of theoretical storm characterization for different climate conditions. *Coastal Engineering, 96*, 71-80.
24. Marzeddu, A., De Leau, J., Mathijs, A., Gironella, X., Bas, H., Gracia, V. & Sanchez Arcilla, A. (2017). Effects of storm duration and sequencing on armour layer damages. Manuscript submitted for publication.
25. Mathijs, A. (2017). *Use of multi-view 3D reconstruction for damage assessment in breakwaters.* Master Thesis. Universitat Politècnica de Catalunya (UPC), Barcelona, Spain.
26. Medina, J. R., Gómez-Martín, M. E. & Corredor, A. (2011). Influence of armour unit placement on armour porosity and hydraulic stability. *Coastal Engineering Proceedings, 1*(32), 41.
27. Medina, J. R., Molines, J. & Gómez-Martín, M. E. (2014). Influence of armour porosity on the hydraulic stability of cube armour layers. *Ocean Engineering*, *88*, 289–297.
28. Melby, J. A. & Kobayashi, N. (1998). Progression and variability of damage on rubble mound breakwaters. *Journal of waterway, port, coastal and ocean engineering, 124(6),* 286-294.
29. Owen, M. W. & Allsop, N. W. H. (1984). Hydraulic modelling of rubble mound breakwaters. *Proceedings of the Conference on Breakwater: Design and Construction* (pp. 71-78). Thomas Telford Publishing, London.
30. Pardo, V., Herrera, M. P., Molines, J. & Medina, J. R. (2013). Placement Test, Porosity, and Randomness of Cube and Cubipod Armor Layers. *Journal of Waterway, Port, Coastal and Ocean Engineering, 140*(5), 04014017.
31. Pierson, W. J. & Moskowitz, L. (1964). A proposed spectral form for fully developed wind seas based on the similarity of SA Kitaigorodskii. *Journal of geophysical research*, *69*(24), 5181-5190.
32. Rice, S.O. (1945). Mathematical analysis of random noise. *Bell System Technical Journal, 24*(1), 46-156.
33. Recomendaciones para obras marítimas (ROM). Acciones en el proyecto de obras marítimas y portuarias (ROM 02-90).
34. Snavely, K. N. (2009). *Scene reconstruction and visualization from internet photo collections.* Doctoral Thesis. University of Washington, Seattle, WA, USA.
35. Soares, C. G. & Scotto, M. (2001). Modelling uncertainty in long-term predictions of significant wave height. *Ocean Engineering, 28*(3), 329-342.

36. Sulisz, W., Paprota, M. & Reda, A. (2016). Extreme waves in the southern Baltic Sea. Olas gigantes en la parte sur del mar Báltico. *Ciencias Marinas, 42*(2), 123-137.
37. Van Buchem, R. V. (2009). *Stability of single top layer of cubes* (Doctoral dissertation, MSc-Thesis, Delft University of Technology, Delft).
38. Van der Meer, J. W. (1987). Stability of breakwater armour layers-design formulae. *Coastal engineering, 11*(3), 219-239
39. Van der Meer, J. W. (1988b). Stability of cubes, tetrapods and accropode. *Proceedings of the breakwaters '88 conference. Design breakwaters* (pp. 59-68). Thomas Telford Publishing, London, UK.
40. Van der Meer, J. W. (1992). Stability of the seaward slope of berm breakwaters. *Coastal Engineering, 16*(2), 205-234
41. Van der Meer, J. W. (1998). Application and stability criteria for rock and artificial units. *Dikes and Revetments*, *Rotterdam/Brookfield: AA Balkema*, *Chapter 11*, 191-215.
42. Van der Meer, J. W. (1999, June). Design of concrete armour layers. In *Proceedings of the Coastal Structures '99. Santander, Spain, 7-10 June 1999 (*Vol. 99, pp. 213-221).
43. Via Estrem, L., Pullen, T. A., Stewart, T. & Allsop, W. (2013). Damage to rubble mound breakwaters-Extracting design guidance from 'old' test data. *ICE Coasts, Marine Structures and Breakwaters conference, 18-20 September 2013, Edinburgh.*
44. Westoby, M. J., Brasington, J., Glasser, N. F., Hambrey, M. J. & Reynolds, J. M. (2012). 'Structure-from-Motion' photogrammetry: A low-cost, effective tool for geoscience applications. *Geomorphology, 179,* 300-314.
45. Wolters, G., Van Gent, M., Allsop, W., Hamm, L & Mühlestein, D. (2009, September). HYDRALAB III: Guidelines for physical model testing of rubble mound breakwaters. *In Proceedings of the 9th International Conference on Coasts, Marine Structures and Breakwaters: Adapting to Change, Edinburgh, United Kingdom* (pp. 659-670).

# APPENDIX: TEST PLANS

In this appendix are presented the test plans for the different sets of the synthetic trapezoidal storm and the real storm, which have been the ones carried out by the author for this research during these months in the flume facility. Also the parameters $N_o$ and $N_{od}$ for the steps available are showed.

The units for the different parameters are for all the tables the ones written below:

- $H_{s,target}$ and $H_{s,measured}$: [m]
- $T_{p,input}$: [s]
- $N_z$: [-]
- $N_o$ $and$ $N_{od}$: [-]

## *Trapezoidal storm*

| Seed nº1 | Trapezium storm | | | | | |
|---|---|---|---|---|---|---|
| ID | Hs_target | Hs_measured | Tp_input | Nz | No | Nod |
| **090217_0** | 0.035 | 0.036 | 1.04 | 387 | | |
| **090217_1** | 0.037 | 0.039 | 1.08 | 760 | | |
| **090217_2** | 0.039 | 0.042 | 1.11 | 1122 | | |
| **090217_3** | 0.042 | 0.043 | 1.15 | 1473 | | |
| **090217_4** | 0.044 | 0.046 | 1.18 | 1814 | | |
| **090217_5** | 0.047 | 0.049 | 1.22 | 2145 | | |
| **090217_6** | 0.049 | 0.050 | 1.25 | 2466 | | |
| **090217_7** | 0.052 | 0.053 | 1.29 | 2779 | | |
| **090217_8** | 0.054 | 0.058 | 1.32 | 3084 | 33 | 1.39 |
| **090217_9** | 0.054 | 0.058 | 1.32 | 3389 | | |
| **090217_10** | 0.054 | 0.058 | 1.32 | 3694 | | |
| **090217_11** | 0.054 | 0.058 | 1.32 | 4000 | | |
| **090217_12** | 0.054 | 0.058 | 1.32 | 4305 | 65 | 2.73 |
| **100217_0** | 0.052 | 0.054 | 1.29 | 4618 | | |
| **100217_1** | 0.049 | 0.051 | 1.25 | 4939 | | |
| **100217_2** | 0.047 | 0.050 | 1.22 | 5269 | | |
| **100217_3** | 0.044 | 0.047 | 1.18 | 5611 | | |
| **100217_4** | 0.042 | 0.043 | 1.15 | 5962 | | |
| **100217_5** | 0.039 | 0.042 | 1.11 | 6324 | | |
| **100217_6** | 0.037 | 0.040 | 1.08 | 6697 | | |
| **100217_7** | 0.035 | 0.037 | 1.04 | 7084 | 83 | 3.49 |

*Table 22. 1st test plan for the trapezoidal storm.*

| Seed nº2 | Trapezium storm | | | | | |
|---|---|---|---|---|---|---|
| ID | Hs_target | Hs_measured | Tp_input | Nz | No | Nod |
| 130217_0 | 0.035 | 0.036 | 1.04 | 387 | | |
| 130217_1 | 0.037 | 0.039 | 1.08 | 760 | | |
| 130217_2 | 0.039 | 0.040 | 1.11 | 1122 | | |
| 130217_3 | 0.042 | 0.043 | 1.15 | 1473 | | |
| 130217_4 | 0.044 | 0.046 | 1.18 | 1814 | | |
| 130217_5 | 0.047 | 0.048 | 1.22 | 2145 | | |
| 130217_6 | 0.049 | 0.050 | 1.25 | 2466 | | |
| 130217_7 | 0.052 | 0.053 | 1.29 | 2779 | | |
| 130217_8 | 0.054 | 0.057 | 1.32 | 3084 | 37 | 1.56 |
| 130217_9 | 0.054 | 0.056 | 1.32 | 3389 | | |
| 130217_10 | 0.054 | 0.057 | 1.32 | 3694 | | |
| 130217_11 | 0.054 | 0.056 | 1.32 | 4000 | | |
| 130217_12 | 0.054 | 0.056 | 1.32 | 4305 | 59 | 2.48 |
| 140217_0 | 0.052 | 0.052 | 1.29 | 4618 | | |
| 140217_1 | 0.049 | 0.050 | 1.25 | 4939 | | |
| 140217_2 | 0.047 | 0.048 | 1.22 | 5269 | | |
| 140217_3 | 0.044 | 0.046 | 1.18 | 5611 | | |
| 140217_4 | 0.042 | 0.043 | 1.15 | 5962 | | |
| 140217_5 | 0.039 | 0.040 | 1.11 | 6324 | | |
| 140217_6 | 0.037 | 0.038 | 1.08 | 6697 | | |
| 140217_7 | 0.035 | 0.036 | 1.04 | 7084 | 62 | 2.61 |

*Table 23. 2nd test plan for the trapezoidal storm.*

| Seed nº3 | Trapezium storm | | | | | |
|---|---|---|---|---|---|---|
| ID | Hs_target | Hs_measured | Tp_input | Nz | No | Nod |
| 150217_0 | 0.035 | 0.034 | 1.04 | 387 | 6 | 0.25 |
| 150217_1 | 0.037 | 0.038 | 1.08 | 760 | 8 | 0.34 |
| 150217_2 | 0.039 | 0.039 | 1.11 | 1122 | 10 | 0.42 |
| 150217_3 | 0.042 | 0.043 | 1.15 | 1473 | 10 | 0.42 |
| 150217_4 | 0.044 | 0.044 | 1.18 | 1814 | 13 | 0.55 |
| 150217_5 | 0.047 | 0.047 | 1.22 | 2145 | 18 | 0.76 |
| 150217_6 | 0.049 | 0.050 | 1.25 | 2466 | 21 | 0.88 |
| 150217_7 | 0.052 | 0.052 | 1.29 | 2779 | 21 | 0.88 |
| 150217_8 | 0.054 | 0.055 | 1.32 | 3084 | 32 | 1.34 |
| 160217_0 | 0.054 | 0.054 | 1.32 | 3389 | 50 | 2.10 |
| 160217_1 | 0.054 | 0.054 | 1.32 | 3694 | 62 | 2.61 |
| 160217_2 | 0.054 | 0.055 | 1.32 | 4000 | 63 | 2.65 |
| 160217_3 | 0.054 | 0.055 | 1.32 | 4305 | 73 | 3.07 |
| 160217_4 | 0.052 | 0.051 | 1.29 | 4618 | 78 | 3.28 |
| 160217_5 | 0.049 | 0.049 | 1.25 | 4939 | 78 | 3.28 |
| 160217_6 | 0.047 | 0.046 | 1.22 | 5269 | 78 | 3.28 |
| 160217_7 | 0.044 | 0.044 | 1.18 | 5611 | 79 | 3.32 |
| 160217_8 | 0.042 | 0.042 | 1.15 | 5962 | 81 | 3.40 |
| 160217_9 | 0.039 | 0.039 | 1.11 | 6324 | 81 | 3.40 |
| 160217_10 | 0.037 | 0.037 | 1.08 | 6697 | 81 | 3.40 |
| 160217_11 | 0.035 | 0.034 | 1.04 | 7084 | 81 | 3.40 |

*Table 24. 3rd test plan for the trapezoidal storm.*

| Seed nº4 | Trapezium storm | | | | | |
|---|---|---|---|---|---|---|
| ID | Hs_target | Hs_measured | Tp_input | Nz | No | Nod |
| 170217_0 | 0.035 | 0.036 | 1.04 | 387 | | |
| 170217_1 | 0.037 | 0.039 | 1.08 | 760 | | |
| 170217_2 | 0.039 | 0.041 | 1.11 | 1122 | | |
| 170217_3 | 0.042 | 0.043 | 1.15 | 1473 | | |
| 170217_4 | 0.044 | 0.047 | 1.18 | 1814 | | |
| 170217_5 | 0.047 | 0.048 | 1.22 | 2145 | | |
| 170217_6 | 0.049 | 0.050 | 1.25 | 2466 | | |
| 170217_7 | 0.052 | 0.055 | 1.29 | 2779 | | |
| 170217_8 | 0.054 | 0.058 | 1.32 | 3084 | 27 | 1.13 |
| 200217_0 | 0.054 | 0.057 | 1.32 | 3389 | | |
| 200217_1 | 0.054 | 0.058 | 1.32 | 3694 | | |
| 200217_2 | 0.054 | 0.058 | 1.32 | 4000 | | |
| 200217_3 | 0.054 | 0.057 | 1.32 | 4305 | 40 | 1.68 |
| 200217_4 | 0.052 | 0.053 | 1.29 | 4618 | | |
| 200217_5 | 0.049 | 0.050 | 1.25 | 4939 | | |
| 200217_6 | 0.047 | 0.048 | 1.22 | 5269 | | |
| 200217_7 | 0.044 | 0.047 | 1.18 | 5611 | | |
| 200217_8 | 0.042 | 0.043 | 1.15 | 5962 | | |
| 200217_9 | 0.039 | 0.041 | 1.11 | 6324 | | |
| 200217_10 | 0.037 | 0.039 | 1.08 | 6697 | | |
| 200217_11 | 0.035 | 0.037 | 1.04 | 7084 | 45 | 1.89 |

*Table 25. 4th test plan for the trapezoidal storm.*

| Seed nº5 | Trapezium storm | | | | | |
|---|---|---|---|---|---|---|
| ID | Hs_target | Hs_measured | Tp_input | Nz | No | Nod |
| 210217_0 | 0.035 | 0.034 | 1.04 | 387 | | |
| 210217_1 | 0.037 | 0.037 | 1.08 | 760 | | |
| 210217_2 | 0.039 | 0.037 | 1.11 | 1122 | | |
| 210217_3 | 0.042 | 0.040 | 1.15 | 1473 | | |
| 210217_4 | 0.044 | 0.043 | 1.18 | 1814 | | |
| 210217_5 | 0.047 | 0.044 | 1.22 | 2145 | | |
| 210217_6 | 0.049 | 0.047 | 1.25 | 2466 | | |
| 210217_7 | 0.052 | 0.048 | 1.29 | 2779 | | |
| 210217_8 | 0.054 | 0.052 | 1.32 | 3084 | 37 | 1.56 |
| 210217_9 | 0.054 | 0.052 | 1.32 | 3389 | | |
| 210217_10 | 0.054 | 0.051 | 1.32 | 3694 | | |
| 210217_11 | 0.054 | 0.052 | 1.32 | 4000 | | |
| 220217_0 | 0.054 | 0.052 | 1.32 | 4305 | 63 | 2.65 |
| 220217_1 | 0.052 | 0.048 | 1.29 | 4618 | | |
| 220217_2 | 0.049 | 0.046 | 1.25 | 4939 | | |
| 220217_3 | 0.047 | 0.044 | 1.22 | 5269 | | |
| 220217_4 | 0.044 | 0.043 | 1.18 | 5611 | | |
| 220217_5 | 0.042 | 0.040 | 1.15 | 5962 | | |
| 220217_6 | 0.039 | 0.037 | 1.11 | 6324 | | |
| 220217_7 | 0.037 | 0.036 | 1.08 | 6697 | | |
| 220217_8 | 0.035 | 0.033 | 1.04 | 7084 | 65 | 2.73 |

*Table 26. 5th test plan for the trapezoidal storm.*

| Seed nº2 | Trapezium storm | | | | | |
|---|---|---|---|---|---|---|
| ID | Hs_target | Hs_measured | Tp_input | Nz | No | Nod |
| 230217_0 | 0.035 | 0.036 | 1.04 | 387 | | |
| 230217_1 | 0.037 | 0.038 | 1.08 | 760 | | |
| 230217_2 | 0.039 | 0.040 | 1.11 | 1122 | | |
| 230217_3 | 0.042 | 0.043 | 1.15 | 1473 | | |
| 230217_4 | 0.044 | 0.045 | 1.18 | 1814 | | |
| 230217_5 | 0.047 | 0.048 | 1.22 | 2145 | | |
| 230217_6 | 0.049 | 0.050 | 1.25 | 2466 | | |
| 230217_7 | 0.052 | 0.052 | 1.29 | 2779 | | |
| 230217_8 | 0.054 | 0.056 | 1.32 | 3084 | 19 | 0.8 |
| 240217_0 | 0.054 | 0.056 | 1.32 | 3389 | | |
| 240217_1 | 0.054 | 0.056 | 1.32 | 3694 | | |
| 240217_2 | 0.054 | 0.056 | 1.32 | 4000 | | |
| 240217_3 | 0.054 | 0.056 | 1.32 | 4305 | 31 | 1.3 |
| 240217_4 | 0.052 | 0.052 | 1.29 | 4618 | | |
| 240217_5 | 0.049 | 0.050 | 1.25 | 4939 | | |
| 240217_6 | 0.047 | 0.047 | 1.22 | 5269 | | |
| 240217_7 | 0.044 | 0.045 | 1.18 | 5611 | | |
| 240217_8 | 0.042 | 0.042 | 1.15 | 5962 | | |
| 240217_9 | 0.039 | 0.040 | 1.11 | 6324 | | |
| 240217_10 | 0.037 | 0.038 | 1.08 | 6697 | | |
| 240217_11 | 0.035 | 0.036 | 1.04 | 7084 | 34 | 1.43 |

*Table 27. 6th test plan for the trapezoidal storm.*

| Seed nº2 | Trapezium storm | | | | | |
|---|---|---|---|---|---|---|
| ID | Hs_target | Hs_measured | Tp_input | Nz | No | Nod |
| 060317_0 | 0.035 | 0.035 | 1.04 | 387 | | |
| 060317_1 | 0.037 | 0.038 | 1.08 | 760 | | |
| 060317_2 | 0.039 | 0.040 | 1.11 | 1122 | | |
| 060317_3 | 0.042 | 0.042 | 1.15 | 1473 | | |
| 060317_4 | 0.044 | 0.045 | 1.18 | 1814 | | |
| 060317_5 | 0.047 | 0.048 | 1.22 | 2145 | | |
| 060317_6 | 0.049 | 0.050 | 1.25 | 2466 | | |
| 060317_7 | 0.052 | 0.052 | 1.29 | 2779 | | |
| 060317_8 | 0.054 | 0.056 | 1.32 | 3084 | 6 | 0.25 |
| 060317_9 | 0.054 | 0.056 | 1.32 | 3389 | | |
| 060317_10 | 0.054 | 0.056 | 1.32 | 3694 | | |
| 070317_0 | 0.054 | 0.035 | 1.32 | 4000 | | |
| 070317_1 | 0.054 | 0.056 | 1.32 | 4305 | 7 | 0.29 |
| 070317_2 | 0.052 | 0.052 | 1.29 | 4618 | | |
| 070317_3 | 0.049 | 0.050 | 1.25 | 4939 | | |
| 070317_4 | 0.047 | 0.048 | 1.22 | 5269 | | |
| 070317_5 | 0.044 | 0.045 | 1.18 | 5611 | | |
| 070317_6 | 0.042 | 0.042 | 1.15 | 5962 | | |
| 070317_7 | 0.039 | 0.040 | 1.11 | 6324 | | |
| 070317_8 | 0.037 | 0.038 | 1.08 | 6697 | | |
| 070317_9 | 0.035 | 0.036 | 1.04 | 7084 | 8 | 0.34 |

*Table 28. 7th test plan for the trapezoidal storm.*

| Seed nº2 | Trapezium storm | | | | | |
|---|---|---|---|---|---|---|
| ID | Hs_target | Hs_measured | Tp_input | Nz | No | Nod |
| 080317_0 | 0.035 | 0.036 | 1.04 | 387 | | |
| 080317_1 | 0.037 | 0.038 | 1.08 | 760 | | |
| 080317_2 | 0.039 | 0.040 | 1.11 | 1122 | | |
| 080317_3 | 0.042 | 0.043 | 1.15 | 1473 | | |
| 080317_4 | 0.044 | 0.045 | 1.18 | 1814 | | |
| 080317_5 | 0.047 | 0.048 | 1.22 | 2145 | | |
| 080317_6 | 0.049 | 0.050 | 1.25 | 2466 | | |
| 080317_7 | 0.052 | 0.052 | 1.29 | 2779 | | |
| 080317_8 | 0.054 | 0.056 | 1.32 | 3084 | 43 | 1.81 |
| 090317_0 | 0.054 | 0.056 | 1.32 | 3389 | | |
| 090317_1 | 0.054 | 0.056 | 1.32 | 3694 | | |
| 090317_2 | 0.054 | 0.056 | 1.32 | 4000 | | |
| 090317_3 | 0.054 | 0.056 | 1.32 | 4305 | 51 | 2.14 |
| 090317_4 | 0.052 | 0.052 | 1.29 | 4618 | | |
| 090317_5 | 0.049 | 0.050 | 1.25 | 4939 | | |
| 090317_6 | 0.047 | 0.047 | 1.22 | 5269 | | |
| 090317_7 | 0.044 | 0.045 | 1.18 | 5611 | | |
| 090317_8 | 0.042 | 0.042 | 1.15 | 5962 | | |
| 090317_9 | 0.039 | 0.040 | 1.11 | 6324 | | |
| 090317_10 | 0.037 | 0.038 | 1.08 | 6697 | | |
| 090317_11 | 0.035 | 0.036 | 1.04 | 7084 | 51 | 2.14 |

*Table 29. 8th test plan for the trapezoidal storm.*

| Seed nº2 | Trapezium storm | | | | | |
|---|---|---|---|---|---|---|
| ID | Hs_target | Hs_measured | Tp_input | Nz | No | Nod |
| 100317_0 | 0.035 | 0.036 | 1.04 | 387 | | |
| 100317_1 | 0.037 | 0.038 | 1.08 | 760 | | |
| 100317_2 | 0.039 | 0.040 | 1.11 | 1122 | | |
| 100317_3 | 0.042 | 0.042 | 1.15 | 1473 | | |
| 100317_4 | 0.044 | 0.045 | 1.18 | 1814 | | |
| 130317_0 | 0.047 | 0.047 | 1.22 | 2145 | | |
| 130317_1 | 0.049 | 0.050 | 1.25 | 2466 | | |
| 130317_2 | 0.052 | 0.052 | 1.29 | 2779 | | |
| 130317_3 | 0.054 | 0.056 | 1.32 | 3084 | 8 | 0.34 |
| 130317_4 | 0.054 | 0.056 | 1.32 | 3389 | | |
| 130317_5 | 0.054 | 0.056 | 1.32 | 3694 | | |
| 130317_6 | 0.054 | 0.056 | 1.32 | 4000 | | |
| 140317_0 | 0.054 | 0.056 | 1.32 | 4305 | 20 | 0.84 |
| 140317_1 | 0.052 | 0.052 | 1.29 | 4618 | | |
| 140317_2 | 0.049 | 0.050 | 1.25 | 4939 | | |
| 140317_3 | 0.047 | 0.048 | 1.22 | 5269 | | |
| 140317_4 | 0.044 | 0.045 | 1.18 | 5611 | | |
| 140317_5 | 0.042 | 0.042 | 1.15 | 5962 | | |
| 140317_6 | 0.039 | 0.040 | 1.11 | 6324 | | |
| 140317_7 | 0.037 | 0.038 | 1.08 | 6697 | | |
| 140317_8 | 0.035 | 0.036 | 1.04 | 7084 | 22 | 0.92 |

*Table 30. 9th test plan for the trapezoidal storm.*

| Seed nº2 | Trapezium storm | | | | | |
|---|---|---|---|---|---|---|
| ID | Hs_target | Hs_measured | Tp_input | Nz | No | Nod |
| 270317_0 | 0.035 | 0.036 | 1.04 | 387 | | |
| 270317_1 | 0.037 | 0.038 | 1.08 | 760 | | |
| 270317_2 | 0.039 | 0.040 | 1.11 | 1122 | | |
| 270317_3 | 0.042 | 0.042 | 1.15 | 1473 | | |
| 270317_4 | 0.044 | 0.045 | 1.18 | 1814 | | |
| 270317_5 | 0.047 | 0.048 | 1.22 | 2145 | | |
| 270317_6 | 0.049 | 0.050 | 1.25 | 2466 | | |
| 270317_7 | 0.052 | 0.052 | 1.29 | 2779 | | |
| 270317_8 | 0.054 | 0.056 | 1.32 | 3084 | 13 | 0.55 |
| 270317_9 | 0.054 | 0.056 | 1.32 | 3389 | | |
| 270317_10 | 0.054 | 0.056 | 1.32 | 3694 | | |
| 270317_11 | 0.054 | 0.056 | 1.32 | 4000 | | |
| 270317_12 | 0.054 | 0.056 | 1.32 | 4305 | 20 | 0.84 |
| 280317_0 | 0.052 | 0.053 | 1.29 | 4618 | | |
| 280317_1 | 0.049 | 0.051 | 1.25 | 4939 | | |
| 280317_2 | 0.047 | 0.048 | 1.22 | 5269 | | |
| 280317_3 | 0.044 | 0.046 | 1.18 | 5611 | | |
| 280317_4 | 0.042 | 0.043 | 1.15 | 5962 | | |
| 280317_5 | 0.039 | 0.041 | 1.11 | 6324 | | |
| 280317_6 | 0.037 | 0.039 | 1.08 | 6697 | | |
| 280317_7 | 0.035 | 0.035 | 1.04 | 7084 | 21 | 0.88 |

*Table 31. 10th test plan for the trapezoidal storm.*

## *Real storm*

| Seed nº3 | Real storm | | | | | |
|---|---|---|---|---|---|---|
| ID | Hs_target | Hs_measured | Tp_input | Nz | No | Nod |
| 290317_0 | 0.033 | 0.034 | 1.13 | 360 | | |
| 290317_1 | 0.038 | 0.038 | 1.16 | 703 | | |
| 290317_2 | 0.043 | 0.042 | 1.11 | 1063 | | |
| 290317_3 | 0.041 | 0.041 | 1.16 | 1406 | | |
| 290317_4 | 0.047 | 0.047 | 1.45 | 1676 | | |
| 290317_5 | 0.044 | 0.043 | 1.11 | 2036 | | |
| 290317_6 | 0.054 | 0.055 | 1.3 | 2341 | 3 | 0.13 |
| 290317_7 | 0.048 | 0.047 | 1.11 | 2701 | | |
| 290317_8 | 0.049 | 0.049 | 1.16 | 3044 | | |
| 290317_9 | 0.050 | 0.051 | 1.55 | 3296 | | |
| 290317_10 | 0.051 | 0.055 | 1.55 | 3548 | | |
| 290317_11 | 0.049 | 0.049 | 1.3 | 3853 | | |
| 290317_12 | 0.053 | 0.056 | 1.55 | 4105 | | |
| 290317_13 | 0.053 | 0.055 | 1.23 | 4429 | 23 | 0.97 |
| 300317_0 | 0.051 | 0.052 | 1.18 | 4772 | | |
| 300317_1 | 0.048 | 0.047 | 1.3 | 5077 | | |
| 300317_2 | 0.049 | 0.050 | 1.16 | 5420 | | |
| 300317_3 | 0.049 | 0.049 | 1.38 | 5708 | | |
| 300317_4 | 0.048 | 0.048 | 1.16 | 6051 | | |
| 300317_5 | 0.047 | 0.046 | 1.3 | 6356 | | |
| 300317_6 | 0.044 | 0.044 | 1.23 | 6680 | | |
| 300317_7 | 0.035 | 0.036 | 1.13 | 7040 | 26 | 1.09 |

*Table 32. 1st test plan for the real storm.*

| Seed nº5 | Real storm | | | | | |
|---|---|---|---|---|---|---|
| ID | Hs_target | Hs_measured | Tp_input | Nz | No | Nod |
| 310317_0 | 0.033 | 0.032 | 1.13 | 360 | 0 | 0 |
| 310317_1 | 0.038 | 0.038 | 1.16 | 703 | 1 | 0 |
| 310317_2 | 0.043 | 0.040 | 1.11 | 1063 | 3 | 0.1 |
| 310317_3 | 0.041 | 0.040 | 1.16 | 1406 | 3 | 0.1 |
| 310317_4 | 0.047 | 0.044 | 1.45 | 1676 | 5 | 0.21 |
| 310317_5 | 0.044 | 0.041 | 1.11 | 2036 | 7 | 0.29 |
| 310317_6 | 0.054 | 0.052 | 1.3 | 2341 | 25 | 1.05 |
| 310317_7 | 0.048 | 0.045 | 1.11 | 2701 | 26 | 1.09 |
| 310317_8 | 0.049 | 0.047 | 1.16 | 3044 | 26 | 1.09 |
| 310317_9 | 0.050 | 0.048 | 1.55 | 3296 | 29 | 1.22 |
| 310317_10 | 0.051 | 0.051 | 1.55 | 3548 | 32 | 1.34 |
| 310317_11 | 0.049 | 0.046 | 1.3 | 3853 | 32 | 1.34 |
| 310317_12 | 0.053 | 0.052 | 1.55 | 4105 | 35 | 1.47 |
| 310317_13 | 0.053 | 0.051 | 1.23 | 4429 | 35 | 1.47 |
| 310317_14 | 0.051 | 0.051 | 1.18 | 4772 | 39 | 1.64 |
| 310317_15 | 0.048 | 0.045 | 1.3 | 5077 | 40 | 1.68 |
| 310317_16 | 0.049 | 0.048 | 1.16 | 5420 | 41 | 1.72 |
| 310317_17 | 0.049 | 0.046 | 1.38 | 5708 | 41 | 1.72 |
| 310317_18 | 0.048 | 0.046 | 1.16 | 6051 | 41 | 1.72 |
| 310317_19 | 0.047 | 0.043 | 1.3 | 6356 | 41 | 1.72 |
| 310317_20 | 0.044 | 0.041 | 1.23 | 6680 | 41 | 1.72 |
| 310317_21 | 0.035 | 0.034 | 1.13 | 7040 | 42 | 1.77 |

*Table 33. 2nd test plan for the real storm.*

| Seed nº5 | Real storm | | | | | |
|---|---|---|---|---|---|---|
| ID | Hs_target | Hs_measured | Tp_input | Nz | No | Nod |
| 030417_0 | 0.033 | 0.032 | 1.13 | 360 | | |
| 030417_1 | 0.038 | 0.038 | 1.16 | 703 | | |
| 030417_2 | 0.043 | 0.040 | 1.11 | 1063 | | |
| 030417_3 | 0.041 | 0.040 | 1.16 | 1406 | | |
| 030417_4 | 0.047 | 0.044 | 1.45 | 1676 | | |
| 030417_5 | 0.044 | 0.041 | 1.11 | 2036 | | |
| 030417_6 | 0.054 | 0.052 | 1.3 | 2341 | 23 | 0.97 |
| 030417_7 | 0.048 | 0.046 | 1.11 | 2701 | | |
| 030417_8 | 0.049 | 0.047 | 1.16 | 3044 | | |
| 030417_9 | 0.050 | 0.048 | 1.55 | 3296 | | |
| 030417_10 | 0.051 | 0.052 | 1.55 | 3548 | | |
| 030417_11 | 0.049 | 0.046 | 1.3 | 3853 | | |
| 030417_12 | 0.053 | 0.052 | 1.55 | 4105 | | |
| 030417_13 | 0.053 | 0.052 | 1.23 | 4429 | 41 | 1.72 |
| 040317_0 | 0.051 | 0.051 | 1.18 | 4772 | | |
| 040317_1 | 0.048 | 0.045 | 1.3 | 5077 | | |
| 040317_2 | 0.049 | 0.048 | 1.16 | 5420 | | |
| 040317_3 | 0.049 | 0.047 | 1.38 | 5708 | | |
| 040317_4 | 0.048 | 0.047 | 1.16 | 6051 | | |
| 040317_5 | 0.047 | 0.044 | 1.3 | 6356 | | |
| 040317_6 | 0.044 | 0.041 | 1.23 | 6680 | | |
| 040317_7 | 0.035 | 0.034 | 1.13 | 7040 | 42 | 1.77 |

*Table 34. 3rd test plan for the real storm.*

| Seed nº7 | Real storm | | | | | |
|---|---|---|---|---|---|---|
| ID | Hs_target | Hs_measured | Tp_input | Nz | No | Nod |
| 050417_0 | 0.033 | 0.032 | 1.13 | 360 | | |
| 050417_1 | 0.038 | 0.037 | 1.16 | 703 | | |
| 050417_2 | 0.043 | 0.041 | 1.11 | 1063 | | |
| 050417_3 | 0.041 | 0.040 | 1.16 | 1406 | | |
| 050417_4 | 0.047 | 0.043 | 1.45 | 1676 | | |
| 050417_5 | 0.044 | 0.042 | 1.11 | 2036 | | |
| 050417_6 | 0.054 | 0.053 | 1.3 | 2341 | 14 | 0.59 |
| 050417_7 | 0.048 | 0.046 | 1.11 | 2701 | | |
| 050417_8 | 0.049 | 0.047 | 1.16 | 3044 | | |
| 050417_9 | 0.050 | 0.047 | 1.55 | 3296 | | |
| 050417_10 | 0.051 | 0.050 | 1.55 | 3548 | | |
| 050417_11 | 0.049 | 0.047 | 1.3 | 3853 | | |
| 050417_12 | 0.053 | 0.051 | 1.55 | 4105 | | |
| 050417_13 | 0.053 | 0.050 | 1.23 | 4429 | 34 | 1.43 |
| 050417_14 | 0.051 | 0.052 | 1.18 | 4772 | | |
| 050417_15 | 0.048 | 0.045 | 1.3 | 5077 | | |
| 050417_16 | 0.049 | 0.047 | 1.16 | 5420 | | |
| 050417_17 | 0.049 | 0.044 | 1.38 | 5708 | | |
| 050417_18 | 0.048 | 0.046 | 1.16 | 6051 | | |
| 050417_19 | 0.047 | 0.044 | 1.3 | 6356 | | |
| 050417_20 | 0.044 | 0.041 | 1.23 | 6680 | | |
| 050417_21 | 0.035 | 0.034 | 1.13 | 7040 | 39 | 1.64 |

*Table 35. 4th test plan for the real storm.*

| Seed nº8 | Real storm | | | | | |
|---|---|---|---|---|---|---|
| ID | Hs_target | Hs_measured | Tp_input | Nz | No | Nod |
| 060417_0 | 0.033 | 0.034 | 1.13 | 360 | | |
| 060417_1 | 0.038 | 0.039 | 1.16 | 703 | | |
| 060417_2 | 0.043 | 0.042 | 1.11 | 1063 | | |
| 060417_3 | 0.041 | 0.042 | 1.16 | 1406 | | |
| 060417_4 | 0.047 | 0.047 | 1.45 | 1676 | | |
| 060417_5 | 0.044 | 0.043 | 1.11 | 2036 | | |
| 060417_6 | 0.054 | 0.057 | 1.3 | 2341 | 19 | 0.80 |
| 070417_0 | 0.048 | 0.047 | 1.11 | 2701 | | |
| 070417_1 | 0.049 | 0.049 | 1.16 | 3044 | | |
| 070417_2 | 0.050 | 0.051 | 1.55 | 3296 | | |
| 070417_3 | 0.051 | 0.055 | 1.55 | 3548 | | |
| 070417_4 | 0.049 | 0.050 | 1.3 | 3853 | | |
| 070417_5 | 0.053 | 0.056 | 1.55 | 4105 | | |
| 070417_6 | 0.053 | 0.055 | 1.23 | 4429 | 35 | 1.51 |
| 070417_7 | 0.051 | 0.054 | 1.18 | 4772 | | |
| 070417_8 | 0.048 | 0.049 | 1.3 | 5077 | | |
| 070417_9 | 0.049 | 0.050 | 1.16 | 5420 | | |
| 070417_10 | 0.049 | 0.048 | 1.38 | 5708 | | |
| 070417_11 | 0.048 | 0.048 | 1.16 | 6051 | | |
| 070417_12 | 0.047 | 0.048 | 1.3 | 6356 | | |
| 070417_13 | 0.044 | 0.044 | 1.23 | 6680 | | |
| 070417_14 | 0.035 | 0.036 | 1.13 | 7040 | 51 | 2.14 |

*Table 36. 5th test plan for the real storm.*